




2018

Rebound Relationships: An Investigation Of Hiv-1 Rebound Dynamics And Host Immune Responses During Analytical Treatment Interruption

Danielle Brenda Salantes

University of Pennsylvania, dsalantes@gmail.com

Follow this and additional works at: <https://repository.upenn.edu/edissertations>

 Part of the [Allergy and Immunology Commons](#), [Genetics Commons](#), [Immunology and Infectious Disease Commons](#), [Medical Immunology Commons](#), and the [Virology Commons](#)

Recommended Citation

Salantes, Danielle Brenda, "Rebound Relationships: An Investigation Of Hiv-1 Rebound Dynamics And Host Immune Responses During Analytical Treatment Interruption" (2018). *Publicly Accessible Penn Dissertations*. 3179.
<https://repository.upenn.edu/edissertations/3179>

Rebound Relationships: An Investigation Of Hiv-1 Rebound Dynamics And Host Immune Responses During Analytical Treatment Interruption

Abstract

In HIV-infected patients, combination antiretroviral therapy (cART) during HIV-1 infection potently suppresses viral replication and slows progression to AIDS. Upon cessation of cART, however, systemic infection is rapidly re-established due to the long-lived pool of latently infected cells, or HIV reservoir, that is seeded early in infection and persists despite years of cART in patients. This long-lived reservoir is the target of novel curative strategies. In order to determine in vivo efficacy of these interventions, closely monitored analytical treatment interruption (ATI) is required. Previously conducted ATI trials have provided important baseline information regarding the kinetics and diversity of viruses emerging from latency. As future HIV curative clinical trials move towards prolonged periods of ATI, studies assessing the effect of ATI on host virus-immune dynamics will provide an important baseline that will further our understanding of trial outcomes. In this thesis, I conducted single genome sequencing (SGS) of HIV-1 env and neutralization assays using autologous antibodies to characterize the viral and immune dynamics of rebound in two clinical trials: a longitudinal ATI study in the absence of any intervention, and a brief ATI study involving administration of the broadly neutralizing antibody VRC01. Our data, consistent with previous studies, demonstrated that viral rebound occurs within four weeks of ATI and is established by multiple latently infected cells in the majority of HIV-infected participants. Analyses of plasma containing VRC01 and/or autologous antibodies show that latent reservoir viruses can experience an antibody-mediated neutralization sieve effect, thus preventing the persistence of antibody-sensitive viruses. Additionally, SGS of latent viruses before and after brief ATI show that the size and composition of the peripheral latent viral reservoir is not significantly altered during ATI, demonstrating that short-term ATI is safe. Taken together, these data highlight the complex virus-host dynamics during ATI, and further suggest that passively infused or host-derived neutralizing antibodies can exert selective pressure, altering the evolution of HIV in its host.

Degree Type

Dissertation

Degree Name

Doctor of Philosophy (PhD)

Graduate Group

Cell & Molecular Biology

First Advisor

Katharine J. Bar

Keywords

AIDS, antibodies, evolution, HIV, latency, rebound

Subject Categories

Allergy and Immunology | Genetics | Immunology and Infectious Disease | Medical Immunology | Virology

REBOUND RELATIONSHIPS: AN INVESTIGATION OF HIV-1 REBOUND DYNAMICS
AND HOST IMMUNE RESPONSES DURING ANALYTICAL TREATMENT

INTERRUPTION

D. Brenda Salantes

A DISSERTATION

in

Cell and Molecular Biology

Presented to the Faculties of the University of Pennsylvania

in

Partial Fulfillment of the Requirements for the

Degree of Doctor of Philosophy

2018

Supervisor of Dissertation

Katharine J. Bar, M.D.

Assistant Professor of Medicine

Graduate Group Chairperson

Daniel S. Kessler, Ph.D. Associate Professor of Cell and Developmental Biology

Dissertation Committee

James L. Riley, Ph.D., Associate Professor of Microbiology

James A. Hoxie, M.D., Professor of Medicine

Dave B. Weiner, Ph.D., Professor of Pathology and Laboratory Medicine

Ronald G. Collman, M.D., Professor of Medicine

Dedication

This thesis is dedicated to those who came before me and sacrificed more than I could imagine to give me this very opportunity. You opened doors for me that did not previously exist, you gave me a voice I did not know I could possess, and have instilled within me the courage to keep on going.

ACKNOWLEDGMENTS

First and foremost, I would like to express my sincerest gratitude to my thesis mentor, Dr. Katie Bar. Without hesitation, Dr. Bar bravely took me on as her first Ph.D. student and put me in the driver's seat of several high-impact clinical studies. Her faith in me as a capable, independent scientist has been paramount to my success in the lab. Throughout my Ph.D., she has also generously provided me the space to pursue several non-academic activities that have allowed me to expand my leadership and advocacy skills. Without Dr. Bar's support, undoubtedly, I would not be the well-rounded scientist I am today.

I'd also like to thank my thesis committee members: Dr. Jim Riley, Dr. Jim Hoxie, Dr. Ron Collman and Dr. Dave Weiner for their scientific guidance and mentorship, as well as previous Bar lab members: Ben Scheinfeld, Kate Kerpen, Tuhina Srivastava, Felicity Mampe, Emily Lindemuth, Erin Reagan, and Anya Bauer, for their boundless support as lab mates and now lifelong friends. I am also indebted to Fang-Hua Lee, Dr. Shuyi Wang, Dr. Fred Bibollet-Ruche, Dr. Gerald Learn and the previous and current SGA Core staff for all of their technical help and scientific expertise along the way.

Finally, I'd like to acknowledge my funding sources, (HIV Pathogenesis T32), the BGS and CAMB faculty and staff for their endless support, our clinical collaborators, and the amazing clinical trial participants who selflessly volunteered for these studies in order to expand the landscape of the HIV cure field.

ABSTRACT

REBOUND RELATIONSHIPS: AN INVESTIGATION OF HIV-1 REBOUND DYNAMICS AND HOST IMMUNE RESPONSES DURING ANALYTICAL TREATMENT

INTERRUPTION

D. Brenda Salantes

Katharine J. Bar, M.D.

In HIV-infected patients, combination antiretroviral therapy (cART) during HIV-1 infection potently suppresses viral replication and slows progression to AIDS. Upon cessation of cART, however, systemic infection is rapidly re-established due to the long-lived pool of latently infected cells, or HIV reservoir, that is seeded early in infection and persists despite years of cART in patients. This long-lived reservoir is the target of novel curative strategies. In order to determine in vivo efficacy of these interventions, closely monitored analytical treatment interruption (ATI) is required. Previously conducted ATI trials have provided important baseline information regarding the kinetics and diversity of viruses emerging from latency. As future HIV curative clinical trials move towards prolonged periods of ATI, studies assessing the effect of ATI on host virus-immune dynamics will provide an important baseline that will further our understanding of trial outcomes. In this thesis, I conducted single genome sequencing (SGS) of HIV-1 *env* and neutralization assays using autologous antibodies to characterize the viral and immune dynamics of rebound in two clinical trials: a longitudinal ATI study in the absence of any intervention, and a brief ATI study involving administration of the broadly neutralizing antibody VRC01. Our data, consistent with previous studies, demonstrated that viral rebound occurs within four weeks of ATI and is established by multiple latently

infected cells in the majority of HIV-infected participants. Analyses of plasma containing VRC01 and/or autologous antibodies show that latent reservoir viruses can experience an antibody-mediated neutralization sieve effect, thus preventing the persistence of antibody-sensitive viruses. Additionally, SGS of latent viruses before and after brief ATI show that the size and composition of the peripheral latent viral reservoir is not significantly altered during ATI, demonstrating that short-term ATI is safe. Taken together, these data highlight the complex virus-host dynamics during ATI, and further suggest that passively infused or host-derived neutralizing antibodies can exert selective pressure, altering the evolution of HIV in its host.

TABLE OF CONTENTS

ACKNOWLEDGMENTS	iii
ABSTRACT.....	iv
LIST OF TABLES.....	viii
LIST OF ILLUSTRATIONS.....	ix
CHAPTER 1.....	1
Introduction	1
Epidemiology of HIV-1.....	1
HIV-1 biology and genetic diversity.....	2
HIV-1 transmission and pathogenesis	3
Dynamics of the autologous antibody response during infection.....	5
Latency and persistence	8
Combination antiretroviral therapy	11
Clinical effects of analytical treatment interruption	13
Goals of this thesis	16
References	19
CHAPTER 2.....	27
Autologous antibody responses drive viral diversity during rebound after analytical treatment interruption.....	27
Abstract	28
Introduction	29
Results.....	31
Tables.....	39
Figures.....	40
Discussion.....	46
Materials and Methods.....	53
References.....	60
CHAPTER 3.....	64
Effect of HIV Antibody VRC01 on Viral Rebound After Treatment Interruption	64
Abstract	65
Introduction	67
Results.....	68
Tables.....	75
Figures.....	76
Discussion.....	85
Materials and Methods.....	88
References	98
CHAPTER 4.....	102

HIV-1 Latent Reservoir Size and Diversity are Stable Following Brief Treatment Interruption	102
.....	
Abstract	103
Introduction	104
Results.....	105
Tables.....	117
Figures.....	118
Discussion.....	126
Materials and Methods.....	129
References.....	136
CHAPTER 5.....	140
DISCUSSION	140
Overview	141
Clonality of the viral rebound quasispecies	142
Rebound kinetics to evaluate effect of treatment.....	144
SGS and neutralization assays elucidate mechanisms of failure.	145
Env evolution and host immune responses during ATI	147
Safety of ATI	149
Discordance between ex-vivo derived latent reservoir viruses and rebound.....	150
In conclusion	151
References.....	153

LIST OF TABLES

Table 2.1: Single-ATI and multiple-ATI participant demographics.....	39
Table 3.1: Characteristics of the participants at baseline for ACTG Clinical Trial A5340, Step 1	75
Table 4.1: Baseline, clinical, and study characteristics from A5340 Step 3.....	117
Table 4.2: Genealogical Sorting Indices.....	117

LIST OF ILLUSTRATIONS

Figure 2.1: Kinetics of viral rebound from single-ATI participants.....	40
Figure 2.2: Maximum-likelihood phylogenetic trees of SGS-derived gp160 env or gp41 sequences from single-ATI participants.....	41
Figure 2.3: Correlations between viral load, the number of rebound/founder lineages, and weeks post-ATI at first detectable rebound.....	42
Figure 2.4: ML phylogenetic trees of SGS-derived HIV-1 gp160 or gp41 from longitudinal ATI time points.....	43
Figure 2.5: Strain-specific autologous antibodies develop during ATI.....	44
Figure 2.6: Viral kinetics, dynamics, and autologous antibody responses in multiple-ATI participants.....	45
Figure 3.1: A5340 Step 1 Study Schema.....	76
Figure 3.2: Early viral rebound despite high plasma levels of VRC01.....	77
Figure 3.3: Plasma viremia and levels of VRC01 in trial participants after discontinuation of ART.....	78
Figure 3.4: VRC01 neutralization titers before ART and during viral rebound.....	79
Figure 3.5: Maximum Likelihood (ML) phylogenetic trees of individual participants.....	81
Figure 3.6: VRC01-resistance of pre-cART and rebound viruses.....	82
Figure 3.7: VRC01 antibody footprint sequence changes from pre-cART to rebound..	83
Figure 4.1: A5340 Step 3 Study Schema.....	118
Figure 4.2: Single copy assay.....	118
Figure 4.3: Quantitative measures of reservoir change.....	119
Figure 4.4: ML phylogenetic trees of SGS-derived gp160 <i>env</i> sequences from pre-ART plasma, rebound plasma, and replication-competent latent viruses (Participants A01, A02, A05, A06, A07)	120
Figure 4.5: ML phylogenetic trees of SGS-derived gp160 <i>env</i> sequences from pre-ART plasma, rebound plasma, and replication-competent latent viruses (Participants A08, A09, A13)	121

Figure 4.6: Neutralization sensitivity to VRC01 and autologous plasma at the time of viral rebound..... 122

Figure 4.7: ML phylogenetic trees of SGS-derived gp160 env sequences from pre-ART plasma, rebound plasma, replication-competent latent viruses (Participants A01, A02, and A05–A07)..... 123

Figure 4.8: ML phylogenetic trees of SGS-derived gp160 env sequences from pre-ART plasma, rebound plasma, replication-competent latent viruses, and genetically intact proviral DNA (Participants A08, A09 and A13)..... 124

Figure 4.9: Comparisons of pairwise Levenshtein Distances between virus populations..... 125

CHAPTER 1

Introduction

Epidemiology of HIV-1

In 1983, human immunodeficiency virus (HIV-1) was discovered as the causative agent of Acquired Immunodeficiency Disease (AIDS) and remains a global health concern with no vaccine and over 60 million infected and 35 million deaths from AIDS-related illnesses^{1,2,3,4}. Early genome sequencing and in vitro viral isolation characterized HIV as a retrovirus with two related types: HIV-1 and HIV-2. HIV-1 leads the majority of human infections globally while HIV-2 is isolated primarily in West African countries⁵. Phylogenetic analyses identified simian immunodeficiency viruses (SIVs) as the closest relative of HIV and determined that the epidemic arose through multiple independent cross-species transmission events between humans and SIV-infected African primates^{5,6}. HIV-1 strains can be categorized into four distinct phylogenetic groups: M, N, O and P, where group M viruses are the principal cause of the AIDS pandemic with an estimated index transmission event occurring between 1910-1930^{7,8}. Further modeling of the most recent common ancestor of HIV-1 Group M viruses identified nine clades (A, B, C, D, F, G, H, J, K), with clade B viruses representing the most common subtype responsible for HIV-1 infection in North America and Europe. In 2017, 37 million people were living with HIV-1 and 1.8 million new people are estimated to have been newly infected this year. Due to the prevalence of Clade B viruses in North America and the focus of clinical trials performed in this region in this thesis, I will primarily highlight clade B infection in human subjects who have previously participated in curative HIV-1 clinical trials.

HIV-1 biology and genetic diversity

HIV-1 is an enveloped virus of the family Retroviridae, and genus, lentivirus, which is derived from the Latin word *lentus*, or slow, indicative of its long incubation periods and persistent viral replication⁹. The genome of HIV-1 is a coding RNA with nine open reading frames that produce 15 proteins and is approximately 9.8 kilobases in length¹⁰. Centrally located genes encode three protein classes: 1. Structural proteins: Gag, Pol, and Env; 2. Regulatory proteins: Tat and Rev; and 3. Accessory proteins: Vpu, Vpr, Vif, and Nef. The 160 kilodalton protein, *env*, mediates viral fusion into host cells and is a critical component of viral immune evasion¹¹. The host protease, Furin, cleaves gp160 into gp41 (transmembrane of *env*) and gp120 (located on surface of the infected cell or virion), which are arranged as a multimer or trimer in their active state¹⁰. Escape mutations within *env* rapidly spread throughout the viral population during chronic infection, and is driven by strong selection pressure imposed by cytotoxic CD8+ T cells and neutralizing antibodies¹². In this thesis, I will primarily focus on neutralizing antibodies as the drivers of HIV-1 Env genetic diversity during viral rebound. HIV-1 has a propensity to infect activated CD4+ T cells through engagement of gp120 to the cell surface receptor, CD4, and upregulated co-receptor proteins (CCR5, CXCR4). Engagement of these receptors triggers conformational change in the *env* glycoprotein which mediate fusion of the virus into the host cytoplasm. Transcription of the viral genome is then initiated through HIV-1 Reverse Transcriptase (RT), which converts single stranded RNA into a double stranded DNA genome called a provirus. Within hours, the provirus is then trafficked into the nucleus where it is integrated into host DNA^{13,14}.

One hallmark feature of HIV-1 among all retroviruses is its extensive genetic diversity. This diversity can be attributed to its rapid turnover rate^{15,16} in combination with a high mutation rate guided by an error-prone RT¹⁷. Mathematical modeling takes both variables into account and estimates that the total HIV-1 production rate is 10.3 virions per day with a nucleotide substitution rate of approximately 2×10^{-5} mutations/base pair/cycle^{15,16,18,19}. This rapid increase in diversity allows HIV-1 virions to quickly escape mounting host immune pressures during viral replication, as well as pressure from monotherapy from a single antiretroviral agent. As such, successful viral suppression requires a multi-pronged approach with a combination of potent antiretrovirals (cART) targeting various stages of HIV-1 replication at once.

HIV-1 transmission and pathogenesis

HIV-1 transmission in humans most commonly occurs through contact with viruses at mucosal surfaces or from percutaneous inoculation^{20,21}. The period between infection of the first host cell to when virus is detectable in the plasma is called the eclipse phase and is estimated to be approximately 7-21 days²²⁻²⁶. Fiebig et al. described 6 sequential stages of acute viremia²⁷. In Fiebig I, only HIV-1 RNA can be detected in the blood. Within 7 days, the viral core protein p24 can be detected in Fiebig II as the HIV viral load rises above 10,000 copies/ml and increases at approximately 0.35 log₁₀HIV RNA per day. Peak viral loads, rapid decline of CD4+ T cells, and virus-specific anti-gp41 IgM antibodies can be detected in Fiebig III. During peak viremia, some infected individuals experience symptoms of acute retroviral syndrome, including fever, rash, severe fatigue, diarrhea, and myalgias. Following the acute stages of infection, there is a precipitous depletion of susceptible CD4+ T cell targets and generation of partially-effective host

immune responses, leading to progression of Fiebig stages IV-VI. These stages include a 2-log decrease in plasma vRNA from peak viremia, and the establishment of the plasma viral setpoint²⁸. Anti-HIV antibodies are also generated at this time, though these antibodies are non-neutralizing and do not mediate antibody-dependent cell-mediated virus inhibition (ADCVI). Neutralizing antibodies that target the variable region of *env* generally appear within 12 weeks of infection in clade B-infected individuals²⁹⁻³². The progression to clinical symptoms can vary among individuals, but often occurs slowly. Until this period, infected individuals are asymptomatic and considered to be chronically infected as viral set point is maintained with large numbers of CD4+ T cells becoming infected and dying each day^{33,34}. AIDS is clinically defined when CD4+ T cell counts are less than 200mm³³⁵⁻³⁷, leading to the establishment of opportunistic infections.

Sequence analysis of viruses from homosexual, heterosexual, mother-to-child or percutaneous transmission pairs have determined that productive infection typically occurs with one or a few transmitted/founder (T/F) variants that rapidly evolve over the course of infection³⁸⁻⁴⁰. In addition, transmission pair analyses have determined that despite increased genetic diversity within the pair donor, the majority (76%) of pair recipients established productive clinical infection through a single virus or virus infected cell, while the minority of recipients (24%) had evidence of infection by at least two to five viruses. This low multiplicity of infection and limited viral evolution preceding peak viremia suggests a mucosal bottleneck occurs during initial infection preventing multiple transmission events from a pool of diverse viruses from the chronically infected donor^{41,42,43}.

Dynamics of the autologous antibody response during infection

Rapid evolution of HIV-1 can also be attributed to viral escape of anti-HIV host immune responses mounted through the course of infection. The early stages of HIV-1 infection have been characterized into distinct Fiebig Stages I-VI²⁷. At the start of infection, humoral immune response against HIV-1 are delayed. Within 1 week, the first B cell responses develop in the form of antibody-immune complexes, followed by anti-gp41 antibodies a few days later, and anti-gp120 antibodies several weeks later. Importantly, these delayed antibodies provide no neutralization activity or selection pressure against circulating viruses. Months after infection autologous strain-specific neutralizing antibodies emerge, but provide no neutralizing activity against heterologous strains^{31,38,39,44}. Longitudinal analyses of the autologous antibody response against contemporaneous and early viruses have shown that neutralizing antibodies drive viral escape, as contemporaneous viruses are less sensitive to autologous antibody responses than earlier viruses^{30,38,45-47}. Structural and sequence analyses have shown that this escape is mediated by mutations within the glycan shield of HIV-1 Env and occurs through single amino acid substitutions, insertions and deletions⁴⁸.

Despite significant challenges with rapid viral escape and low strain-specificity, depletion of B cells using anti-CD20 antibodies in nonhuman primate models demonstrate that the autologous antibody response maintains some clinical benefit during infection. Passively transferred antibodies used as a prophylactic strategy against SIV or chimeric simian/human immunodeficiency viruses (SHIV, described in the next section), in nonhuman primates have shown that the dose and timing of autologous antibody administration may have a role in limiting infection⁴⁹⁻⁵². Additionally, recent advances in

B cell cloning have led to the isolation of HIV-specific broadly neutralizing antibodies (bNAbs), which are capable of potently neutralizing cell-free viruses from multiple clades circulating worldwide⁵³⁻⁵⁶. Passive infusions of CD4 binding site (CD4bs) bNAbs have recently entered the clinical trial pipeline and have shown significant and prolonged viral load reduction in the majority of viremic participants⁵⁷. Only 10-30% of infected individuals produce bNAbs during the course of infection, with 1-2% having elite neutralizing activity. While efforts to create an effective vaccine that will produce potent bNAbs in vivo are underway, it is important to note that in passively infused bNAb trials, successful viral suppression in some viremic individuals will not be achieved due to the emergence of high-level resistant variants. Additionally, the finding of pre-existing bNAb resistance in chronically infected individuals presents a significant challenge in using passive infusion of bNAbs as a monotherapeutic cure strategy. Further discussion of pre-existing resistance to the passively infused CD4 binding site antibody, VRC01, will be described in Chapter 3 of this thesis.

For many infectious diseases, the presence of non-neutralizing antibodies have also been implicated in disease prevention and control⁵⁸. While neutralization activity of HIV-1 specific bNAbs requires high affinity Env binding of the variable Fab region of the antibody, antiviral activity can also be mediated indirectly by activation of the Fc region through interactions with the Fcγ receptor expressed on the surface of lymphocytes⁵⁹. Fcγ-mediated effector functions are facilitated through engagement of Fcγ with the Fc region of IgG subtype antibodies and include antibody-dependent cellular cytotoxicity (ADCC), antibody-dependent phagocytosis (ADCP) or antibody-dependent cellular viral inhibition (ADCVI) on infected cells⁶⁰. Previous studies have demonstrated several protective roles mediated through Fc receptors engagement. In a multicenter AIDS

Cohort Study, the ability of polyclonal antibodies to induce ADCC correlated inversely with disease progression⁶¹. Additionally, antibodies with ADCVI activity develop weeks to months prior to neutralizing antibodies, and have been shown to inhibit autologous and heterologous strains of HIV-1 and are inversely correlated with plasma viremia⁶². The protective effect mediated by ADCVI antibodies was also observed during oral challenge with SIVmac251 in newborn macaques, where passive infusion of non-neutralizing, but potent ADCVI antibodies from the serum of SIV-infected macaques protected newborns from infection⁶³.

Differential Fc receptor binding capacities has been shown across various IgG subclasses, where IgG1 and IgG3 are associated with increased affinity and stronger activation of FcγR, while IgG2 and IgG4 have weak activity⁶⁴. These less functional antibodies compete for antigen occupancy with circulating IgG1 and IgG3. By depleting IgG2 and IgG4 in vitro, a higher functional antibody response was observed, suggesting an antagonistic role of IgG2 and IgG4⁶⁵. The protective effect mediated by IgG1 and IgG3 were described in the RV144 phase 2B HIV vaccine trial (ALVAC-HIV vCP1521 prime and recombinant gp120 AIDSVAX B/E boost). While poor humoral immune responses were generated through vaccination, a reduced risk of HIV acquisition was observed^{66,67}. Further analyses of the subclasses of antibodies generated in vaccinated recipients show that polyfunctional antibodies are able to simultaneously recruit multiple effector functions, where IgG1 and IgG3 antibodies are associated with stronger activation of Fc effector functions through increased affinity for the Fc receptor compared to IgG2 and IgG4 antibodies⁶⁵.

The complexity and diversity of the autologous antibody response generated during viral replication is partially driven by the constant evolution of HIV. This creates a “cat-and-mouse” game of viral escape, where the neutralizing antibody responses is continuously lagging behind viral evolution. Sequence analyses of viruses and isolated antibodies from longitudinal time points of active viral replication adds to our understanding of the molecular mechanisms that drive potent autologous antibody responses in vivo, and is an important area of research for HIV-1 vaccine development.

Latency and persistence

The principal barrier to eradicating HIV-1 is the ability of the virus to integrate its genome and establish a viral reservoir within a small pool of long-lived latently infected resting memory CD4+ T cells. Characterization of reservoir dynamics is an important area of study, as mechanisms of viral persistence under fully suppressive cART are not completely understood. Recent advances in next generation molecular sequencing methods have revealed several findings that offer potential explanations. One hypothesis is that there are ongoing, low levels of viral replication due to poor anatomical penetrance of cART in lymphoid tissues^{68,69}. While suboptimal intracellular drug penetrance is a valid concern, there is no clear evidence that supports reduced cART concentration in lymphoid tissues in fully suppressed subjects when lymphoid tissue samples are tested after six months of complete viral suppression with cART. Time points earlier than six months cannot completely eliminate residual viremia. A second alternative mechanism by which low level viral replication occurs during cART is intracellular transmission through direct cell-to-cell contact^{70,71}. While infections originating from a cell-free virus markedly decrease during cART, cell-to-cell transmission of virus would be less sensitive to cART allowing the spread of virus to

occur without acquiring drug-resistant mutations. These studies, however, have largely been restricted to in vitro assays, with no direct evidence of cell-to-cell spread occurring in vivo.

In contrast to ongoing viral replication during cART, others have described low-level antigen-driven proliferation of CD4+ central memory cells and IL-7 mediated homeostatic proliferation as an explanation for reservoir persistence⁷². Independent sampling of identical viral sequences 6+ months apart supports this hypothesis. Additionally, studies using integration site analysis provide direct evidence of infected cell proliferation, further demonstrating that sites of integration are variable and widely distributed throughout the host genome. Identification of large expanded clonal populations within the reservoir along with cells with the same integration site suggests that latently infected cells clonally expand, thus contributing to the stability and persistence of the reservoir under suppressive cART. Furthermore, longitudinal sequence analysis of viruses sampled before cART initiation and during structured treatment interruption in the Swiss HIV Cohort Study show that HIV *env* C2-V3-C3 regions from rebounding viruses do not have an increased genetic distance to the most recent common ancestor (MRCA) compared to pretreatment viruses⁷³. More recent studies, including one presented in Chapter 4 of this thesis, support the hypothesis that the stability of the latent reservoir is instead driven by the clonal expansion of latently-infected cells, as determined by single genome sequence analyses of identical viruses from samples collected at independent time points⁷⁴⁻⁷⁸.

In addition to reservoir persistence under cART, substantial efforts have been made to determine the temporal dynamics of reservoir initiation in order to develop treatment

strategies that limit or prevent reservoir establishment. These efforts were guided by post exposure prophylaxis (PEP) studies in rhesus macaques, where cART was initiated at days 3, 7, 10 or 14 post intrarectal exposure of SIV. After 24 weeks of fully suppressive subcutaneous cART, viral rebound (plasma vRNA >50 copies/ml) occurred in all animals, while animals treated with cART on day 3 experienced a 3-fold delay in rebound kinetics compared to those treated at later time points⁷⁹. Other studies in rhesus macaques have shown that infection can be decreased significantly if PEP is administered orally⁸⁰ or subcutaneously⁸¹ within 72 hours of exposure of SIVmac251, and followed by a brief period of daily dosing. These examples of increased protection in animal models with early PEP initiation suggest reservoir establishment is not immediate, though there is a finite window of opportunity where PEP can effectively prevent permanent seeding of the viral reservoir. With this data, New York guidelines now recommend that PEP is taken within 36 hours of possible HIV exposure and continued for 4 weeks in order to reduce the chances of HIV acquisition⁸². Adherence and completion rates of this short-term regimen, however, remain a significant challenge as studies have shown that only 67% of individuals complete the 28-day course of PEP. One method that has been used to improve retention rates include providing counseling to individuals during PEP therapy. A meta-analysis of sexual assault victims who received PEP show that psychological support through telephone, an adherence diary or in-person counseling throughout the course of treatment is correlated with increased drug adherence. This suggests that continuous emotional support may have a profound impact on PEP efficacy and should be implemented when possible^{83,84}.

Viral dynamics of SIVmac251 in vivo are substantially different from HIV-1 infection in humans, with peak plasma viral load levels ranging from 2.1×10^7 to 7.4×10^7 vRNA

copies/ml by two weeks post infection⁸⁵, compared to a log fold decrease at 10^6 vRNA copies/ml with HIV-1, peaking within 3 weeks post infection⁸⁶. Additionally, variability in the time to set-point viremia, differences in viral decay, as well as distinct innate and adaptive immune responses in SIV infected macaques highlight key differences between SIV and HIV-1 pathogenesis⁸⁷. The creation of SHIVs, which contain an HIV-1 Env cloned into an SIV backbone, helps to address the differences between SIV and HIV in nonhuman primates⁸⁸. Recently developed SHIVs incorporating HIV-1 Envs of clinically relevant viruses demonstrate several key aspects of HIV-1 infection including productive pathogenesis, high antigenicity, the ability to elicit autologous neutralizing antibodies, viral persistence and progression to AIDS⁸⁹. SHIV models will be an invaluable tool in understanding the early events that guide the establishment of latency and resulting host immune responses in the near future.

Combination antiretroviral therapy

Advances in the development of highly effective combination antiretroviral therapy (cART) has led to improved patient outcomes, reduced HIV-associated comorbidity, prolonged survival and decreased risk of HIV transmission⁹⁰⁻⁹². The effectiveness of cART is based off of a combinatorial dosage of drugs that affect several specific viral enzymes responsible for replication, including RT, protease and integrase. Viral suppression can be rapidly achieved to below levels of detection (<50 copies/ml) with genetic screening for mutant viruses, and consistent treatment. The recommended frontline cART regimen for most patients consists of two nucleoside reverse transcriptase inhibitors (NRTIs) and an integrase strand transfer inhibitor (InSTI). Other common clinical regimens include nonnucleoside reverse transcriptase inhibitors (NNRTIs) or boosted protease inhibitors with two NRTIs. Drug tolerability, potency, and

convenience of delivery are critical factors in achieving viral suppression. However, due to a pool of long-lived latently infected cells, daily adherence of cART is required for the lifetime of the patient⁹³⁻⁹⁶. Additionally, even as tremendous efforts have been made to reduce barriers to access of long-term cART, the stability and size of the latent reservoir remains unaffected by prolonged periods of suppressive cART, and as such, cART alone will never be an effective method of eradicating HIV.

It is important to note that while early initiation of cART has substantial clinical benefits, in countries with limited economic resources accessibility of cART remains a significant barrier, thus highlighting the need of additional strategies to effectively target and eradicate the viral reservoir. Proof-of-concept clinical studies exploring cART initiation during the earliest stage of acute infection (Fiebig I) show that all patients experienced viral rebound following cART cessation, further indicating rapid reservoir establishment in humans²⁷. Treatment during Fiebig I was found to have several clinical benefits including preserved immunity, reduced HIV reservoir size, and no seroconversion. However, additional studies assessing the magnitude of gastrointestinal (GI) tract damage show that while individuals treated during acute infection resolved GI tract inflammation and immune activation back to baseline with 24 weeks of cART, histological evaluation of CD4+ T cells in the gut show that CD4+ T cells increase but do not return to baseline after 96 weeks of cART. Attenuation of residual inflammation within the GI tract during early cART is not to be overlooked, however, as activated cells and increased inflammation are drivers of HIV persistence and returning these states close to baseline levels can be an effective way to reduce the size of the reservoir⁹⁷. Control of viral replication with cART at the earliest clinically feasible time point is now the standard of care, and “test and treat” strategies are implemented when possible in

an effort to immediately reduce the size and genetic diversity of the reservoir as well as the clinical manifestations of acute infection.

Clinical effects of analytical treatment interruption

While the advent of cART changed patient outcome during the HIV epidemic in the late 1990s by significantly reducing HIV-related morbidity and mortality, several limitations and concerns regarding continuous cART treatment arose. In the early 2000s, comorbidity, pill burden and adverse drug effects with cART were common reasons why infected patients would switch drug regimens or pause therapy within the first year of treatment despite the increased risk of viral rebound and progression to AIDS. This regimen change or pause in therapy often led to reduced retention rates of long-term suppression with cART, and increased the risk of drug resistance mutations⁹⁸⁻¹⁰⁰. Although modern cART regimens have seen drastic improvements in drug adherence due to greater tolerability and decreased pill burdens to once daily treatment regimens, there is considerable interest in developing novel therapeutic strategies that would lead to cART-free remission. Furthermore, access to daily cART remains a significant issue for infected individuals living in regions of the world without adequate healthcare and economic resources.

Studies that have tested the clinical benefits of cART interruption are known as analytical treatment interruptions (ATI). ATIs have been an invaluable method in understanding the immune dynamics and viral kinetics that occur upon cessation of cART. From 2000-2006, ATI clinical trials assessed the clinical benefits and risks associated with cART cessation in chronically infected individuals. Participants underwent weeks to months of ATI with periodic sampling of plasma viral load levels,

CD4+ T cell counts, as well as other markers of immune activation. “Drug holidays” were also prescribed, allowing participants to pause cART during weekends or holidays in order to improve quality of life, decrease cART toxicity, and reduce the emergence of drug-resistant variants¹⁰¹.

In 2006, concerns regarding metabolic and cardiovascular complications during continuous, long-term cART in chronically infected participants were assessed in studies utilizing episodic cART regimens in the Strategies for Management of Antiretroviral Therapy (SMART) trial¹⁰². In the SMART trial, treatment interruption was guided by CD4+ T cell counts and primary endpoints included increased development of opportunistic disease or death from any cause with secondary endpoints being major cardiovascular, renal, and hepatic disease. Ultimately, the SMART trial did not reduce the risk of adverse events previously associated with continuous cART treatment, nor did it boost host immune responses in the face of active viral replication. Instead, participants saw a significant increase in the risk of opportunistic infections and death, as well as an increased risk to multidrug resistance. These concerns led to a brief halt in prolonged cART interruption methods in future clinical trials.

Other studies have considered the time to cART initiation as a potential variable affecting rebound kinetics and dynamics. Retrospective ATI studies on patients treated with cART at the time of primary HIV-1 infection identified a 15.6% frequency of post-treatment controllers (PTCs) in acutely-treated patients, marked by sustained viral suppression and significantly slower decline in CD4+ T cell counts after cART discontinuation, vs. <0.5% in other patient cohorts⁸⁹. While mechanisms of viral control in acutely-treated PTCs is unclear, early cART initiation is thought to have significantly

decreased the initial size of the viral reservoir, as well as preserve the capacity to develop potent anti-HIV-1 specific host immune responses during ATI. Interestingly, studies investigating rebound viral dynamics in individuals who began cART during acute infection show no further delay in viral rebound than those who began cART during chronic infection¹⁰³.

Additional work assessing functional cure strategies with broadly neutralizing antibodies in chronically infected patients have also relied on ATI methods as a means of assessing the potency of bNabs on reducing the viral reservoir. While time to viral rebound was significantly delayed compared to historical controls without bNAb intervention, the size of the reservoir pre- and post-ATI and VRC01 infusion did not change. These studies emphasize the importance of ATI methods in delineating latent reservoir dynamics and viral diversity and establish that brief, closely monitored ATIs are safe and well tolerated in chronically infected patient populations.

While significant efforts have been made to develop immunotherapeutics that target and eradicate latently infected cells in chronically infected patients, the viral and host immune dynamics that occur during ATI is still not completely understood. Therapeutic efficacy of these novel treatment strategies is typically assessed by significant delays in the time to viral rebound compared to previously conducted ATI trials in the absence of therapeutic intervention (21 days post-ATI), but provides no information on the total size or diversity of the reservoir. Others have used quantitative methods to determine the size of the latent reservoir through HIV DNA and RNA analyses from PBMCs, but due to the large portion of defective virions, these measures provide a vast overestimation of the reservoir. Recently, single genome sequencing methods (SGS) of plasma viruses

that arise at first detectable rebound provide a critical, but minimal snapshot of the diversity of the latent reservoir (described in Chapter 2 of this thesis). For SGS, cDNA derived from plasma vRNA is serially diluted to 1 copy per reaction, followed by direct amplicon sequencing to preclude *in vitro* recombination and nucleotide misincorporation errors mediated by Taq-polymerase. In contrast to bulk PCR methods, SGS allows for the genetic inference of a single viral template rather than a composite of the sequences comprising a major fraction of the viral quasispecies. Through SGS, one can identify minority viral variants as well as linkage of mutations on the same genome^{85,99,104}. These robust sequencing methods can also be utilized in *ex vivo* quantitative viral outgrowth assays (QVOA) in order to determine the composition of the viral reservoir while the infected participant is cART-suppressed (described in Chapter 4 of this thesis). While the QVOA assay provides valuable quantitative and qualitative information about the replication reservoir in cART-suppressed participants, the assay itself is extremely labor and material intensive, requiring millions of resting CD4+ T cells per assay. Furthermore, when QVOA output is assessed by phylogenetic analyses with rebound and pre-cART viruses, in the majority of infected participants, QVOA viruses form distinct lineages and are not predictive of lineages that arise *in vivo* during treatment interruption. These findings highlight that reservoir analyses by QVOA only provides a minimal snapshot of the replication-competent viruses under cART.

Goals of this thesis

In this thesis, I address several key unanswered questions related to the viral and immune dynamics that occur during ATI in two previously conducted clinical trials in chronically infected participants suppressed with cART. First, I investigated the kinetics and diversity of viral rebound using single genome sequencing methods and maximum

likelihood phylogenetic trees on plasma samples archived from first detectable rebound. I hypothesized that sequence analyses would reveal multiple low-diversity lineages that would evolve over the course of treatment interruption. With access to longitudinal ATI samples, I found that rebound arises with 2 to more than 8 distinct clonal lineages, and in the majority of participants, select lineages will either persist or clear over subsequent ATI time points. Using autologous plasma from contemporaneous and subsequent rebound time points, I found that the autologous antibody response generated during rebound exerts antibody pressure on specific rebound variants and this pressure is associated with the clearance of these lineages at later time points (Chapter 2). Second, our lab led the virologic studies in the ACTG Clinical Trial, A5340. Here, I assessed whether the broadly neutralizing antibody, VRC01, was able to exert additional immune pressure on the latent reservoir during ATI. I hypothesized that VRC01 would delay the time to first detectable rebound and select for VRC01 resistant variants (Chapter 3). Through analyses of available pre-cART and rebound viruses from chronically infected participants in this study, I found that there was an increased prevalence of VRC01 resistance, and this resistance led to only modest delays of viral rebound compared to historic ATI controls. Additionally, through phylogenetic analyses, I determined that VRC01 restricted the clonality of rebounding viruses, where highly resistant participants had polyclonal rebound lineages, while participants with pre-circulating pre-cART viruses with variable VRC01 resistance had monoclonal or oligoclonal rebound upon treatment interruption and VRC01 infusion. Finally, with access to archived leukapheresis samples from A5340, I asked whether ex vivo replication competent latent reservoir viruses could predict the clonality of viruses that rebounded in vivo during ATI (Chapter 4). I hypothesized that sequence analyses would reveal that brief ATI would not lead to the expansion of the viral reservoir. Quantitative and qualitative analyses of pre- and post-

trial infected resting CD4+ T reveal that the size of the reservoir does not change upon ATI, nor does it significantly alter the composition of replication-competent viruses in the majority of chronically infected participants. Interestingly, through these analyses, I also identified large, expanded clonal populations of viruses derived by QVOA and proviral DNA sequencing. In participants where the majority of latent viruses represented a single expanded clone, I did not find identical sequences from these clones in the rebound viral quasispecies. Furthermore, I found that while these expanded clones did not harbor increased VRC01 sensitivity, they have increased sensitivity to autologous antibodies compared to rebound viruses, suggesting autologous antibodies are able to exert some immune pressure from select latent viruses. Collectively, these data suggest that multiple latently infected cells are able to reactivate in vivo to establish viral rebound in chronically infected participants. The diversity of the rebounding viral quasispecies, however, is influenced by autologous antibodies and additional immune pressures exerted by infused broadly neutralizing antibodies. Pre-existing resistance to the antibody response may affect the ability of these variants to persist over subsequent viral rebound time points. Additionally, through the assessment of pre- and post-trial latent, pre-cART and rebound viruses from the A5340 clinical trial, I conclude that brief, closely monitored ATIs are safe and well tolerated, and do not lead to severe clinical risks or expansion of the viral reservoir as observed in previously conducted historic ATI trials.

References

1. Barre-Sinoussi, F. *et al.* Isolation of a T-lymphotropic retrovirus from a patient at risk for acquired immune deficiency syndrome (AIDS). *Science* **220**, 868–871 (1983).
2. Global HIV & AIDS statistics — 2018 fact sheet. Available at: <http://www.unaids.org/en/resources/fact-sheet>. (Accessed: 23rd August 2018)
3. Gallo, R. C. *et al.* Frequent detection and isolation of cytopathic retroviruses (HTLV-III) from patients with AIDS and at risk for AIDS. *Science* **224**, 500–503 (1984).
4. Popovic, M., Sarngadharan, M. G., Read, E. & Gallo, R. C. Detection, isolation, and continuous production of cytopathic retroviruses (HTLV-III) from patients with AIDS and pre-AIDS. *Science* **224**, 497–500 (1984).
5. Sharp, P. M. & Hahn, B. H. Origins of HIV and the AIDS Pandemic. *Cold Spring Harb Perspect Med* **1**, (2011).
6. Hahn, B. H., Shaw, G. M., De, K. M., Cock & Sharp, P. M. AIDS as a Zoonosis: Scientific and Public Health Implications. *Science* **287**, 607–614 (2000).
7. Korber, B. *et al.* Timing the ancestor of the HIV-1 pandemic strains. *Science* **288**, 1789–1796 (2000).
8. Worobey, M. *et al.* Direct evidence of extensive diversity of HIV-1 in Kinshasa by 1960. *Nature* **455**, 661–664 (2008).
9. Desrosiers, R. C. & Letvin, N. L. Animal Models for Acquired Immunodeficiency Syndrome. *Rev Infect Dis* **9**, 438–446 (1987).
10. Watts, J. M. *et al.* Architecture and secondary structure of an entire HIV-1 RNA genome. *Nature* **460**, 711–716 (2009).
11. Johnson, W. E. & Desrosiers, R. C. Viral Persistence: HIV's Strategies of Immune System Evasion. *Annu. Rev. Med.* **53**, 499–518 (2002).
12. Zanini, F. & Neher, R. A. Quantifying Selection against Synonymous Mutations in HIV-1 env Evolution. *Journal of Virology* **87**, 11843–11850 (2013).
13. Mohammadi, P. *et al.* 24 Hours in the Life of HIV-1 in a T Cell Line. *PLOS Pathogens* **9**, e1003161 (2013).
14. Mohammadi, P. *et al.* Dynamics of HIV Latency and Reactivation in a Primary CD4+ T Cell Model. *PLOS Pathogens* **10**, e1004156 (2014).
15. Wei, X. *et al.* Viral dynamics in human immunodeficiency virus type 1 infection. *Nature* **373**, 117–122 (1995).

16. Coffin, J. M. HIV population dynamics in vivo: implications for genetic variation, pathogenesis, and therapy. *Science* **267**, 483–489 (1995).
17. Kati, W. M., Johnson, K. A., Jerva, L. F. & Anderson, K. S. Mechanism and fidelity of HIV reverse transcriptase. *J. Biol. Chem.* **267**, 25988–25997 (1992).
18. Perelson, A. S., Neumann, A. U., Markowitz, M., Leonard, J. M. & Ho, D. D. HIV-1 dynamics in vivo: virion clearance rate, infected cell life-span, and viral generation time. *Science* **271**, 1582–1586 (1996).
19. Ho, Y.-C. *et al.* Replication-Competent Noninduced Proviruses in the Latent Reservoir Increase Barrier to HIV-1 Cure. *Cell* **155**, 540–551 (2013).
20. Shattock, R. J. & Moore, J. P. Inhibiting sexual transmission of HIV-1 infection. *Nature Reviews Microbiology* **1**, 25–34 (2003).
21. Shaw, G. M. & Hunter, E. HIV transmission. *Cold Spring Harb Perspect Med* **2**, (2012).
22. Gaines, H., von Sydow, M., Pehrson, P. O. & Lundbegh, P. Clinical picture of primary HIV infection presenting as a glandular-fever-like illness. *BMJ* **297**, 1363–1368 (1988).
23. Schacker, T. Clinical and Epidemiologic Features of Primary HIV Infection. *Annals of Internal Medicine* **125**, 257 (1996).
24. Little, S. J., McLean, A. R., Spina, C. A., Richman, D. D. & Havlir, D. V. Viral Dynamics of Acute HIV-1 Infection. *Journal of Experimental Medicine* **190**, 841–850 (1999).
25. Lindbäck, S. *et al.* Viral dynamics in primary HIV-1 infection. Karolinska Institutet Primary HIV Infection Study Group. *AIDS* **14**, 2283–2291 (2000).
26. Clark, S. J. *et al.* High titers of cytopathic virus in plasma of patients with symptomatic primary HIV-1 infection. *N. Engl. J. Med.* **324**, 954–960 (1991).
27. Fiebig, E. W. *et al.* Dynamics of HIV viremia and antibody seroconversion in plasma donors: implications for diagnosis and staging of primary HIV infection. *AIDS* **17**, 1871 (2003).
28. Robb, M. L. *et al.* Prospective Study of Acute HIV-1 Infection in Adults in East Africa and Thailand. <https://doi.org/10.1056/NEJMoa1508952> (2016). doi:10.1056/NEJMoa1508952
29. Moore, P. L., Gray, E. S. & Morris, L. Specificity of the autologous neutralizing antibody response. *Curr Opin HIV AIDS* **4**, 358–363 (2009).

30. Bunnik, E. M., Pisas, L., Nuenen, A. C. van & Schuitemaker, H. Autologous Neutralizing Humoral Immunity and Evolution of the Viral Envelope in the Course of Subtype B Human Immunodeficiency Virus Type 1 Infection. *Journal of Virology* **82**, 7932–7941 (2008).
31. Davis, K. L. *et al.* High titer HIV-1 V3-specific antibodies with broad reactivity but low neutralizing potency in acute infection and following vaccination. *Virology* **387**, 414–426 (2009).
32. Wei, X. *et al.* Antibody neutralization and escape by HIV-1. *Nature* **422**, 307–312 (2003).
33. Ho, D. D. *et al.* Rapid turnover of plasma virions and CD4 lymphocytes in HIV-1 infection. *Nature* **373**, 123–126 (1995).
34. Coffin, J. & Swanstrom, R. HIV Pathogenesis: Dynamics and Genetics of Viral Populations and Infected Cells. *Cold Spring Harbor Perspectives in Medicine* **3**, (2013).
35. Moir, S., Chun, T.-W. & Fauci, A. S. Pathogenic Mechanisms of HIV Disease. *Annual Review of Pathology: Mechanisms of Disease* **6**, 223–248 (2011).
36. Lackner, A. A., Lederman, M. M. & Rodriguez, B. HIV Pathogenesis: The Host. *Cold Spring Harbor Perspectives in Medicine* **2**, (2012).
37. Fauci, A. S. The human immunodeficiency virus: infectivity and mechanisms of pathogenesis. *Science* **239**, 617–622 (1988).
38. Bar, K. J. *et al.* Early Low-Titer Neutralizing Antibodies Impede HIV-1 Replication and Select for Virus Escape. *PLOS Pathogens* **8**, e1002721 (2012).
39. Keele, B. F. *et al.* Identification and characterization of transmitted and early founder virus envelopes in primary HIV-1 infection. *PNAS* **105**, 7552–7557 (2008).
40. Poss, M. & Overbaugh, J. Variants from the diverse virus population identified at seroconversion of a clade A human immunodeficiency virus type 1-infected woman have distinct biological properties. *J. Virol.* **73**, 5255–5264 (1999).
41. Iyer, S. S. *et al.* Resistance to type 1 interferons is a major determinant of HIV-1 transmission fitness. *PNAS* **114**, E590–E599 (2017).
42. Kariuki, S. M., Selhorst, P., Ariën, K. K. & Dorfman, J. R. The HIV-1 transmission bottleneck. *Retrovirology* **14**, 22 (2017).
43. Joseph, S. B., Swanstrom, R., Kashuba, A. D. M. & Cohen, M. S. Bottlenecks in HIV-1 transmission: insights from the study of founder viruses. *Nat Rev Microbiol* **13**, 414–425 (2015).
44. Tomaras, G. D. *et al.* Initial B-cell responses to transmitted human immunodeficiency virus type 1: virion-binding immunoglobulin M (IgM) and IgG

antibodies followed by plasma anti-gp41 antibodies with ineffective control of initial viremia. *J. Virol.* **82**, 12449–12463 (2008).

45. Lee, F.-H. *et al.* Breakthrough Virus Neutralization Resistance as a Correlate of Protection in a Nonhuman Primate Heterologous Simian Immunodeficiency Virus Vaccine Challenge Study. *Journal of Virology* **89**, 12388–12400 (2015).

46. Slatkin, M. & Maddison, W. P. A cladistic measure of gene flow inferred from the phylogenies of alleles. *Genetics* **123**, 603–613 (1989).

47. Moog, C., Fleury, H. J., Pellegrin, I., Kirn, A. & Aubertin, A. M. Autologous and heterologous neutralizing antibody responses following initial seroconversion in human immunodeficiency virus type 1-infected individuals. *Journal of Virology* **71**, 3734–3741 (1997).

48. Crooks, E. T. *et al.* Vaccine-Elicited Tier 2 HIV-1 Neutralizing Antibodies Bind to Quaternary Epitopes Involving Glycan-Deficient Patches Proximal to the CD4 Binding Site. *PLOS Pathogens* **11**, e1004932 (2015).

49. Rompay, V. *et al.* Passive Immunization of Newborn Rhesus Macaques Prevents Oral Simian Immunodeficiency Virus Infection. *J Infect Dis* **177**, 1247–1259 (1998).

50. Mascola, J. R. *et al.* Protection of Macaques against Pathogenic Simian/Human Immunodeficiency Virus 89.6PD by Passive Transfer of Neutralizing Antibodies. *Journal of Virology* **73**, 4009–4018 (1999).

51. Baba, T. W. *et al.* Human neutralizing monoclonal antibodies of the IgG1 subtype protect against mucosal simian–human immunodeficiency virus infection. *Nature Medicine* **6**, 200–206 (2000).

52. Parren, P. W. H. I. *et al.* Antibody Protects Macaques against Vaginal Challenge with a Pathogenic R5 Simian/Human Immunodeficiency Virus at Serum Levels Giving Complete Neutralization In Vitro. *Journal of Virology* **75**, 8340–8347 (2001).

53. Scheid, J. F. *et al.* Sequence and Structural Convergence of Broad and Potent HIV Antibodies That Mimic CD4 Binding. *Science* **333**, 1633–1637 (2011).

54. Scheid, J. F. *et al.* Broad diversity of neutralizing antibodies isolated from memory B cells in HIV-infected individuals. *Nature* **458**, 636–640 (2009).

55. Simek, M. D. *et al.* Human immunodeficiency virus type 1 elite neutralizers: individuals with broad and potent neutralizing activity identified by using a high-throughput neutralization assay together with an analytical selection algorithm. *J. Virol.* **83**, 7337–7348 (2009).

56. Lynch, R. M. *et al.* The Development of CD4 Binding Site Antibodies during HIV-1 Infection. *Journal of Virology* **86**, 7588–7595 (2012).

57. Caskey, M. *et al.* 3BNC117 a Broadly Neutralizing Antibody Suppresses Viremia in HIV-1-Infected Humans. *Nature* **522**, 487–491 (2015).
58. Horwitz, J. A. *et al.* Non-neutralizing Antibodies Alter the Course of HIV-1 Infection In Vivo. *Cell* **170**, 637-648.e10 (2017).
59. Bournazos, S. *et al.* Broadly neutralizing anti-HIV-1 antibodies require Fc effector functions for in vivo activity. *Cell* **158**, 1243–1253 (2014).
60. Huber, M. *et al.* Complement Lysis Activity in Autologous Plasma Is Associated with Lower Viral Loads during the Acute Phase of HIV-1 Infection. *PLOS Medicine* **3**, e441 (2006).
61. Baum, L. L. *et al.* HIV-1 gp120-specific antibody-dependent cell-mediated cytotoxicity correlates with rate of disease progression. *J. Immunol.* **157**, 2168–2173 (1996).
62. Forthal, D. N., Landucci, G. & Daar, E. S. Antibody from Patients with Acute Human Immunodeficiency Virus (HIV) Infection Inhibits Primary Strains of HIV Type 1 in the Presence of Natural-Killer Effector Cells. *Journal of Virology* **75**, 6953–6961 (2001).
63. Forthal, D. N. *et al.* Rhesus Macaque Polyclonal and Monoclonal Antibodies Inhibit Simian Immunodeficiency Virus in the Presence of Human or Autologous Rhesus Effector Cells. *Journal of Virology* **80**, 9217–9225 (2006).
64. Yates, N. L. *et al.* Vaccine-Induced Env V1-V2 IgG3 Correlates with Lower HIV-1 Infection Risk and Declines Soon After Vaccination. *Science Translational Medicine* **6**, 228ra39-228ra39 (2014).
65. Schroeder, H. W. & Cavacini, L. Structure and Function of Immunoglobulins. *J Allergy Clin Immunol* **125**, S41–S52 (2010).
66. Rerks-Ngarm, S. *et al.* Vaccination with ALVAC and AIDSVAX to Prevent HIV-1 Infection in Thailand. *New England Journal of Medicine* **361**, 2209–2220 (2009).
67. Chung, A. W. *et al.* Dissecting polyclonal vaccine-induced humoral immunity against HIV using Systems Serology. *Cell* **163**, 988–998 (2015).
68. Fletcher, C. V. *et al.* Persistent HIV-1 replication is associated with lower antiretroviral drug concentrations in lymphatic tissues. *PNAS* **111**, 2307–2312 (2014).
69. Persaud, D. *et al.* Continued production of drug-sensitive human immunodeficiency virus type 1 in children on combination antiretroviral therapy who have undetectable viral loads. *J. Virol.* **78**, 968–979 (2004).
70. Bracq, L., Xie, M., Benichou, S. & Bouchet, J. Mechanisms for Cell-to-Cell Transmission of HIV-1. *Front Immunol* **9**, (2018).

71. Sigal, A. *et al.* Cell-to-cell spread of HIV permits ongoing replication despite antiretroviral therapy. *Nature* **477**, 95–98 (2011).
72. Chomont, N. *et al.* HIV reservoir size and persistence are driven by T cell survival and homeostatic proliferation. *Nat. Med.* **15**, 893–900 (2009).
73. Joos, B. *et al.* HIV rebounds from latently infected cells, rather than from continuing low-level replication. *Proc Natl Acad Sci U S A* **105**, 16725–16730 (2008).
74. Lee, G. Q. *et al.* Clonal expansion of genome-intact HIV-1 in functionally polarized Th1 CD4+ T cells. *J Clin Invest* **127**, 2689–2696
75. Salantes, D. B. *et al.* HIV-1 latent reservoir size and diversity are stable following brief treatment interruption. (2018). doi:10.1172/JCI120194
76. Simonetti, F. R. *et al.* Clonally expanded CD4+ T cells can produce infectious HIV-1 in vivo. *Proc Natl Acad Sci U S A* **113**, 1883–1888 (2016).
77. Bui, J. K. *et al.* Proviruses with identical sequences comprise a large fraction of the replication-competent HIV reservoir. *PLOS Pathogens* **13**, e1006283 (2017).
78. Hosmane, N. N. *et al.* Proliferation of latently infected CD4+ T cells carrying replication-competent HIV-1: Potential role in latent reservoir dynamics. *J. Exp. Med.* **214**, 959–972 (2017).
79. Whitney, J. B. *et al.* Rapid Seeding of the Viral Reservoir Prior to SIV Viremia in Rhesus Monkeys. *Nature* **512**, 74–77 (2014).
80. Bourry, O. *et al.* Effect of a short-term HAART on SIV load in macaque tissues is dependent on time of initiation and antiviral diffusion. *Retrovirology* **7**, 78 (2010).
81. García-Lerma, J. G. *et al.* Intermittent Prophylaxis with Oral Truvada Protects Macaques from Rectal SHIV Infection. *Science Translational Medicine* **2**, 14ra4-14ra4 (2010).
82. Sultan, B., Benn, P. & Waters, L. Current perspectives in HIV post-exposure prophylaxis. *HIV AIDS (Auckl)* **6**, 147–158 (2014).
83. Chacko, L., Ford, N., Sbaiti, M. & Siddiqui, R. Adherence to HIV post-exposure prophylaxis in victims of sexual assault: a systematic review and meta-analysis. *Sex Transm Infect* **88**, 335–341 (2012).
84. Ford, N. *et al.* Adherence to HIV postexposure prophylaxis: a systematic review and meta-analysis. *AIDS* **28**, 2721–2727 (2014).
85. Lopker, M. J. *et al.* Derivation and Characterization of Pathogenic Transmitted/Founder Molecular Clones from Simian Immunodeficiency Virus SIVsmE660 and SIVmac251 following Mucosal Infection. *J Virol* **90**, 8435–8453 (2016).

86. Ribeiro, R. M. *et al.* Estimation of the initial viral growth rate and basic reproductive number during acute HIV-1 infection. *J. Virol.* **84**, 6096–6102 (2010).
87. Williams, K. C. & Burdo, T. H. HIV and SIV infection - the role of cellular restriction and immune responses in viral replication and pathogenesis. *APMIS* **117**, 400–412 (2009).
88. Kumar, N., Chahroudi, A. & Silvestri, G. Animal models to achieve an HIV cure. *Current Opinion in HIV and AIDS* **11**, 432 (2016).
89. Li, H. *et al.* Envelope residue 375 substitutions in simian–human immunodeficiency viruses enhance CD4 binding and replication in rhesus macaques. *Proc Natl Acad Sci U S A* **113**, E3413–E3422 (2016).
90. Sempowski, G. D. & Haynes, B. F. Immune reconstitution in patients with HIV infection. *Annu. Rev. Med.* **53**, 269–284 (2002).
91. Ghosn, J., Taiwo, B., Seedat, S., Autran, B. & Katlama, C. HIV. *The Lancet* **0**, (2018).
92. Current status and prospects of HIV treatment. *Current Opinion in Virology* **18**, 50–56 (2016).
93. Finzi, D. & Siliciano, R. F. Viral Dynamics in HIV-1 Infection. *Cell* **93**, 665–671 (1998).
94. Chun, T. W. *et al.* Quantification of latent tissue reservoirs and total body viral load in HIV-1 infection. *Nature* **387**, 183–188 (1997).
95. Palella, F. J. *et al.* Declining morbidity and mortality among patients with advanced human immunodeficiency virus infection. HIV Outpatient Study Investigators. *N. Engl. J. Med.* **338**, 853–860 (1998).
96. Finzi, D. *et al.* Latent infection of CD4+ T cells provides a mechanism for lifelong persistence of HIV-1, even in patients on effective combination therapy. *Nat. Med.* **5**, 512–517 (1999).
97. Deleage, C. *et al.* Impact of early cART in the gut during acute HIV infection. *JCI Insight* **1**, (2016).
98. Kousignian, I. *et al.* Maintaining antiretroviral therapy reduces the risk of AIDS-defining events in patients with uncontrolled viral replication and profound immunodeficiency. *Clin. Infect. Dis.* **46**, 296–304 (2008).
99. Palmer, S. *et al.* Multiple, Linked Human Immunodeficiency Virus Type 1 Drug Resistance Mutations in Treatment-Experienced Patients Are Missed by Standard Genotype Analysis. *Journal of Clinical Microbiology* **43**, 406–413 (2005).

100. Pougă, L. *et al.* New Resistance Mutations to Nucleoside Reverse Transcriptase Inhibitors at Codon 184 of HIV-1 Reverse Transcriptase (M184L and M184T). *Chemical Biology & Drug Design* doi:10.1111/cbdd.13378
101. 'Drug holidays' provide no benefits in HIV treatment. *Public Health Rep* **119**, 97 (2004).
102. Strategies for Management of Antiretroviral Therapy (SMART) Study Group *et al.* CD4+ count-guided interruption of antiretroviral treatment. *N. Engl. J. Med.* **355**, 2283–2296 (2006).
103. Stephenson, K. E. *et al.* Antibody Responses After Analytic Treatment Interruption in Human Immunodeficiency Virus-1-Infected Individuals on Early Initiated Antiretroviral Therapy. *Open Forum Infect Dis* **3**, (2016).
104. Salazar-Gonzalez, J. F. *et al.* Genetic identity, biological phenotype, and evolutionary pathways of transmitted/founder viruses in acute and early HIV-1 infection. *J Exp Med* **206**, 1273–1289 (2009).

CHAPTER 2

Autologous antibody responses drive viral diversity during rebound after analytical treatment interruption

D. Brenda Salantes, Ben Scheinfeld, Felicity Mampe, Tuhina Srivastava, Grant Eilers, Katherine Kerpen, Manolis Papasavvas, Luis Montaner and Katharine J. Bar

Abstract

Analytical treatment interruptions (ATI) in chronically infected, cART-suppressed participants provide a unique opportunity to assess the characteristics of viruses that emerge from the latent reservoir. This assessment of rebound viruses can be used to inform future therapeutic strategies aimed at reducing or clearing the reservoir to achieve cART-free HIV remission. Previous clinical trials utilizing ATI methods have determined that in the majority of participants, plasma viremia can be observed within 2-4 weeks of cART cessation, though the viral and immune dynamics that occur during this period are unclear. In this study, I used single genome sequencing methods (SGS) and neutralization assays on archived rebound plasma samples from a previously conducted ATI clinical trial to describe the genotypic and phenotypic characteristics of viruses that emerge from the latent reservoir. Consistent with recently published studies, I observe that first detectable viremia occurs within a median of 4 weeks post-ATI, and arises from multiple latently infected cells. Additional sequence analyses of longitudinal rebound time points also revealed that select rebound variants can either persist or clear from the viral quasispecies, and newly emerging, distinct viral variants can emerge over time. Of note, early rebounding viruses that were cleared at subsequent ATI time points were shown to have greater sensitivity to contemporaneous and longitudinal plasma. These data demonstrate that the autologous antibody response is able to exert selective immune pressure on viruses emerging from the reservoir, thus influencing the composition of the rebounding viral quasispecies.

Introduction

The primary barrier to HIV cure is the persistent latent reservoir. Combination antiretroviral therapy (cART) potently suppresses ongoing virus replication, but it does not eradicate latently infected cells. When cART is stopped, reactivating virus quickly reinitiates systemic replication in the vast majority of people living with HIV. Thus, the study of viral rebound allows a better understanding of the underlying latent reservoir and the impact of eradication strategies.

Studies involving viral rebound after an analytical treatment interruption (ATI) have been conducted for multiple reasons over the past 30 years. Early trials tested the immunologic and drug-sparing effects of relatively open-ended ATI, with CD4+ T cell counts and viral load thresholds used as cART restart criteria¹⁻³. These trials showed minimal immune enhancement as a result of rebound viremia in terms of clinical or immunologic outcomes. Further, extended periods of rebound viremia were associated with poorer clinical outcomes, including a significant increase in the risk of opportunistic infections and death, as well as an increased risk of developing multidrug resistance to cART¹. Collectively, these ATI studies show minimal immune enhancement from rebound viremia in terms of clinical or immunologic outcomes, resulting in reluctance to conduct clinical trials involving prolonged ATI. Recent studies of short, closely monitored treatment interruptions, in contrast, have provided reassurance that ATIs can be conducted safely, with little or no measured change to immune parameters or the size or composition of the latent reservoir after re-initiation of cART⁴⁻⁷. Moving forward, the ability to suppress or delay viral rebound remains a key goal of clinical trials of HIV

therapy and cure strategies. Thus, as novel treatment strategies targeting the latent reservoir have emerged, closely monitored analytical treatment interruptions (ATI) of cART are likely to remain critical components of HIV clinical trials.

Having access to clinical trial samples at the time of viral rebound also allows the unique opportunity to examine viruses that until very recently were part of the replication competent latent reservoir. Recent studies of viral rebound, including a human clinical trial of intensively monitored ATI by Rothenberger and colleagues, demonstrated that virus reactivates from multiple infected cells at sites throughout the body¹⁴. Studies sampling plasma virus weekly or bi-weekly support these findings, suggesting that initial plasma rebound virus is comprised of a diverse virus population that reactivated from multiple, genetically distinct, latently infected cells. Two reports regarding two independent ATI trials found that viruses arising during rebound were not identical to genetically intact or replication-competent viruses from the periphery^{15,16}. The viral kinetics of rebound in the days and weeks after initial viremia, however, are less well characterized. Further, the role of host immune responses in driving virus evolution in the days and weeks after durable cART suppression are unclear. As the field moves to test immunologically active interventions and other cure strategies within the context of ATI, the viral and immune parameters of rebound will become even more relevant.

Here, I performed in-depth analyses on the virus populations that rebound in participants undergoing a prolonged ATI in a previously conducted clinical trial⁸. Using single genome sequencing (SGS), phylogenetic analyses, and neutralization assays of Env pseudotypes against contemporaneous and longitudinal plasma, I found that the virus

populations circulating systemically during ATI substantially evolve over time and that autologous antibody responses are an important driver of that process.

Results

Participant characteristics

To evaluate the viral and immune kinetics of rebound, we studied samples from a previously conducted clinical trial that tested the effect of ATI in participants who initiated cART during chronic infection and had been durably virally suppressed on cART for at least six months (NCT00051818)⁸. The trial compared the effects of a single open-ended ATI for up to 47 weeks, and multiple-ATI with structured ATIs of 2, 4, 6, and 12 weeks in duration. The time to rebound, adverse events, viral setpoint pre and post-initiation of cART, immune parameters and effectiveness of resuppression on cART were examined. Results demonstrated no significant differences in clinical outcome between the two arms. For our analyses, we randomly selected participants (n=11 from the single ATI arm and n=2 from the multiple ATI arm) who experienced viral rebound to >1,000 copies/ml and for whom plasma samples were available. Demographic and clinical characteristics of the 13 participants of this study are described in Table 2.1. In summary, these 13 participants' characteristics were similar to the parental trial cohort, with a median age of 42 years (single-ATI) and 46 years (multiple-ATI); these participants were 80% male, 40% African-American, 40% Caucasian, 20% LatinX, and reported sexual HIV transmission. They had been on ART for a median of 4.5 years, with a median CD4 T cell count of 637 cells/mm³ (single-ATI) and 658 cells/mm³ (multiple-ATI) at enrollment. The participants were on ART regimens of either protease

inhibitors (n=6) or non-nucleosidase reverse transcription inhibitors (n=8) and two NRTIs. In the trial, participants stopped their ART and had plasma samples collected every two to five weeks.

Kinetics and clonality of viral rebound

Viral kinetics of rebound for the single ATI participants are shown in Figure 1. Participants were sampled every four to five weeks, and 10 of 11 had experienced viral rebound by week 4, consistent with other reports of time to rebound after ATI in the absence of any intervention^{2,5,7,14,17-19}. Plasma viral loads at week 4 post-ATI ranged from 834 to 26,468 copies/ml.

To estimate the number of virus-infected cells rebounding from latency to contribute to systemic rebound, we performed SGS of *env* on the plasma virus from first detectable viremia in eleven participants. Depending on plasma viral load, we performed either full gp160 *env* sequencing (n=9) or gp41 *env* (n=2). ML phylogenetic trees of *env* sequences are shown in Figure 2. Maximum within-participant genetic diversity at this time point ranged from 1.1% to 6.1%, reflecting the diverse virus populations comprising the latent reservoir in individuals initiating ART in chronic HIV infection. Within these diverse virus populations, discrete identical and low-diversity lineages can be discerned in multiple participants, reflecting clonal expansion from a recently reactivated virus-infected cell. To better understand early evolution during viral rebound, the mathematical model and Monte Carlo stimulation presented by Lee et al. can be used to distinguish between two unique variants^{8,9}. We estimate that the time to cART washout is approximately two weeks, and that immune selection events have not yet occurred during this period. Here, I used the conservative cut-off of 0.15% diversity (or ~3

nucleotides per gp160 env sequence) to discriminate between virus evolution during viral rebound vs. prior to ART initiation, and estimate the minimal number of virus populations contributing to systemic viral rebound. Further, when the total rebound viral quasispecies is analyzed together, the data fails to conform to a Poisson distribution, but when each lineage is examined independently, the Poisson distribution is maintained. Examining each of the participants, we find multiple genetically distinct virus populations establish rebound viremia with between 2 and more than 10 founder virus populations fitting independent Poisson distributions, with a median of distinct 5 populations in each participant. For example, Participant S25's (Fig 2A) viruses cluster in four genetically distinct lineages, suggesting rebound from at least four distinct virus-infected cells. Participant S21's viruses (Fig 2B) cluster into three distinct populations (two lineages with multiple closely related viruses, with diversity <0.15%), and a single genetically distinct sequence representing a less deeply sampled lineage. While these estimates have several important caveats, including the limited sampling depth and issues of recombination and APOBEC-mediated mutation, these results mirror those of other studies estimating the clonality of the rebounding virus population¹⁴⁻¹⁶. When I examined the relationship between time to rebound, viral clonality, and viral load at first detectable rebound in this single ATI cohort, I found no significant correlation between these variables (Spearman's rank correlation coefficient $p > 0.05$, Figure 2.3), suggesting that the number of founder viruses does not affect the timing or magnitude of viral rebound.

Rebound virus populations rapidly evolve over time and early dominant viruses are cleared

To assess changes in rebound diversity over time, we performed SGS of HIV-1 Env over the duration of up to 47 weeks of ATI in eight participants with available longitudinal sampling and analyzed each participant's sequences in ML phylogenetic trees (Figs 2.4). In all participants, total virus diversity increased (In participant S25, max diversity at first detectable rebound was 1.1% within 4 weeks of ATI vs. 11.9% within 47 weeks of ATI). Across the cohort, the increased diversification over time was driven by expansion of the initial virus populations sampled at first detectable rebound and the addition of new, genetically distinct lineages arising from continued reactivation from latency or the recombination of previously sampled lineages. Many of the virus lineages sample at first detectable rebound persisted over time, with identical or similar *env* sequences sampled at later time points. In the majority of participants, however, a substantial number of the rebound founder lineages (those sampled at first detectable rebound) were not sampled longitudinally, suggesting they were cleared from circulation or substantially reduced in relative frequency compared to other variants. For example, in Participant S53, the 4 lineages sampled at first detectable rebound (week 4 post-ATI, in black in Fig. 2.4B) are not sampled subsequently at weeks 8, 12 or 17 post-ATI. In a similar but more extreme example, participant S25 (Fig. 2.4D) had 5 genetically distinct lineages with a max diversity of 1.1% sampled at first detectable rebound. Four weeks later, all of these viruses were cleared, and a genetically distant virus population with a max diversity of 11.6% was sampled, which persisted for the next 30 weeks. To be sure sample mix-ups were not responsible for this extreme shift in virus populations, we performed mitochondrial sequencing of host DNA in each plasma sample, which confirmed the shared identity of these samples. In other participants, including S05 (Fig. 2.4A) and S60 (Fig. 2.4C), there was a mixed picture, with some initially sampled lineages persisting and others being cleared. In participant S05, plasma virus at 4 weeks post-ATI clustered

into 4 lineages; the most populous of these lineages (39% total sequences) is not sampled 6 weeks later, while the 3 relatively minor lineages persist, with identical or nearly identical viruses sampled at week 10. Of the seven participants with adequate longitudinal sampling, two participants had all initial lineages cleared by the next time point, four had most or the predominant lineage cleared by the next timepoint, while just one participant had the majority of lineages persist. With the caveats that limited sampling depth and recombination may account for some virus population shifts, these dramatic shifts in virus populations over the first weeks of rebound suggest a strong selective pressure against cleared viral lineages.

Autologous neutralizing antibody responses (nAb) drive virus population shifts during early rebound

While autologous nAbs have been shown to drive virus clearance in acute and early infection²⁰⁻²⁵, titers wane substantially during ART suppression²⁶. Thus, it is unclear whether they can drive viral clearance during early ATI and rebound. To test the hypothesis that autologous nAb responses have a role in shaping the rebound virus quasispecies, we generated Env pseudoviruses from the consensus of early rebound lineages that persisted or were cleared in participants S05, S60 and S53 and assessed their neutralization sensitivity to early ATI plasmas (see Fig 2.4 for cloned Envs).

Figure 2.5A and B display the autologous plasma nAb titers against virus lineages that were either cleared or persisted in these three participants. In participant S05, initial nAb titers at the time of first detectable rebound (week 4 post-ATI) are modest against the circulating rebound virus populations (titers between 1:200 and 1:400). By week 10,

when the cleared viruses are no longer sampled, the titers against the cleared viruses have markedly increased, while the titers against the lineage that persist remain modest. In participant S60, first sampled at week 5 post-ATI, titers against the viruses that will ultimately be cleared are already about 1 log higher than against those that persist; the increased titers against the cleared viruses remain higher through week 13. By week 17 post-ATI, 9 weeks since the cleared viruses were last sampled, the nAb response to the persisting lineages appear roughly similar. In participant S53, nAb titers increase more than 1 log between weeks 4 and 8, coincident with the clearance of the rebound founding virus populations. When the titers are compared at the time point in which the population shift occurred across the 3 participants, the autologous nAb responses were statistically greater against cleared than persistent viruses (Fig. 2.5C, median reciprocal IC50 titer 906 vs. 153, $p=0.0286$ by Wilcoxon/Mann-Whitney test).

To estimate the timing of the emergence of autologous nAb response during ATI, we tested the potency of plasma IgG prior to and during ATI in two participants. At least 1ml of pre-ATI plasma (timepoint 0) was heat inactivated and IgG was further purified from circulating cART through column isolation with the rProtein A/Protein G GraviTrap (GE Healthcare), followed by quantification with the Pierce BCA Protein Assay kit. IgG was then diluted to meet circulating IgG concentrations found in human plasma during cART suppression¹⁰ (see methods). In each participant, IgG increased in potency with the emergence of antigen in viral rebound (Fig. 2.5D). The quantity of IgG required to reach an IC50 against early rebounding variants was between 9-fold and 33-fold greater than total μg IgG required from contemporaneous plasma ($P=0.0079$, Wilcoxon/Mann-Whitney test), suggesting anti-HIV IgG responses are modestly present prior to viral rebound and rapidly amplify within the first weeks of viral rebound. Additionally, strain

specificity can also be observed in pre-ATI plasma, where persisting viral lineages had an IC₅₀ of >2000 µg/ml IgG, while cleared lineages were neutralized with 174 µg/ml to 1295 µg/ml of IgG.

Autologous nAb responses drive virus selection through sequential ATIs.

We next asked whether nAb responses would similarly drive rebound virus evolution in the participants undergoing multiple structured ATIs. I studied two participants who underwent three serial ATIs of 2, 4, 6 and 12 week intervals followed by brief periods of virus suppression with cART (Fig. 2.6A and C). In both participants, each ATI led to rapid viral rebound within 2-5 weeks. We generated gp160 *env* sequences via SGS for each participant using samples from the time of first detectable plasma viremia over 200 copies/milliliter. For participant S04, viruses from first detectable viremia in ATI timepoint 1 (ATI 1) clustered into six lineages (three major lineages and three genetically distinct single viruses, Fig. 2.6B). For participant S23, virus during ATI 1 did not rise over 200 copies; initial plasma rebound during ATI 2 was characterized by 7 lineages (Fig. 2.6D).

To determine the effects of nAbs on virus evolution, we examined the viruses that emerged during subsequent ATIs. A significant limitation to this analysis is the minimal time of ART suppression between each ATI time point. Because there was not enough time for the virus population to re-enter steady state latency¹¹, rebound virus during subsequent ATIs likely arose either from recently infected, short-lived cells or ongoing, low-level virus replication in the absence of long-term, durable ART suppression. We reasoned, therefore, that virus circulating during subsequent ATIs would be biased towards the virus populations reactivating during the initial ATI. What we found,

however, was that in both participants several of the initial virus populations were cleared. In S04, one of the three major and all three minor lineages failed to be sampled subsequently (Fig. 2.6B). Two of the original virus populations persisted and were sampled along with new distinct virus populations at subsequent ATI timepoints. In participant S23, three of seven initial lineages in ATI 2 were no longer sampled, while four others persisted through ATIs 3 and 4 (Fig. 2.6D). When representative viruses from persisting and cleared lineages from each participant were cloned and tested as pseudoviruses for sensitivity to autologous plasma (Fig. 2.6E), the cleared viruses had a trend towards higher autologous nAb titers than the persisting at ATI 2, meaning that the cleared viruses were more neutralization sensitive to paired contemporaneous autologous plasma than persisting viruses (IC₅₀ reciprocal plasma dilution for persisting lineages=208 versus cleared lineages=0.223, P= 0.200 by Wilcoxon/Mann-Whitney test). Thus, our results from multiple-ATI participants are consistent with our findings from the single-ATI participants.

Tables

	Single-ATI	Multiple-ATI
Male	81%	100%
Years on cART	4.5 (4, 6.7)	7 (6, 11)
CD4+ T cell count at recruitment (cells/mm ³) (median [25%, 85% quartiles])	637 (481, 793)	658 (506.5, 815.8)
Drug classes used at entry ^a		
PI	4/11	1/2
NNRTI	7/11	1/2

^A Numbers include cases of PINNRTI combined use at study entry
AA, African American; C, Caucasian; LX, LatinX; IV, Intravenous drug use; PI, protease inhibitor; NNRTI, non-nucleoside reverse transcriptase inhibitor; S, sexual transmission

Table 2.1 Single-ATI and multiple-ATI participant demographics

Figures

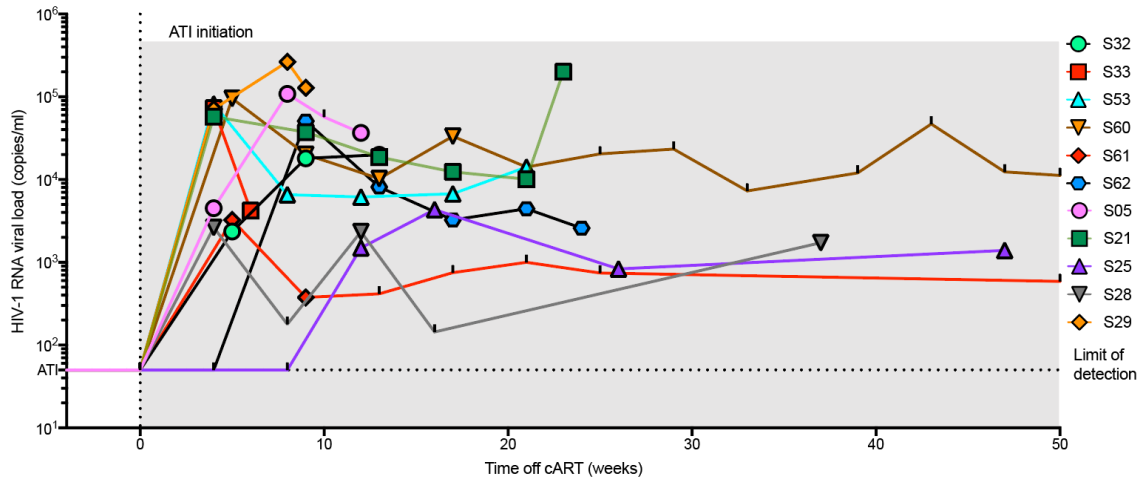


Figure 2.1 Kinetics of viral rebound from single-ATI participants

This graph displays measured plasma HIV-1 RNA viral loads from the nine participants who underwent single-ATI. Shapes represent time points in which archived plasma was available for single genome sequencing and neutralization assays. Tick marks represent time points where plasma was not available for analysis.

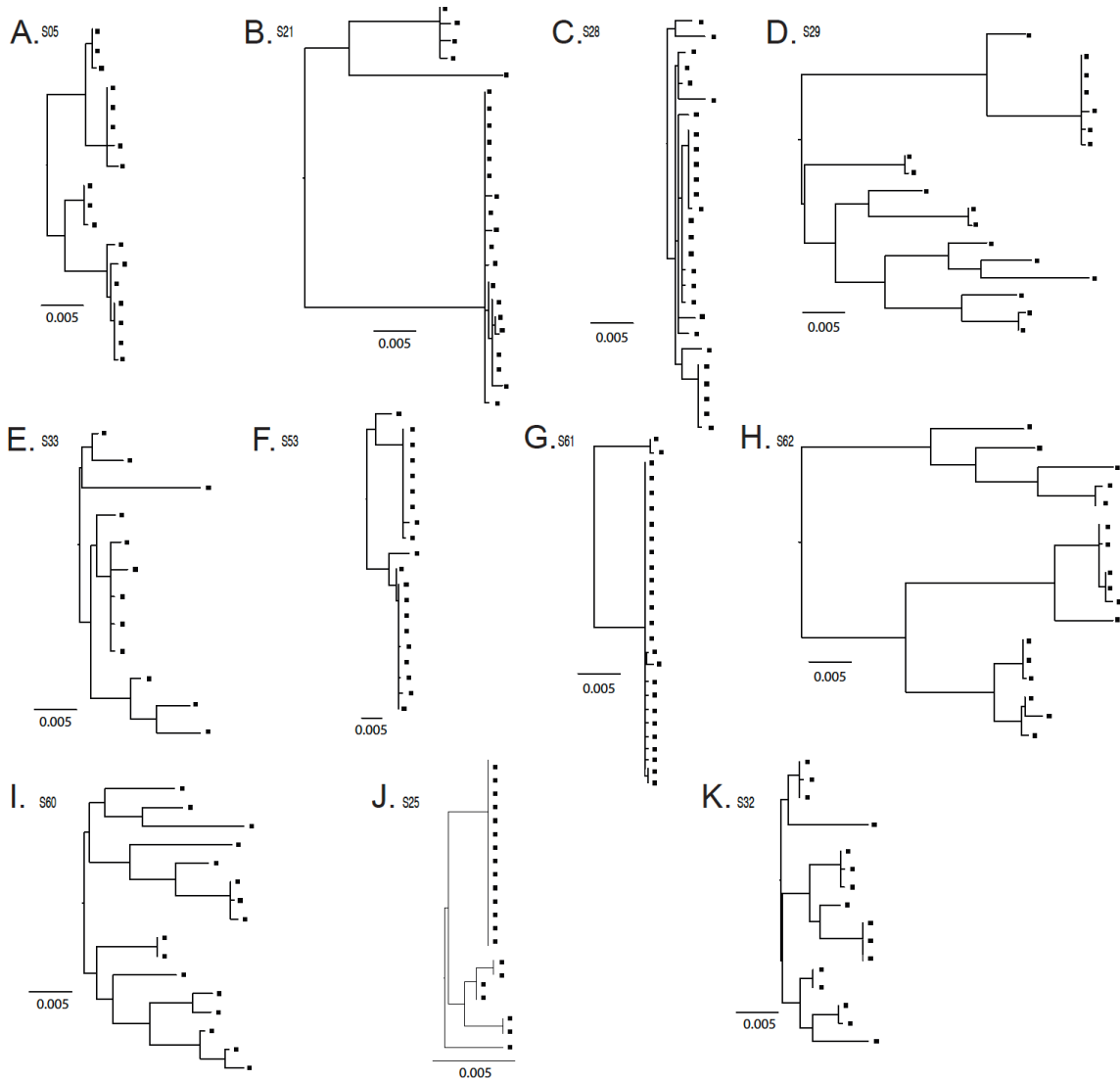


Figure 2.2 Maximum-likelihood phylogenetic trees of SGS-derived gp160 env or gp41 sequences from single-ATI participants (A-K: S05, S21, S28, S29, S33, S53, S61, S62, S60, S25 and S32). Env sequences from first detectable rebound are shown in black squares. Genetic distance is shown by the scale bar, indicating percent difference.

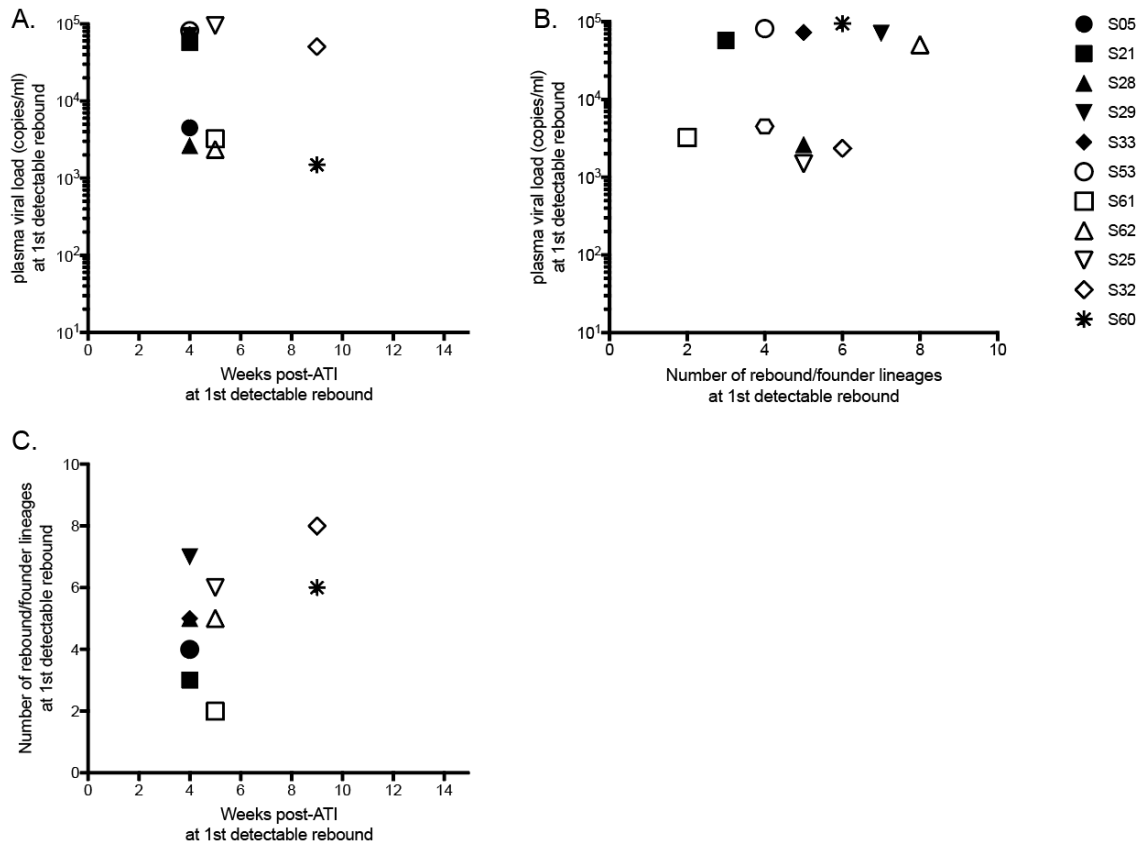


Figure 2.3 Correlations between viral load, the number of rebound/founder lineages, and weeks post-ATI at first detectable rebound. No correlation was observed in either measure, (A) $P=0.226$, (B) $P=0.81$, (C) $P=0.217$, as determined by Spearman's correlation coefficient.

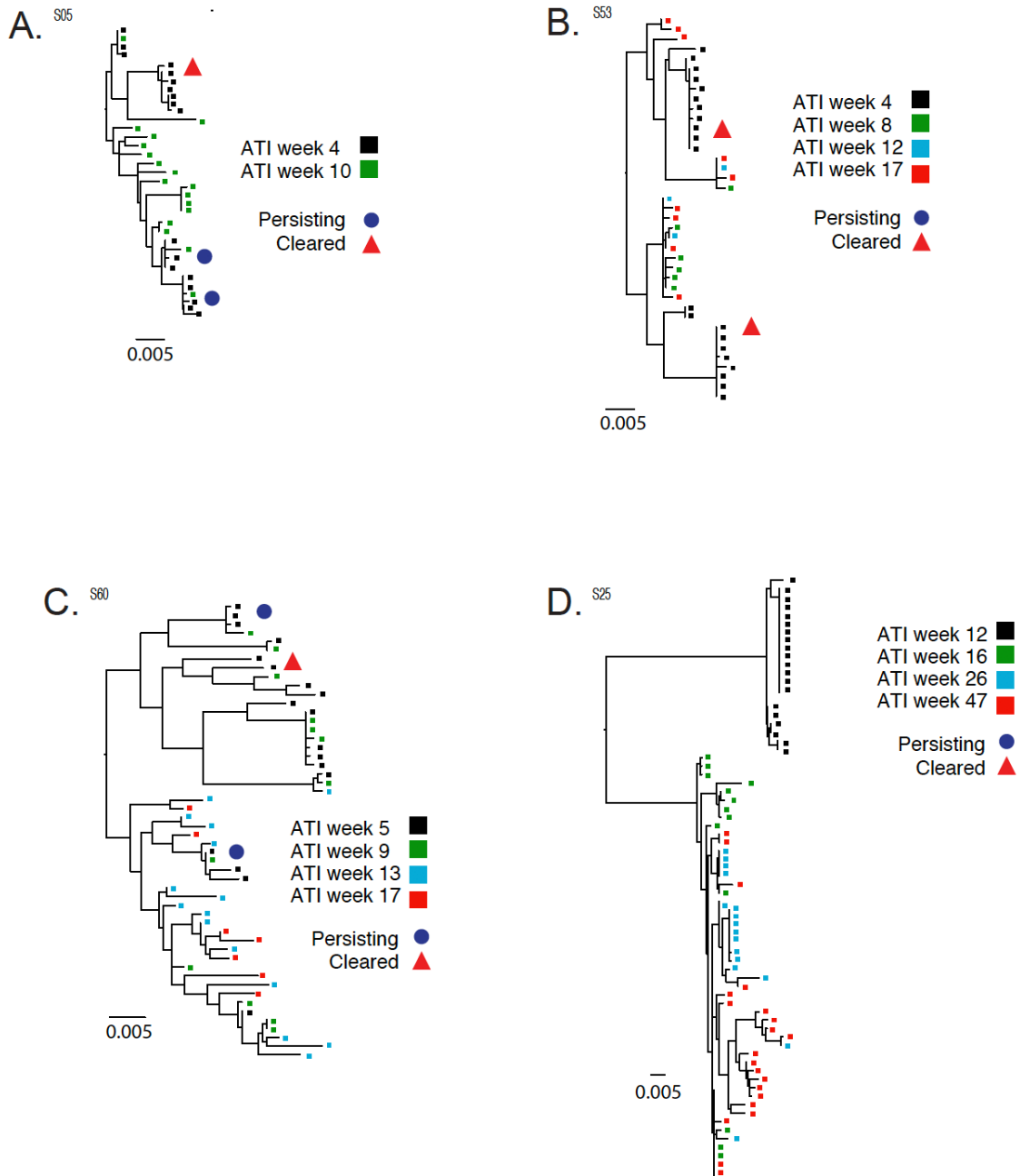


Figure 2.4 ML phylogenetic trees of SGS-derived HIV-1 gp160 or gp41 from longitudinal ATI time points Participants S05, S53, S60 and S25 shown above (A-D). Squares depict a single virus. Black, green, blue, and red depict viruses sequenced from first, second, third and fourth ATI time points, respectively. Blue circles (persisting lineages) and red triangles (cleared lineages) highlight first detectable rebound gp160 *envs* that were used for Env Pseudotype generation and neutralization analyses.

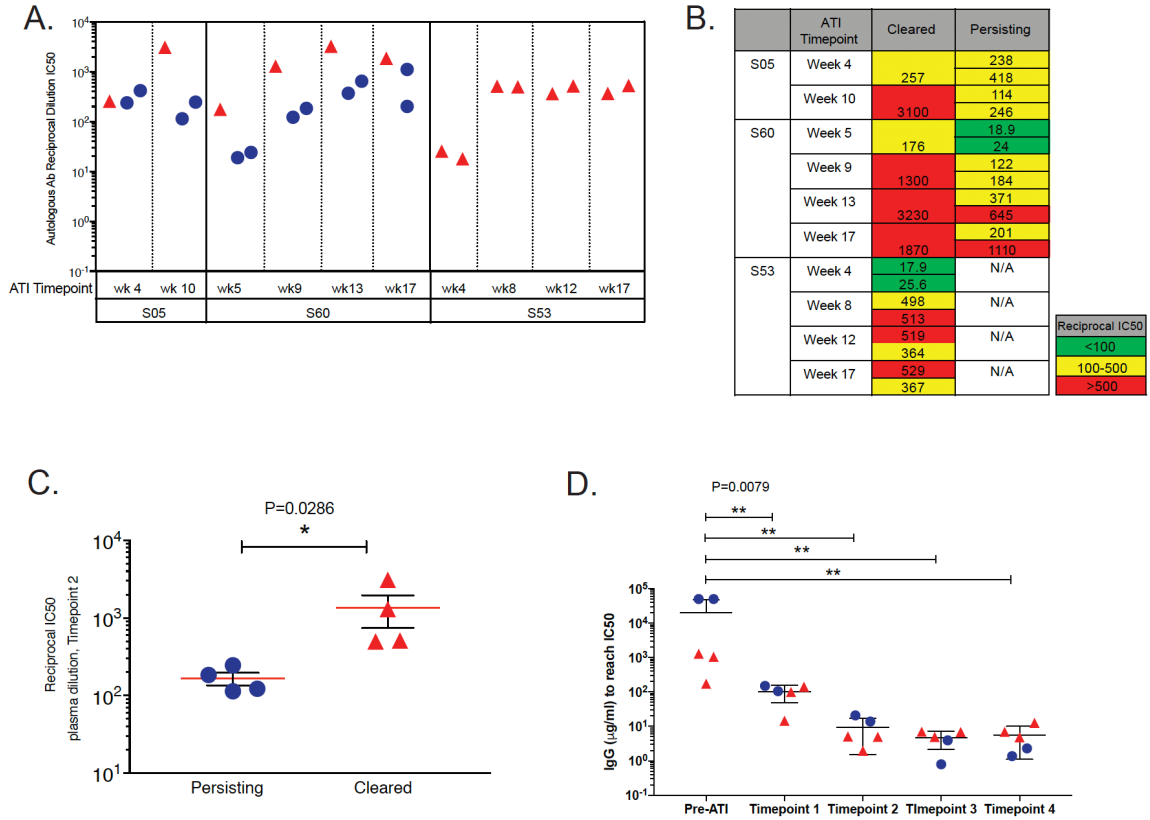


Figure 2.5 Strain-specific autologous antibodies develop during ATI. A. Participants S05, S60 and S53 have persisting (circle) and cleared (triangle) viruses with differing neutralization sensitivity to antibodies from contemporaneous and longitudinal ATI time points. B. Summary of IC50s. C. Isolated IgG from pre-ATI time points from participants S53 and S60 show neutralizing antibody responses develop during rebound. D. Total IgG required to reach IC50s against persisting and cleared viral lineages.

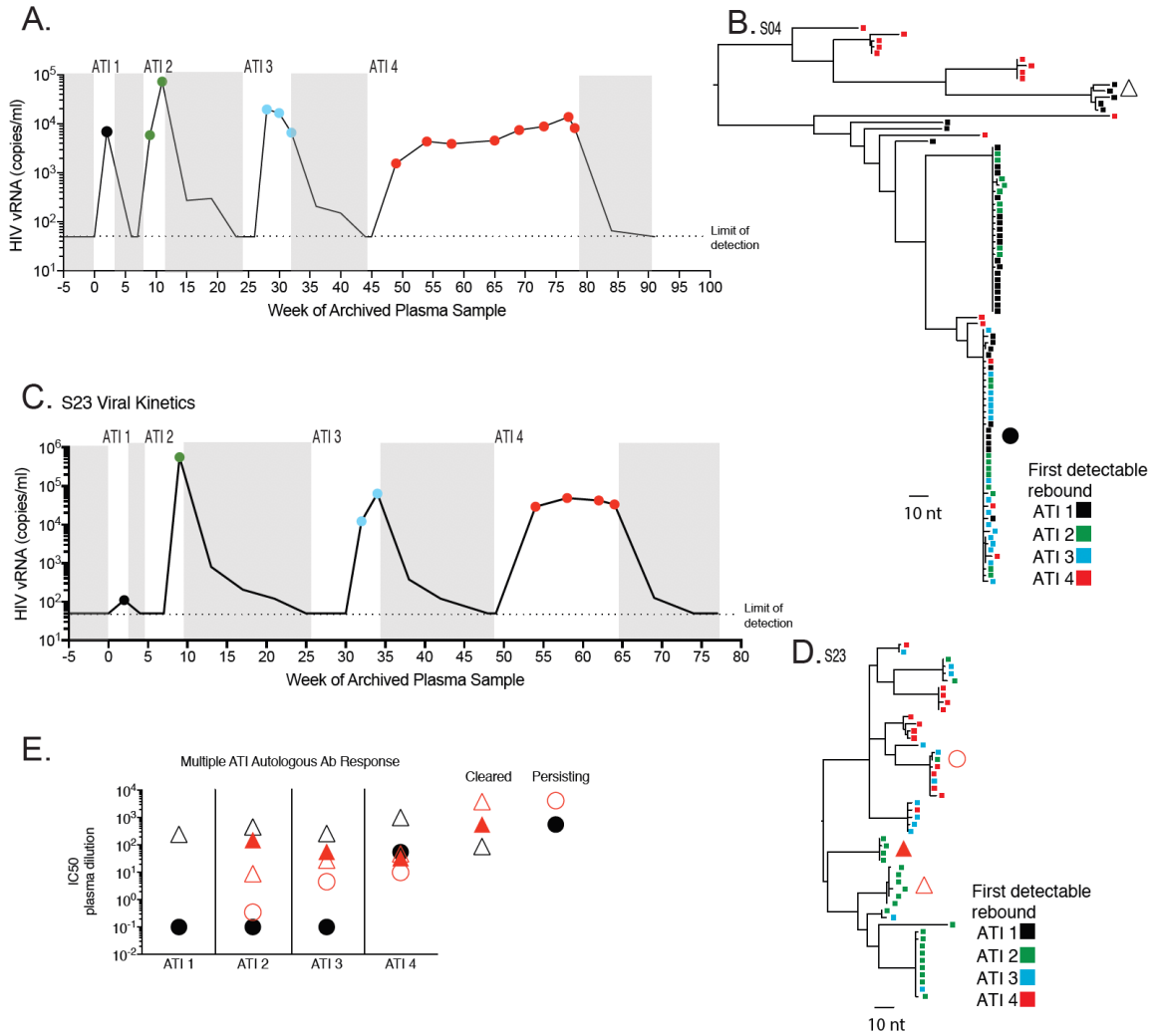


Figure 2.6 Viral kinetics, dynamics, and autologous antibody responses in multiple-ATI participants. Participant S04 shown in (A) and (B), participant S23 shown in (C), (D). (E) The autologous antibody response at first detectable rebound in ATI time points 1-4 displayed as reciprocal IC₅₀ plasma dilution. The HIV-1 Env variant cloned for neutralization assays can be found in each participant's respective phylogenetic tree, indicated as a triangle (cleared lineage) or circle (persisting lineage).

Discussion

While cART is effective at stopping ongoing virus replication, sustained viral suppression currently requires a lifetime of daily cART due to the persistence of latently infected cells. These cells are the target of novel therapeutics that aim to eradicate or suppress the latent reservoir to induce cART-free remission. Without a validated biomarker of the reservoir, however, ATIs are an important empiric test of the efficacy of suppressive or curative strategies against HIV. Many of these strategies engage the human immune system, making elucidation of the viral dynamics and host immune responses during ATI and rebound highly relevant.

Several parallels exist between the biology of HIV transmission and acute infection and that of viral rebound during ATI. In both scenarios, a viral inoculum initiates systemic infection and is met with innate and adaptive immune responses. In acute infection, the size of the inoculum¹²⁻¹⁵, and the timing of the ensuing innate¹⁶⁻¹⁹ and adaptive responses²⁰⁻²⁴ have been well characterized. Rebound after ATI has recently been shown in several human studies to follow reactivation of multiple viruses from multiple sites²⁵. The timing and magnitude of innate and adaptive immune responses, however, are not well characterized. The kinetics of adaptive immune responses, in particular, are highly relevant to the array of CTL and Ab-based therapeutics being currently developed.

Previous studies have shown that exhausted CD8+ T cells expand and CD4+ T cells decline with increased viral replication during primary infection²⁶ and viral rebound²,

suggesting a similar temporal association between antigen load and anti-HIV T cell responses. Additionally, upon initiation of cART in both groups, rapid reconstitution of lymphocytes, cytokines, chemokines and additional elevated inflammatory markers is observed, though these levels do not completely return to baseline levels²⁷⁻²⁹. Partial immune reconstitution can also be observed in participants who underwent multiple ATI strategies². Key differences between transmission and rebound include the number of variants that establish plasma viremia. During acute infection, 80% of mucosally transmitted variants are from a single transmitted founder virus (T/F) in HIV-1 clade B and clade C infections^{13,30}, while multiple genetically distinct variants establish viral rebound²⁵. Additionally, while increased titers of neutralizing antibodies against heterologous isolates were found at 8 weeks of ATI and were associated with lower viral loads during rebound, no analyses of strain-specific neutralization were measured³¹. Determining the kinetics and potency of the host antibody response against autologous viruses is pivotal to our understanding of viral rebound dynamics during ATI and could potentially provide an additional mechanism by which neutralization-sensitive latent viruses are unable to sustain systemic replication in the absence of cART.

Here, we used archived plasma samples from a previously conducted single-ATI and multiple-ATI clinical trial to assess the genotypic and phenotypic characteristics of the rebounding viral quasispecies. Consistent with previous ATI trials^{1,7,26,32,33}, we found that viral rebound occurs within 2-4 weeks of ATI (median 4 weeks) (Fig 1) while phylogenetic analyses of plasma viruses from this time point revealed a substantial increase in diversity (range, 1.1-6.07%) compared to the diversity of viral populations observed during acute infection (range, 0.08-0.47%)¹³, suggesting viral and host immune dynamics during rebound are distinct from early infection.

A hallmark of chronic HIV-1 infection is the expansive intra-patient genetic diversity driven by the accumulation of viral immune escape mutations as well as rapid and error-prone replication rates. While cART can reduce plasma viral loads to undetectable levels, infected cells with genetically distinct viruses can remain transcriptionally inactive until cART is removed, thus contributing to the overall diversity of the latent reservoir. In this study, we identified multiple genetically distinct viruses emerging from latency utilizing SGS methods on plasma viruses from first detectable rebound by identifying clonal viral lineages. The criteria we used to identify a clonal virus includes the base pair *in vivo* evolution rate of HIV-1 ($4.1\text{-}1.7 \times 10^{-3}$ per base per cell), multiplied by the length of gp160 (approximately 2,700 nucleotides) and gp41 (1,400 nucleotides). Using these criteria, we find that the maximum number of mutations allowed from the consensus viral sequence is 3.78 mutations, and 1.96 mutations respectively, accounting for minor PCR-induced *in vitro* errors. We identified 2 to more than 8 clonal lineages per participant at first detectable rebound, with evidence of recombinant viruses scattered throughout the phylogeny (6 of 11 participants). The accumulation of recombinant rebound viruses during ATI was recently described in an ATI trial with infusion of 3BNC117, a CD4 binding site broadly neutralizing antibody⁶. In this study, parent viruses were frequently found in the latent reservoir, but did not productively expand *in vivo*, suggesting that the increase in rebound virus diversity can be attributed to recombination events occurring with two or more distinct reservoir viruses upon cART cessation. While our analyses were limited to circulating plasma viruses, we identified multiple recombinant variants at first detectable rebound in addition to parent viral strains. These findings suggest that while recombination events may contribute to viral diversity, they are not the only factor guiding systemic virus replication during rebound.

We next assessed correlations between rebound viral diversity, viral loads, and time to first detectable rebound. According to our results, no significant correlation was observed between viral load and the number of clonal lineages at first detectable rebound ($P=0.226$), viral load and the number of weeks to first detectable rebound ($P=0.81$), or the number of weeks of detectable rebound and the number of clonal lineages ($P=0.217$) (measured by Spearman's correlation coefficient).

The genetic complexity of the viral reservoir in chronically infected individuals can be observed by sequence analyses of the viral quasispecies over longitudinal ATI time points. In eight participants with sufficient plasma samples for SGS analyses, we observe the emergence of multiple, genetically-distinct viruses throughout the course of ATI, as well as the persistence and clearance of select viral lineages. The viral rebound dynamics observed at baseline highlight how quickly the diversity of the viral quasispecies can accumulate in the absence of cART and significant selection pressures. This is in contrast to Bar et al.'s findings with ATI and VRC01 infusion, where VRC01 is able to exert potent selection pressure on pre-existing VRC01 sensitive variants, resulting in monoclonal/oligoclonal populations of VRC01-resistant rebound lineages³³. These data led us to investigate possible host-mediated mechanisms guiding the clearance of select viral lineages.

Neutralization sieve analysis from autologous antibodies can elucidate mechanistic correlates of immune protection by blocking the transmission of more sensitive viruses^{34–39}. While neutralization sieve analyses have been extensively studied in vaccine trials to identify viruses that establish “breakthrough” infections^{40–43}, the kinetics and potency of neutralizing antibodies that arise during ATI have not yet been characterized. Using

archived plasma samples and Env pseudotypes of consensus envs from cleared and persisting lineages, we asked whether autologous antibody responses generated at the time of virus reactivation implemented significant neutralization pressure on select lineages, thus preventing ongoing persistence at later ATI time points. In four out of nine participants, we found that cleared lineages had a 3.4-fold increase in sensitivity to autologous plasma (mean reciprocal plasma dilution=631.7, $P=0.0079$) (Fig. 2.5B). Isolated IgG from pre-ATI time points show up to a 33-fold increase in total μg IgG required to neutralize 50% of early rebounding variants, suggesting anti-HIV antibodies rapidly emerge shortly after viral rebound (Fig. 2.5D).

The viral and immune dynamics under multiple courses of ATI are unclear. In this study we assessed viral rebound and autologous antibody responses in two participants who participated in multiple ATIs conducted in 2, 4, 6 and 12 week intervals to determine whether autologous neutralizing antibodies prevent the persistence of rebound lineages over episodic ATI time points. While the brief periods of cART treatment of ATIs prevent an accurate analysis of viruses emerging from latency, similar to our findings in single-arm ATI, multiple latently infected cells contribute to viral rebound at each ATI time point. Interestingly, we also observe viral persistence during multiple ATI timepoints, demonstrated by multiple identical viruses arising at first detectable rebound, as well as clearance of specific viral lineages. Cleared viral lineages were also found to be more sensitive to autologous antibodies collected from the first detectable rebound time point of each ATI period in participant S04 (1 of 2 cleared) and S23 (2 of 3 cleared), consistent with our previous findings with cleared viruses from single-arm ATI participants. These data suggest that the initial autologous antibody response generated during the first ATI time point is able to apply a neutralization sieve against select rebounding variants at

multiple-ATI timepoints, even as viral loads decrease to undetectable levels under intermittent periods of cART.

This study has several important limitations. First, our analyses were limited to participants with available plasma to assess by neutralization assays and/or SGS methods. Further work on larger and more diverse cohorts with extensive samples of archived plasma meeting sequencing viral load requirements is warranted. Secondly, viral load analyses in the single-arm ATI cohort began after 4 to 5 weeks of treatment interruption. This delay in viral load sampling fails to capture early, minor rebounding variants that may have emerged sooner, but were rapidly cleared from the viral quasispecies or were less fit compared to the dominant lineage, thus preventing accurate assessment of first detectable rebound viruses. Our likelihood of missing infrequent variants was also increased by our limited sampling depth by SGS methods. Power studies on plasma vRNA sequences show that when the total number of sequences (n) is ≥ 30 , one can be 95% confident not to have missed any variant that comprised at least 10% of the total viral population, whereas when n is between 10 and 20, there is at least an 80% chance to detect a variant represented in $\geq 15\%$ of the population¹³. In the present study, 11/11 single-ATI participants and 1/2 multiple-ATI participants had less than 30 sequences available for analyses for at least one ATI timepoint. Prolonged ATI studies with greater plasma sample availability may help to address this sampling issue. Third, in the multiple-ATI cohort, it is notable that while both participants experienced waning viral loads upon cART reinitiation between ATI time points, they did not achieve complete (< 50 copies/ml) and prolonged viral suppression throughout the course of this study. The short period of cART and

incomplete viral suppression between treatment interruptions prevent a clear distinction between viruses rebounding from latency and ongoing replication and infection of short- or medium-lived cells. Future studies assessing participants with multiple ATIs should consider at least 6 months of cART and undetectable plasma viremia before reinitiating ATI to provide a more accurate assessment of viruses rebounding from latency.

In summary, this study highlights several distinctions between HIV-1 transmission and viral rebound. Consistent with recently published studies, I found that unlike HIV-1 transmission, viral rebound is quickly established by multiple, distinct viral lineages reactivating from latency^{4,7,25,32,33}. Additionally, longitudinal sampling of rebound variants demonstrates that early rebound lineages are susceptible to nAb immune pressure, resulting in selective sweeps of nAb-sensitive lineages within weeks of ATI. This finding is notable as previous studies have suggested that memory B cell responses have a decreased functional profile once chronic HIV infection has been established^{44,45}. Instead, my data shows that strain-specific nAbs are preserved during cART suppression, and are able to produce strain-specific nAbs within 4 weeks of ATI, resulting in viral clearance of nAb-sensitive lineages at subsequent ATI timepoints of up to 78 weeks. This autologous antibody sieving effect occurs more rapidly than in chronic infection, where strain-specific neutralizing antibodies take years to develop³⁷. Additionally, through IgG isolation of pre-ATI plasma, I show that strain-specific antibodies can be found in the plasma at pre-ATI timepoints, suggesting plasma B cells are actively producing low titers of nAbs in the absence of plasma viremia. This finding is significant, as it provides an additional host-mediated mechanism of viral control during ATI. Together, these virologic and immunologic findings provide new insight on the baseline events that occur during ATI and viral rebound, which will be critical for our

understanding of treatment efficacy in future curative therapies operating under ATI conditions.

Materials and Methods

Clinical trial and participant selection

We studied eleven participants from a previously conducted trial comparing a single vs. multiple ATI schema (NCT00051818²). We randomly selected eleven participants with available plasma samples and viral rebound ≥ 1000 copies/ml from the single ATI arm and two participants from the multiple ATI arm. The study was approved by local Institutional Review Boards. Eligibility criteria for the clinical trial are published, but generally included >18 years of age, cART suppression <500 copies/ml for more than 6 months, <50 copies/ml at recruitment of ATI study, CD4⁺ counts >400 cells/ μ l on ART and a nadir no less than 100 cells/ μ l. For gp160 and gp41 *env* analyses during viral rebound, all participants were selected based on first detectable rebound plasma viral loads >1000 copies/ml and >800 copies/ml, respectively, and successful viral suppression <50 copies/ml after cART reinitiation. The trial participants from the single-arm ATI cohort received continuous cART for 1 year, followed by open-ended ATI with the first plasma collection at 4 to 5 weeks, and biweekly monitoring of plasma viremia. Multiple-arm ATI participants interrupted therapy sequentially for 2, 4, 6 and 12 week intervals sequentially, with 2, 12 and 16 weeks of cART-mediated resuppression between each ATI and biweekly monitoring and a final open-ended interruption for up to 1 year. In both cohorts, participants on NNRTIs were instructed to stop these drugs one day earlier than the remaining drug regimen. The primary outcome of the parent study was time to viral rebound during ATI (>5000 copies/ml).

Viral RNA extraction, cDNA synthesis, single genome sequencing (SGS)

SGS enables proportional representation of the complex HIV-1 virus quasispecies with linkage across the sequenced region with minimal in vitro errors⁴⁶. Viral RNA extraction, cDNA synthesis, and SGS were performed to amplify gp41 or gp160 env as previously described³³. In order to ensure a majority of sequences would be generated from a single template, cDNA was diluted so that PCR positive wells were < 30% of the total products. Single cDNA templates for gp41 were amplified with the following hemi-nested gp41 primers: 1st and 2nd round forward primer for gp41, FOR13: GAGAAAGAGCAGAA-GACAGTGG ; 1st round reverse primer 3Envout: TTGCTACTTGTGATTGCTCCATGT; 2nd round reverse primer 3Envin: GTCTCGAGATACTGCTCCCACCC. PCR was performed in MicroAmp 96-well reaction plates (Applied Biosystems, Foster City, CA) with the following PCR parameters: 1 cycle of 94°C for 2 min; 35 cycles of a denaturing step of 94°C for 15 s, an annealing step of 55°C for 30 s, an extension step of 68°C for 1min 30 s, followed by a final extension of 68°C for 10 min. The product of the 1st round PCR was subsequently used as a template in the 2nd round PCR under same conditions but with a total of 45 cycles. 1.5kb amplicons were inspected on precasted 1% agarose E-gels 96 (Invitrogen Life Technologies, Carlsbad, CA). All PCR procedures were carried out under PCR clean room conditions using procedural safeguards against sample contamination, including pre-aliquoting of all reagents, use of dedicated equipment, and physical separation of sample processing from pre- and post-PCR amplification steps. Single cDNA templates for gp160 were amplified with the following nested env primers: 1st round forward primer 5out: TAGAGCCCTGGAAGCAT-CCAGGAAG, 2nd round forward primer 5in: CACCAAGCTTTAGGCATCTC-CTATGGCAGGAAGAAG ; 1st round reverse primer 3Envout: TTGCTACTTGTGATTGC-

TCCATGT; 2nd round reverse primer 3Envin: GTCTCGAGATACTGCTCCCACCC. PCR parameters included: 1 cycle of 94°C for 2 min; 35 cycles of a denaturing step of 94°C for 15 s, an annealing step of 55°C for 30 s, an extension step of 68°C for 3min 30 s, followed by a final extension of 68°C for 10 min. The product of the 1st round PCR was subsequently used as a template in the 2nd round PCR under same conditions but with a total of 45 cycles. Amplicons were inspected using similar methods to gp41, with a target amplicon size of 3kb. Sequences that contained stop codons, large deletions, or mixed bases were removed from further analysis.

Phylogenetic analyses

Sequences from each participant were aligned using Geneious 11.0.3 and alignments were adjusted as necessary by visual inspection. Maximum likelihood phylograms for each participant were inferred using PhyML 3.0, which jointly estimates the tree and the parameters of the evolutionary model. Within-participant alignments were aligned sequentially using Geneious 11.0.3. Pairwise diversity estimates were performed by DIVEIN⁴⁷. To determine the clonality of rebound viremia, sequences were analyzed by modified version of a previously described model of neutral virus evolution^{3,46}, which assumes virus undergoes rapid expansion without selection. Under this model, low-diversity sequence lineages display a star-like phylogeny and a Poisson distribution of mutations, coalesce to an unambiguous founder sequence enabling estimates of time from a MRCA^{46,48}. We estimate that two weeks of ATI is sufficient for cART washout, and that first detectable rebound arises from multiple pre-existing HIV-1 variants archived in latently infected cells. Rebound viruses forming identical or low diversity lineages with <3bp mutations in HIV-1 env or <1bp mutation in gp41 (maximum number of mutations used to distinguish between pre-existing and de novo mutations using the in vivo

evolution rate of HIV-1: $4.1 \times 1.7 \times 10^{-3}$ per base per cell)⁴⁹ are categorized as a clonal lineage, derived from the clonal expansion of a single recrudescence virus. All sequences will be deposited in GenBank (accession numbers to be determined).

Env cloning and pseudovirus titering

Select env sequences from first detectable rebound were molecularly cloned for the production of pseudovirus and phenotypic analyses as described previously³³. Correctly sized amplicons identified by gel electrophoresis were gel-purified by using the QIAquick gel purification kit according to the recommendations of the manufacturer (Qiagen), ligated into the pcDNA 3.1 Zeo (+) Expression Vector (Invitrogen) and transformed into NEB 5-alpha Competent E. coli. 100 µl of transformed bacteria were plated on LB agar plates supplemented with 50 µg/ml ampicillin and cultured at 37°C for 24 hours. Single colonies were selected and grown overnight in liquid LB broth at 37°C with 250 rpm shaking followed by plasmid isolation. Finally, each molecular clone was sequence-confirmed to be identical to the previously determined env sequence of the amplicon. Pseudovirus was prepared by transfecting overnight cultured 0.5×10^6 293T cells in 9.4cm² tissue culture dishes with 500 ng of rev/env expression plasmid and 500ng of pSG3Δenv Backbone using Fugene 6 (Roche Applied Science, Indianapolis, IN) in Dulbecco's Modified Eagle Medium (DMEM). Culture supernatants were harvested 48 hours after transfection, cleared of cellular debris by 0.45-micron filter and stored in aliquots at -80°C. Pseudoviruses were titrated on TZM-bl reporter cells (8129; NIH AIDS Research and Reference Reagent Program), which contain a Tat-inducible 11 luciferase and a β-galactosidase gene expression cassette. Infectious titers were measured on 24-well plates based on β-galactosidase production, representing the number of infection events per µL of virus stock (IU/µL) as described previously^{4,33}.

Neutralization assays

Virus neutralization by plasma was assessed on TZM-bl cells as described previously^{4,33,50}. TZM-bl cells were seeded at 1×10^4 cells per well and cultured in 96-well plates overnight. Virus stock dilutions were made to final concentrations in Dulbecco's modified Eagle's medium (DMEM) containing 6% fetal bovine serum (FBS) and 40 µg/ml DEAE-dextran (Sigma-Aldrich, St. Louis, MO) to achieve 2,000 IU/well. Viruses with low numbers of IU per microliter were added at no less than 1,500 IU/well. Equal-volume virus dilutions and 5-fold serially diluted sera or MAbs were mixed and incubated at 37°C for 1 h. Supernatants were then removed, and 80 µl of these mixtures was added. Medium-only and virus-only control wells were included as background and 100% infectivity, respectively. Luciferase activity was measured after 48 h of incubation at 37°C by using Bright-Glo according to the manufacturer's instructions (Promega). All assays were done in triplicate in each of at least two independent experiments. To calculate the concentration of antibody that neutralized 50% of virus infection (50% inhibitory concentration [IC₅₀]), the antibody dose-response curves were fit with a four-parameter logistic equation by using Prism 7.0 (GraphPad Software, Inc., San Diego, CA). When 50% neutralization was not achieved at the highest concentration of plasma or antibody used, the IC₅₀ was recorded as being higher than the highest concentration used.

Isolation and quantification of pre-ATI IgG

Approximately 1ml of pre-ATI plasma samples from S53 and S60 were collected at 6 and 8 weeks before ATI and heat inactivated at 56° for 45 minutes. Purified IgG was

isolated using the rProtein A/Protein G GraviTrap (GE Healthcare Life Sciences 28-9852-56) following manufacturer's instructions. Isolated IgG concentrations were determined using the BCA protein assay kit (Pierce) using manufacturer's instructions and analyzed with the following microplate procedure: 10 μ l of the standard solutions from Bovine Gamma Globulin Standard Pre-Diluted Set (Pierce) was pipetted into a 96-Well polystyrene plate (Pierce) in replicates, water was used as a blank. The protein was diluted in PBS to make 25 μ l dilutions ranging from 1:10 – 1:30. 10 μ l of each dilution mixture was added to the plate in replicates. 200 μ l of the Working Reagent (50 parts of BCA Reagent A to one part of BCA Reagent B) was added to all the wells containing protein and standard solution. The plate was covered in plastic, mixed thoroughly on a plate shaker for 30 seconds, and placed in a 37° incubator. After 30 minutes, the plate was removed from the incubator and allowed to cool for 10 minutes at room temperature. The absorbance was measured at 562 nm on a plate reader. A standard curve was prepared by plotting the average Blank-corrected 562 nm measurement for each prediluted standard vs. its concentration in μ g/mL. Final IgG concentrations per ml were determined using the standard curve. Mean IgG collected was 22.3mg/ml per participant. In order to recapitulate the amount of human IgG circulating in the plasma in HIV-1 infected, cART-treated individuals (29577+/-607 mg/dl)⁴⁷, we diluted total collected IgG to 20 mg/ml followed by a 1:20 top dilution (1000 μ g/ml) and 4-fold serial dilutions for neutralization analyses. All assays were done in triplicate in each of at least two independent experiments.

Statistical methods.

Statistical analyses. Given the small sample size (n=11, n=2), non-parametric tests were used for all comparisons. The test for within-person change from persisting to cleared

lineages were carried out by Wilcoxon rank sum test. Spearman correlation testing was used to test the association between measures. Analyses were conducted in Statistical Analysis System (SAS), version 9.4.

Acknowledgement: I am grateful for the technical assistance from the NGS Sequencing Core (Miguel Ramirez, Catharine Bahari, Andrew Smith, and Alex Shazad), Gerald H. Learn for sequence and phylogenetic analyses, Fang-Hua Lee for neutralization analyses, and the study volunteers who participated in the previously conducted clinical trial. I also thank Drs. Luis Montaner and Manolis Papanicolaou of the Wistar Institute for their valuable suggestions on subject selection and experimental analyses. This work was primarily supported by R01 DA037244 and 2T32AI007632. I also acknowledge support from multiple Cores of the Penn Center for AIDS Research (P30-AI045008).

References

1. Strategies for Management of Antiretroviral Therapy (SMART) Study Group *et al.* CD4+ count-guided interruption of antiretroviral treatment. *N. Engl. J. Med.* **355**, 2283–2296 (2006).
2. Papasavvas, E. *et al.* Randomized, Controlled Trial of Therapy Interruption in Chronic HIV-1 Infection. *PLoS Med* **1**, (2004).
3. Li, J. Z. *et al.* The Size of the Expressed HIV Reservoir Predicts Timing of Viral Rebound after Treatment Interruption. *AIDS* **30**, 343–353 (2016).
4. Salantes, D. B. *et al.* HIV-1 latent reservoir size and diversity are stable following brief treatment interruption. (2018). doi:10.1172/JCI120194
5. Papasavvas, E. *et al.* Analytical antiretroviral therapy interruption does not irreversibly change pre-interruption levels of cellular HIV: *AIDS* **32**, 1763–1772 (2018).
6. Cohen, Y. Z. *et al.* Relationship between latent and rebound viruses in a clinical trial of anti-HIV-1 antibody 3BNC117. *The Journal of Experimental Medicine* jem.20180936 (2018). doi:10.1084/jem.20180936
7. Clarridge, K. E. *et al.* Effect of analytical treatment interruption and reinitiation of antiretroviral therapy on HIV reservoirs and immunologic parameters in infected individuals. *PLOS Pathogens* **14**, e1006792 (2018).
8. Lee, H. Y. *et al.* Modeling Sequence Evolution in Acute HIV-1 Infection. *J Theor Biol* **261**, 341–360 (2009).
9. Keele, B. F. Identifying and Characterizing Recently Transmitted Viruses. *Curr Opin HIV AIDS* **5**, 327–334 (2010).
10. Ifeanyichukwu, Ositadimma, M., Bright, O. E., C, M. S. & Okechukwu, O. C. Effect of HIV Infection on Some Haematological Parameters and Immunoglobulin Levels in HIV Patients in Benin City, Southern Nigeria. *Journal of HIV & Retro Virus* **2**, (2016).
11. Havlir, D. V. *et al.* Productive Infection Maintains a Dynamic Steady State of Residual Viremia in Human Immunodeficiency Virus Type 1-Infected Persons Treated with Suppressive Antiretroviral Therapy for Five Years. *Journal of Virology* **77**, 11212–11219 (2003).
12. Haaland, R. E. *et al.* Inflammatory Genital Infections Mitigate a Severe Genetic Bottleneck in Heterosexual Transmission of Subtype A and C HIV-1. *PLoS Pathog* **5**, (2009).
13. Keele, B. F. *et al.* Identification and characterization of transmitted and early founder virus envelopes in primary HIV-1 infection. *PNAS* **105**, 7552–7557 (2008).

14. Abrahams, M.-R. *et al.* Quantitating the Multiplicity of Infection with Human Immunodeficiency Virus Type 1 Subtype C Reveals a Non-Poisson Distribution of Transmitted Variants. *J Virol* **83**, 3556–3567 (2009).
15. Shaw, G. M. & Hunter, E. HIV transmission. *Cold Spring Harb Perspect Med* **2**, (2012).
16. Benecke, A., Gale, M. & Katze, M. G. Dynamics of innate immunity are key to chronic immune activation in AIDS: *Current Opinion in HIV and AIDS* **7**, 79–85 (2012).
17. Iwasaki, A. Innate Immune Recognition of HIV-1. *Immunity* **37**, 389–398 (2012).
18. Doehle, B. P., Hladik, F., McNevin, J. P., McElrath, M. J. & Gale, M. Human Immunodeficiency Virus Type 1 Mediates Global Disruption of Innate Antiviral Signaling and Immune Defenses within Infected Cells. *Journal of Virology* **83**, 10395–10405 (2009).
19. Borrow, P. Innate immunity in acute HIV-1 infection. *Curr Opin HIV AIDS* **6**, 353–363 (2011).
20. Bunnik, E. M., Pisas, L., Nuenen, A. C. van & Schuitemaker, H. Autologous Neutralizing Humoral Immunity and Evolution of the Viral Envelope in the Course of Subtype B Human Immunodeficiency Virus Type 1 Infection. *Journal of Virology* **82**, 7932–7941 (2008).
21. Borrow, P., Lewicki, H., Hahn, B. H., Shaw, G. M. & Oldstone, M. B. Virus-specific CD8⁺ cytotoxic T-lymphocyte activity associated with control of viremia in primary human immunodeficiency virus type 1 infection. *Journal of Virology* **68**, 6103–6110 (1994).
22. Koup, R. A. *et al.* Temporal association of cellular immune responses with the initial control of viremia in primary human immunodeficiency virus type 1 syndrome. *Journal of Virology* **68**, 4650–4655 (1994).
23. Price, D. A. *et al.* Positive selection of HIV-1 cytotoxic T lymphocyte escape variants during primary infection. *Proc Natl Acad Sci U S A* **94**, 1890–1895 (1997).
24. Wilson, J. D. *et al.* Direct visualization of HIV-1-specific cytotoxic T lymphocytes during primary infection. *AIDS* **14**, 225–233 (2000).
25. Rothenberger, M. K. *et al.* Large number of rebounding/founder HIV variants emerge from multifocal infection in lymphatic tissues after treatment interruption. *PNAS* **112**, E1126–E1134 (2015).
26. Davey, R. T. *et al.* HIV-1 and T cell dynamics after interruption of highly active antiretroviral therapy (HAART) in patients with a history of sustained viral suppression. *PNAS* **96**, 15109–15114 (1999).

27. Hogg, R. S. *et al.* Improved Survival Among HIV-Infected Individuals Following Initiation of Antiretroviral Therapy. *JAMA* **279**, 450–454 (1998).
28. Autran, B. *et al.* Positive effects of combined antiretroviral therapy on CD4+ T cell homeostasis and function in advanced HIV disease. *Science* **277**, 112–116 (1997).
29. Hammer, S. M. *et al.* A Trial Comparing Nucleoside Monotherapy with Combination Therapy in HIV-Infected Adults with CD4 Cell Counts from 200 to 500 per Cubic Millimeter. *New England Journal of Medicine* **335**, 1081–1090 (1996).
30. Salazar-Gonzalez, J. F. *et al.* Genetic identity, biological phenotype, and evolutionary pathways of transmitted/founder viruses in acute and early HIV-1 infection. *J Exp Med* **206**, 1273–1289 (2009).
31. McLinden, R. J. *et al.* Association of HIV neutralizing antibody with lower viral load after treatment interruption in a prospective trial (A5170). *AIDS* **26**, 1452 (2012).
32. Caskey, M. *et al.* 3BNC117 a Broadly Neutralizing Antibody Suppresses Viremia in HIV-1-Infected Humans. *Nature* **522**, 487–491 (2015).
33. Bar, K. J. *et al.* Effect of HIV Antibody VRC01 on Viral Rebound after Treatment Interruption. *N. Engl. J. Med.* **375**, 2037–2050 (2016).
34. Richman, D. D., Wrin, T., Little, S. J. & Petropoulos, C. J. Rapid evolution of the neutralizing antibody response to HIV type 1 infection. *Proc Natl Acad Sci U S A* **100**, 4144–4149 (2003).
35. Wei, X. *et al.* Antibody neutralization and escape by HIV-1. *Nature* **422**, 307–312 (2003).
36. Lee, F.-H. *et al.* Breakthrough Virus Neutralization Resistance as a Correlate of Protection in a Nonhuman Primate Heterologous Simian Immunodeficiency Virus Vaccine Challenge Study. *Journal of Virology* **89**, 12388–12400 (2015).
37. Moody, M. A. *et al.* Strain-Specific V3 and CD4 Binding Site Autologous HIV-1 Neutralizing Antibodies Select Neutralization-Resistant Viruses. *Cell Host & Microbe* **18**, 354–362 (2015).
38. Liao, H.-X. *et al.* Co-evolution of a broadly neutralizing HIV-1 antibody and founder virus. *Nature* **496**, 469–476 (2013).
39. Korber, B. *et al.* Evolutionary and immunological implications of contemporary HIV-1 variation. *Br. Med. Bull.* **58**, 19–42 (2001).
40. Rolland, M. *et al.* Increased HIV-1 vaccine efficacy against viruses with genetic signatures in Env V2. *Nature* **490**, 417–420 (2012).
41. Rolland, M. *et al.* Genetic impact of vaccination on breakthrough HIV-1 sequences from the STEP trial. *Nature Medicine* **17**, 366–371 (2011).

42. Edlefsen, P. T. *et al.* Comprehensive sieve analysis of breakthrough HIV-1 sequences in the RV144 vaccine efficacy trial. *PLoS Comput. Biol.* **11**, e1003973 (2015).
43. Roederer, M. *et al.* Immunological and virological mechanisms of vaccine-mediated protection against SIV and HIV. *Nature* **505**, 502–508 (2014).
44. Moir, S. & Fauci, A. S. B cells in HIV infection and disease. *Nat Rev Immunol* **9**, 235–245 (2009).
45. Moir, S. *et al.* B cells in early and chronic HIV infection: evidence for preservation of immune function associated with early initiation of antiretroviral therapy. *Blood* **116**, 5571–5579 (2010).
46. Halper-Stromberg, A. & Nussenzweig, M. C. Towards HIV-1 remission: potential roles for broadly neutralizing antibodies. *J Clin Invest* **126**, 415–423 (2016).
47. Phylogeny/Divergence/Diversity. Available at: <https://indra.mullins.microbiol.washington.edu/DIVEIN/diver.html>. (Accessed: 26th August 2018)
48. Balazs, A. B. *et al.* Antibody-based protection against HIV infection by vectored immunoprophylaxis. *Nature* **481**, 81–84 (2012).
49. Cuevas, J. M., Geller, R., Garijo, R., López-Aldeguer, J. & Sanjuán, R. Extremely High Mutation Rate of HIV-1 In Vivo. *PLOS Biology* **13**, e1002251 (2015).
50. Bar, K. J. *et al.* Early Low-Titer Neutralizing Antibodies Impede HIV-1 Replication and Select for Virus Escape. *PLOS Pathogens* **8**, e1002721 (2012).

CHAPTER 3

Effect of HIV Antibody VRC01 on Viral Rebound After Treatment Interruption

This work was published in the following publication:

Bar KJ, Sneller MC, Harrison LJ, Justement JS, Overton ET, Petrone ME, Salantes DB, Seamon CA, Scheinfeld B, Kwan RW, Learn GH, Proschan MA, Kreider EF, Blazkova J, Bardsley M, Refsland EW, Messer M, Clarridge KE, Tustin NB, Madden PJ, Oden K, O'Dell SJ, Jarocki B, Shiakolas AR, Tressler RL, Doria-Rose NA, Bailer RT, Ledgerwood JE, Capparelli EV, Lynch RM, Graham BS, Moir S, Koup RA, Mascola JR, Hoxie JA, Fauci AS, Tebas P, Chun, T-W. *N. Engl. J. Med.* **375**, 2037–2050 (2016).

Abstract

Significant advances in the field of single-cell antibody cloning have led to the discovery of multiple exceptionally potent broadly neutralizing antibodies (bNAbs) in HIV infected individuals. BNAbs target conserved regions of the HIV-1 Env glycoprotein to neutralize the majority of diverse HIV strains, making these monoclonal antibodies an exciting new addition to potential HIV cure strategies currently being tested in humans. While a recent clinical trial of a single bNAb infusion was found to be safe and effective at reducing HIV-1 rebound viremia in the majority of infected patients, variability in the diversity and kinetics of rebounding viruses suggests bNAb monotherapy may affect individuals differently¹. Elucidating the within-host dynamics of HIV during passive bNAb infusion and ATI will be a critical step in informing the development of future treatment strategies for HIV-1 eradication.

In this study, I determine the within-host viral dynamics of HIV during passive bNAb infusion in the AIDS Clinical Trials Group study A5340 taking place at the University of Pennsylvania. The CD4 binding site (CD4 bs) bNAb, VRC01, was administered intravenously to 15 chronically infected individuals, where recrudescence during bNAb infusion represented viruses that were able to “breakthrough” VRC01 intervention and were used as a metric of therapeutic effect. Using archived plasma samples, I performed genotypic and phenotypic analyses on viruses from pre-cART and rebound time points using SGS, molecular cloning, and neutralization assays. Through phylogenetic analyses, I identified multiple participants with VRC01-mediated restriction of viral lineages that emerged from latency. Phenotypic analyses through Env cloning confirmed the prevalence of clinically significant pre-existing resistance to VRC01, which

correlated with viral rebound kinetics. This assessment of VRC01-resistant viruses breaking through ATI and VRC01 infusion highlight future challenges of monotherapy with bNAbs. The degree of baseline VRC01 resistance was striking, and confirms the need for more broad, potent bNAbs that are able to target a diversity of viral epitopes. Additionally, this work emphasizes a need for standardized clinical assays that can accurately assess for low frequencies of resistant viruses before participants undergo bNAb infusion and ATI.

Introduction

Advances in B cell cloning have led to the isolation of HIV-specific broadly neutralizing antibodies (bNAbs) capable of potently neutralizing cell-free viruses from multiple clades circulating worldwide¹⁻⁸. Combinatorial infusion of bNAbs targeting various epitopes on the Env glycoprotein greatly contribute to viremic suppression in humanized mouse and rhesus macaque models of HIV-1 infection⁹. Additionally, macaques treated with bNAb cocktails show reductions in measured proviral DNA and increases in HIV-specific cellular immune responses, suggesting that bNAb infusion may directly or indirectly target cell-associated virus within the latent reservoir and “boost” adaptive immune responses¹⁰⁻¹¹. In the parent AIDS Clinical Trials Group Study A5340 being conducted at the University of Pennsylvania, we will determine whether VRC01, a bNAb targeting the CD4 receptor binding site (CD4bs) of the HIV envelop glycoprotein, can suppress viral rebound in chronically infected humans during brief analytical treatment interruption (ATI) of ART (see Figure 1 for A5340 schema).

VRC01 has been shown to neutralize approximately 90% of 190 group M HIV Env pseudoviruses with a mean 50% inhibitory concentration (IC₅₀) of 0.33 µg per milliliter. Recent studies implementing passive bNAb immunotherapy in mice and macaques suggest that in addition to potent viral suppression, bNAbs may also enhance host immune responses and reduce levels of proviral DNA across compartments¹²⁻¹⁵. These findings have raised enthusiasm for bNAb’s potential ability to eradicate HIV, but need to be confirmed in human studies. The benefits of HIV-1 specific bNAbs over cART include their ability to be delivered as long-acting agents through Fc engineering⁶ or vectored delivery^{15, 16}. Additionally, unlike cART, the Fc portion of bNAbs enable possible

engagement with host immune cells and contribute to the killing of infected cells and mediate clearance of the persistent viral reservoir^{4, 17, 18, 19}.

Previous clinical trials in humans have shown that VRC01 administration is safe and well tolerated in uninfected individuals, as well as viremic or cART-suppressed individuals^{22, 24}. In the majority of viremic individuals, a 1.1 to 1.8 log₁₀ decrease in plasma viral loads were observed shortly after VRC01 infusion. Interestingly, further analysis showed that 25% of participants did not achieve viral suppression due to a minor pool of circulating VRC01-resistant strains. Other studies assessing VRC01 sensitivity in HIV-1 viral isolates from cART-suppressed participants show that while some participants harbor a low frequency of VRC01-resistant replication competent viruses within the viral reservoir, the majority of cART-suppressed participants contain latent viruses that are sensitive to VRC01 in vitro. The identification of VRC01-resistant variants also raised the question of whether these minority resistant variants would emerge during VRC01 infusion and ATI. My goal in this study was to determine if passive infusion of VRC01 would restrict the clonality and phenotype of viruses rebounding from the latent reservoir. These studies highlight the complexity of viral rebound dynamics during high levels of circulating bNAbs and further inform our understanding of archived resistance in chronically infected participants.

Results

Participant demographics

We enrolled 14 participants, all of whom were male, with a median age 38 years

(interquartile range, 34-44), 7 (50%) African American and 7 (50%) Caucasian. CD4 T-cell count at enrollment was 896 cells per cubic millimeter (interquartile range, 579 to 1053) and a median duration from the initiation of cART to study entry of 4.7 years (interquartile range, 3.8-6.0) and 10 (71%) were on INSTI and 4 (29%) on PI cART regimens (see table 3.1 for summary of baseline characteristics). One participant was excluded from the analyses of time to viral rebound because he discontinued ART before the administration of VRC01. All remaining participants completed the three infusions VRC01 per protocol, with only one serious adverse event reported that was not related to VRC01. The safety and tolerability profile of VRC01 are consistent with separate, larger ongoing clinical trials of the same product. All participants were rapidly suppressed with their original cART regimen upon two consecutive confirmations of plasma viral rebound at 500 copies per milliliter. The median time of cART cessation was 6 weeks (range, 3 to 13) and the median time from the first detectable HIV RNA level of 200 copies per milliliter or more to the first suppressed HIV level of less than 200 copies per milliliter after ART reinitiation was 6 weeks (range, 3 to 14). Throughout ATI, no participant had measurable CD4 T cell counts below 350 cell per milliliter. Additional participant demographics and clinical characteristics can be found in Table 3.1.

Treatment procedures, study objectives, and study outcomes

In step 1 of the A5340 trial, 14 participants received up to three doses of VRC01 (40 mg per kilogram of body weight administered intravenously) at 3-week intervals (Fig. 3.1). Participants then discontinued cART after the first VRC01 infusion and were followed weekly until HIV RNA levels reached ≥ 200 copies/ml followed by a confirmation level of

≥1,000 copies/ml, or three consecutive measurements of ≥200 copies/ml, or until they had confirmed CD4 T cell counts of <350 cells/mm³. Upon confirmation of viral rebound or decreased CD4 T cells, participants entered step 2 of A5340, at which point cART was reinitiated and participants were followed until plasma viral loads were <50copies/ml. The objectives of this clinical study was to assess the safety and side-effect profile of VRC01 infusions in cART-suppressed individuals, and to estimate the proportion of participants with viral rebound in the presence of high plasma concentrations of VRC01 at 8 weeks of ATI. Secondary objectives included the frequency of rebound viremia at 4 weeks as well as the evaluation of the pharmacokinetic characteristics of VRC01. In this study, the key exploratory objectives were the frequency of anti-idiotypic antibodies against VRC01 as well as the genetic and phenotypic characterization of the rebound virus. With 13 participants with evaluable data, we had 95% power to detect a difference of 40 percentage points¹⁴ at a two-sided alpha level of 0.10. Of the 14 enrolled participants, 13 completed the clinical trial with evaluable data.

Time to viral rebound

Interestingly, while measured plasma VRC01 were above 50µg/ml (median 175, range 68-1,494) (Fig. 3.2) 12 of 13 participants did not experience durable suppression of plasma viremia for more than 8 weeks. The median time to rebound was 4 weeks which is a small delay in viral rebound kinetics compared to kinetics observed in historical controls from previous ACTG studies; 38% of A5340 participants remain virally suppressed at week 4 versus 13% of historical controls (P = 0.04 by a two-sided Fisher's exact test) and 8% and 3%, respectively, were suppressed at week 8 (P = 0.44 by a two-

sided Fisher's exact test) (Fig. 3.3). Participant A07 had prolonged viral suppression and detectable viremia at week 11 of ATI, when plasma levels of VRC01 waned to 25µg per milliliter. Participant A11 was excluded from evaluation due to a premature pause in cART, causing detectable plasma viremia at the time of VRC01 infusion. Throughout the course of the trial, no anti-idiotypic antibodies were identified in any of the participants.

Sequence evidence of VRC01-mediated virus restriction

To characterize the genotype of rebounding viral populations, I generated cDNA from extracted viral RNA from samples collected from pre-cART plasma (8 participants) as well as plasma collected from the first and second weeks of detectable viremia (13 participants). Next, nested PCR HIV-1 gp160 primers were used to amplify full-length env sequences from each participant and single-genome sequencing methods were used to determine the genome of individual pre-cART and/or rebound sequences. These sequences were analyzed together in a maximum likelihood (ML) phylogenetic tree and showed independent clustering, confirming the relatedness of pre-cART and rebound viruses (Fig. 3.4).

Independent studies (including the ATI clinical trial discussed in Chapter 2 of this thesis) that assessed the diversity of the rebounding viral quasispecies have shown that in the absence of therapeutic intervention, first detectable viral rebound is polyclonal due to the activation of multiple latently infected cells²⁷⁻²⁹. In this study, I assessed for genetic evidence of VRC01-mediated viral restriction by comparing the number of genetically distinct virus populations compared to historical controls. In 3 of 12 participants (25%)

who rebounded in the presence of high plasma concentrations of VRC01, sequence evidence suggested VRC01-mediated restriction of viral rebound. In participant A04, A02 (Fig. 3.4), and A12 (Fig. 3.5) pre-cART plasma virus formed characteristic unstructured phylogenetic trees characteristic of chronic HIV infection. Rebound lineages from these participants, however, clustered into low-diversity lineages of nearly identical sequences and conformed to a strict model of neutral virus evolution, where the genetic distance of the most recent common ancestor of these low-diversity rebound lineages suggests recent clonal expansion of a single virus. The remaining 9 of 12 participants (75%) had polyclonal rebound similar to what is observed in historical analytic treatment interruption without resistance. Rebound viruses from participant A05 clustered into multiple genetically distinct rebound lineages that align throughout the pre-ART virus phylogeny, while Participant A03 had rebound sequences that clustered unevenly within the pre-ART virus population, supporting sequence compartmentalization (Fig. 3.4). In participant A07, first detectable rebound was observed at week 11 with lower plasma levels of VRC01 (Fig. 3.4). I observed two closely related rebound lineages in this participant that were distinct from the pre-cART viral quasispecies.

Further, we identified specific amino acid changes within the VRC01 antibody-binding site with the use of neutralization-based epitope prediction identified in or near the VRC01 epitope (located within the V5 loop and the CD4-binding loop). These data suggest that VRC01 is mediating selective pressure on rebounding virus (Fig. 3.7)

Selection for VRC01-Resistant Rebounding Viruses

Next, I determined the role of resistance to VRC01 at viral rebound in the presence of high VRC01 concentrations. I hypothesized that early viral rebound and viral restriction of select lineages from latency was caused by pre-existing resistant variants emerging from the latent reservoir. To test this, I cloned select pre-cART and rebound *envs* from throughout the participant's viral quasispecies and expressed these *envs* via pseudoviruses to determine *env* VRC01 sensitivity in standardized *in vitro* HIV-1 neutralization assays. All participants who had rapid viral rebound with high concentrations of circulating VRC01 also contained rebound *envs* with IC50 neutralization titers greater than 1 µg/ml (median 4.55 µg/ml, range 1.1 µg/ml- >50 µg/ml), conferring moderate resistance to VRC01^{5, 32, 33}. I also compared pre-cART and rebound Envs in the 8 participants who contained sequences from both time points. I observed a trend towards increased VRC01-resistance at rebound (mean increase by a factor of 3.79, P = 0.004 by a two-sided random-effects model). Overall, participants in A5340 had greater baseline resistance to VRC01 in comparison to previous HIV-1 panels (p=0.003, two-sided Wilcoxon rank sum test)⁵. Summaries of the IC50 titers of pre-cART and rebound viruses from each participant can be found in Fig. 3.4 and Fig. 3.6.

When comparing rebound kinetics and pre-cART resistance to VRC01 in participants with available plasma samples, I also found that the timing of viral rebound was associated with increased pre-existing VRC01 resistance. Participants A02 and A07, who had the longest delay in viral rebound (8 and 11 weeks respectively), also had a mean pre-cART IC50s of <1µg/ml with the emergence of VRC01 sensitive monoclonal or oligoclonal viral lineages. In contrast, participants A05, A06, and A09 harbored

multiple VRC01-resistant pre-cART variants. Infusion of VRC01 in these participants was followed by the rapid emergence of polyclonal rebound viruses that were highly resistant to VRC01. Interestingly, in participants with a range of pre-cART VRC01 sensitivities (Participant A03, A04 and A12), I found that while rebound also occurred soon after ATI (range, 2-6 weeks), sequence analyses of rebound variants show monoclonal or compartmentalized rebound.

Tables

Table 1. Characteristics of the Participants at Baseline.*		
Characteristic	A5340 Trial (N=14)	Historical Controls from Previous ACTG Studies (N=61)
Sex — no. (%)		
Male	14 (100)	53 (87)
Female	0	8 (13)
Age — yr		
Median (IQR)	38 (34–44)	44 (40–50)
Range	27–52	27–73
Race or ethnic group — no. (%)†		
White non-Hispanic	6 (43)	41 (67)
Black non-Hispanic	6 (43)	13 (21)
Hispanic, regardless of race	2 (14)	7 (11)
Weight — kg		
Median (IQR)	86 (77–102)	NA
Range	60–115	NA
HIV RNA — copies/no. (%)		
<50 copies/ml	13 (93)	61 (100)
≥50 copies/ml	1 (7)	0
CD4 T-cell count — cells/mm ³		
Median (IQR)	896 (579–1053)	852 (686–1048)
Range	470–1586	350–1667
Nadir CD4 T-cell count — no. (%)		
<201 cells/mm ³	0	3 (5)
201–500 cells/mm ³	12 (86)	39 (64)
>500 cells/mm ³	2 (14)	16 (26)
Unknown	0	3 (5)
Duration from initiation of ART to study entry — yr		
Median (IQR)	4.7 (3.8–6.0)	5.6 (4.1–6.7)
Range	2.7–14.5	0.7–16.8
Duration of suppression — yr		
Median (IQR)	NA	NA
Range	NA	NA
ART regimen — no. (%)		
Abacavir–lamivudine–dolutegravir	4 (29)	0
Abacavir–lamivudine–atazanavir	0	0
Emtricitabine–tenofovir–ritonavir–boosted atazanavir	1 (7)	0
Emtricitabine–tenofovir–ritonavir–boosted darunavir	3 (21)	0
Emtricitabine–tenofovir–dolutegravir	2 (14)	0
Emtricitabine–tenofovir–efavirenz	0	0
Emtricitabine–tenofovir–elvitegravir–cobicistat	3 (21)	0
Emtricitabine–tenofovir–raltegravir	1 (7)	0
Emtricitabine–tenofovir–rilpivirine	0	0
Zidovudine–lamivudine–nelfinavir	0	15 (25)
Zidovudine–lamivudine–indinavir	0	10 (16)
Zidovudine–lamivudine–ritonavir–boosted indinavir	0	4 (7)
Stavudine–lamivudine–indinavir	0	6 (10)
Stavudine–lamivudine–nelfinavir	0	5 (8)
Stavudine–didanosine–nelfinavir	0	2 (3)
Other protease inhibitor–based regimen	0	19 (31)

Table 3.1 Characteristics of the participants at baseline for ACTG Clinical Trial A5340, Step 1. From N Engl J Med., Bar et al., Effect of HIV Antibody VRC01 on Viral Rebound after Treatment Interruption, 375(21). Copyright © (2016) Massachusetts Medical Society. Reprinted with permission.

Figures

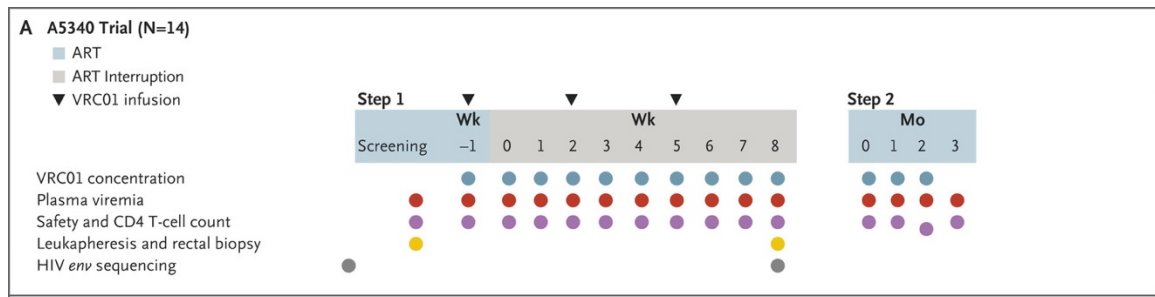


Figure 3.1 A5340 Step 1 Study Schema. The A5340 trial had two steps. In step 1, participants received an intravenous infusion of VRC01 (at a dose of 40 mg per kilogram of body weight) (triangles) 1 week before and 2 and 5 weeks after discontinuation of antiretroviral therapy (ART). ART was discontinued 1 week after the first VRC01 infusion. The treatment interruption was open-ended, and participants were monitored weekly until viral rebound. On confirmed plasma viral rebound, participants entered step 2 and ART was reinitiated. Participants were then followed until plasma viremia decreased below 50 copies per milliliter. HIV *env* sequencing (gray circles) was performed with the use of plasma samples obtained before the initiation of ART and after viral rebound. From N Engl J Med., Bar et al., Effect of HIV Antibody VRC01 on Viral Rebound after Treatment Interruption, 375(21). Copyright © (2016) Massachusetts Medical Society. Reprinted with permission.

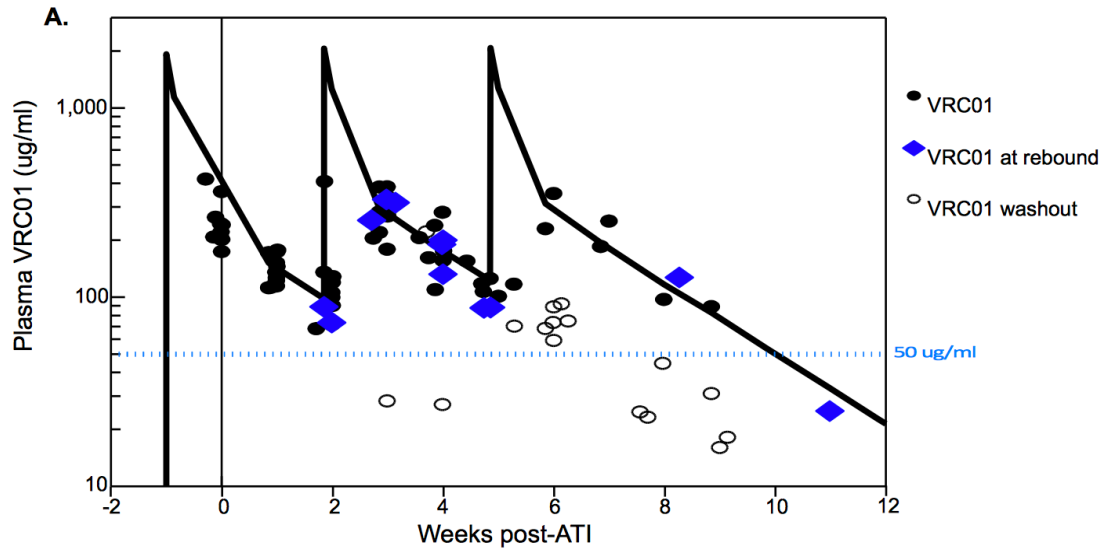


Figure 3.2 Early viral rebound despite high plasma levels of VRC01. A. Plasma concentrations of VRC01 for all participants are plotted against time of ATI. All participants maintained plasma levels of VRC01 greater than 50 $\mu\text{g/ml}$ for more than 8 weeks and 12/13 participants experienced viral rebound with these levels. Solid circles indicate measured levels before viral rebound; open circles were obtained after viral rebound. The blue diamonds indicate levels of VRC01 at the time point of first detectable viremia. Modeling of VRC01 pharmacokinetics shown by black line. From N Engl J Med., Bar et al., Effect of HIV Antibody VRC01 on Viral Rebound after Treatment Interruption, 375(21). Copyright © (2016) Massachusetts Medical Society. Reprinted with permission.

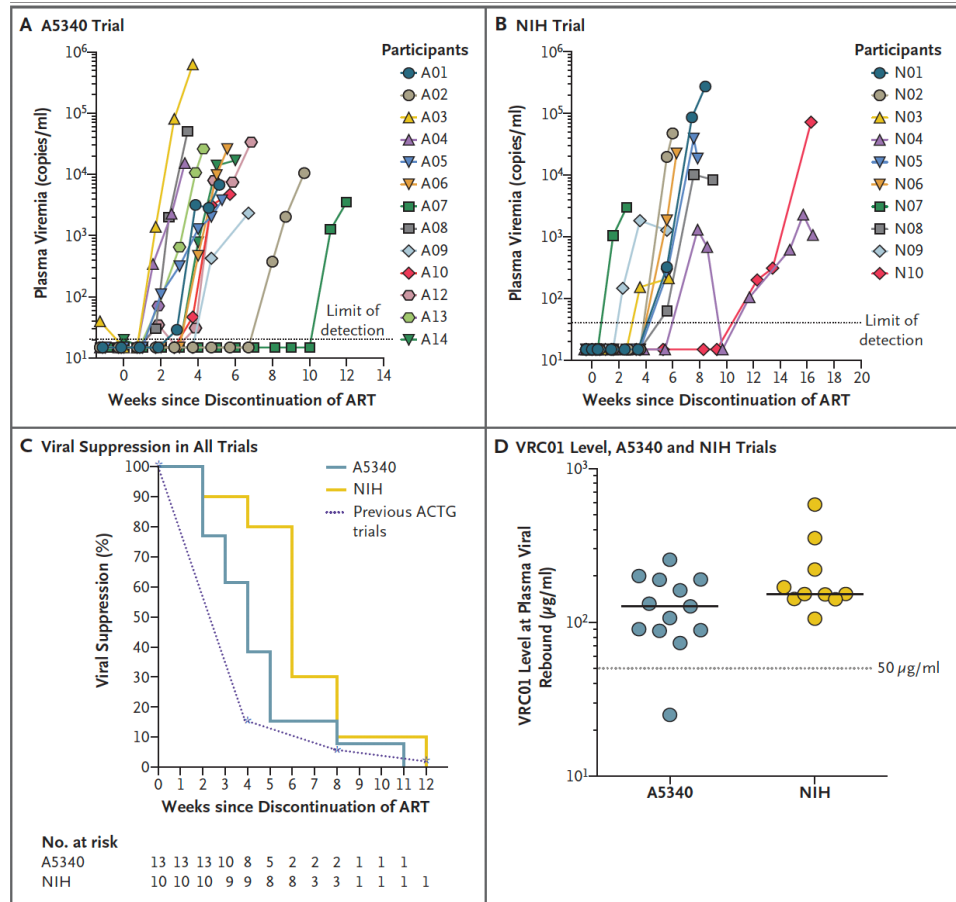


Figure 3.3 Plasma viremia and levels of VRC01 in trial participants after discontinuation of ART. Panel A shows the plasma viremia of participants in the A5340 trial after initiation of ATI. Gray dotted line indicated limit of detection of the assay (HIV RNA level, 20 copies per milliliter). Panel B shows the plasma viremia of NIH trial participants after ATI. The gray dotted line indicates the limit of detection in the assay (HIV RNA level, 40 copies per milliliter). Panel C shows the Kaplan-Meier curve of plasma viral suppression (<200 copies per milliliter) after VRC01 administration and ATI in A5340 and NIH trial participants as compared with historical participants in AIDS Clinical Trials Group (ACTG) trials who underwent ATI without other immunotherapeutic interventions. Panel D shows in vivo plasma levels of VRC01 at first detectable viremia. The limit of detection of VRC01 was less than 0.98 μg per milliliter. From *N Engl J Med.*, Bar et al., Effect of HIV Antibody VRC01 on Viral Rebound after Treatment Interruption, 375(21). Copyright © (2016) Massachusetts Medical Society. Reprinted with permission.

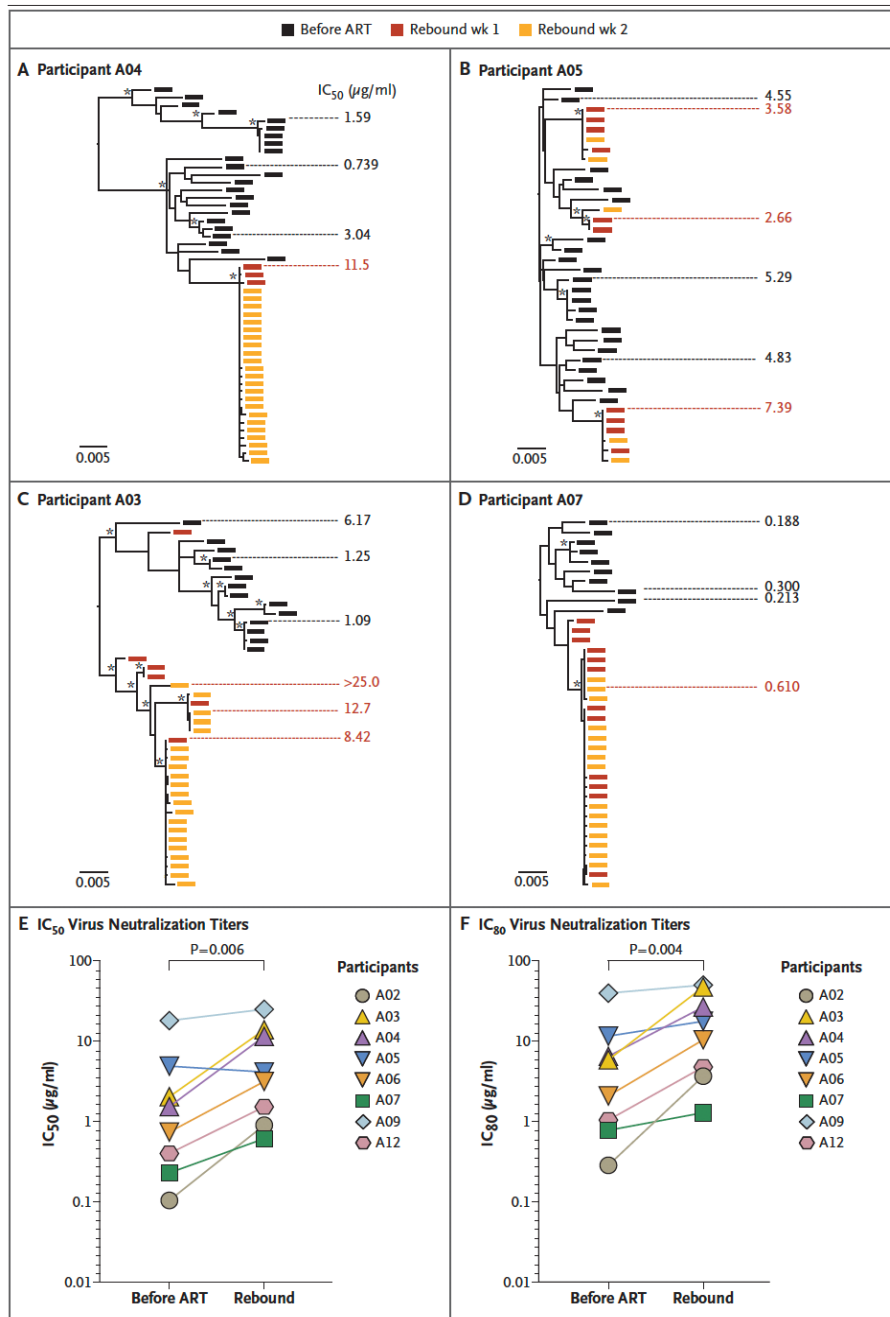


Figure 3.4 VRC01 neutralization titers before ART and during viral rebound.

Panels A through D show maximum likelihood phylogenetic trees of single-genome sequencing–derived env sequences from pre-ART and rebound plasma virus and neutralization titers to VRC01 from four participants. Participants A04, A05, and A03 had early viral rebound despite high levels of VRC01; Participant A07 had delayed rebound with lower plasma VRC01 levels. Black rectangles indicate pre-ART plasma env sequences, and red and orange rectangles indicate the env sequences from the first and second weeks of detectable viremia. The scale bar indicates genetic distance. Fifty

percent inhibitory concentration (IC50) neutralization titers are shown to the side of each tree aligned to the specific envelope glycoprotein that was cloned and tested for phenotypic features. Asterisks indicate bootstrap support of greater than 80%. As shown in Panel A, Participant A04 had monoclonal rebound with VRC01-resistant virus. As shown in Panel B, Participant A05 had polyclonal rebound with VRC01-resistant virus. As shown in Panel C, Participant A03 had polyclonal rebound with VRC01-resistant virus. Multiple rebound lineages arise clustered within one area of the phylogeny. Sequences from Participant A03 were tested for clustering; Slatkin–Maddison and Hudson’s “nearest neighbor” tests support sequence compartmentalization ($P < 0.001$ and $P = 0.004$, respectively). As shown in Panel D, Participant A07 had polyclonal rebound of VRC01-sensitive virus. As shown in Panels E and F, pre-ART and rebound Env pseudotyped virus from the eight participants with available samples were compared for changes in neutralization sensitivity by IC50 (truncated at 25 μg per milliliter) (Panel E) and 80% inhibitory concentration (IC80) (truncated at 50 μg per milliliter) (Panel F) with the use of multilevel random-effects models (random intercept and slope) to account for multiple clones per participant at each time point. A two-sided P value for the estimated difference in pre-ART and rebound resistance was calculated. Mean titers are shown for pre-ART virus on the left and rebound virus on the right. From *N Engl J Med.*, Bar et al., Effect of HIV Antibody VRC01 on Viral Rebound after Treatment Interruption, 375(21). Copyright © (2016) Massachusetts Medical Society. Reprinted with permission.

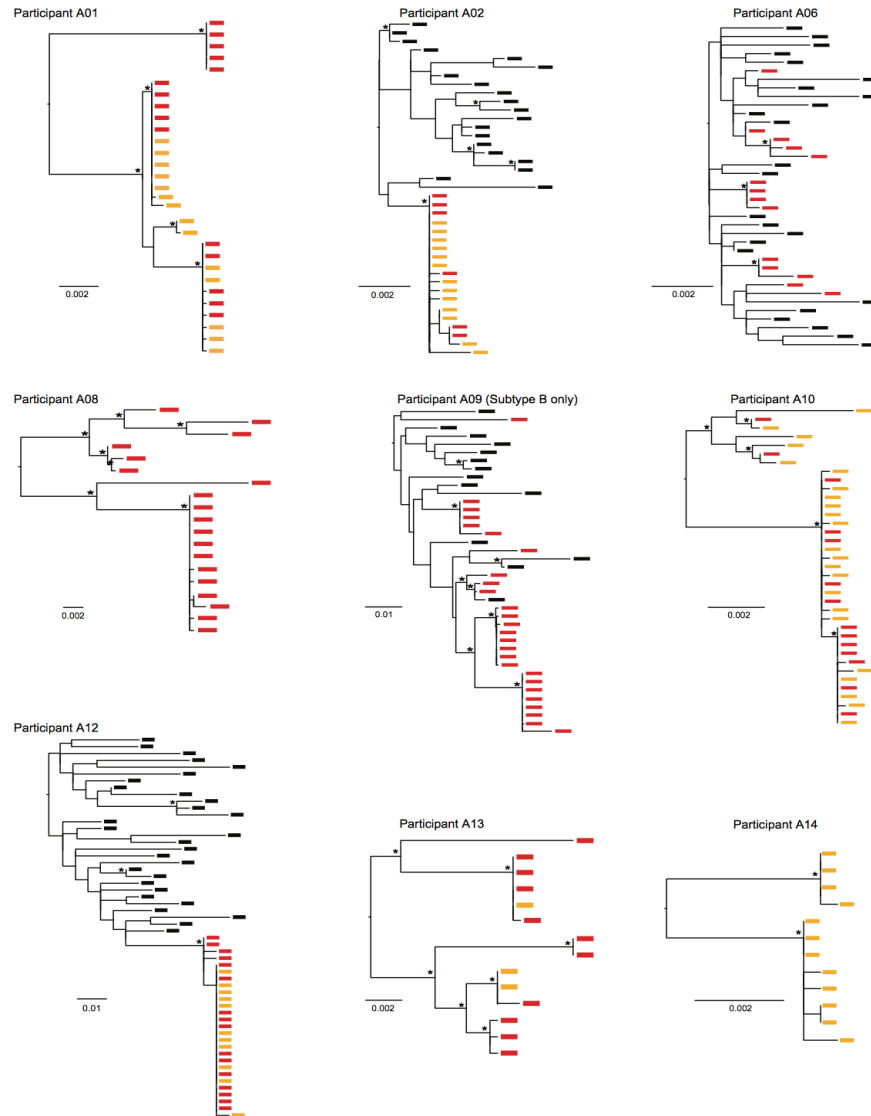


Figure 3.5 Maximum Likelihood (ML) phylogenetic trees of individual participants. Maximum likelihood phylogenetic trees of gp160 env sequences from participants not displayed in Figure 3 are shown, except Participant 11, whose sequences were not evaluated due to early discontinuation of ART. Pre-ART sequences are shown in black, rebound sequences from weeks 1 and 2 of detectable viremia are shown in red and orange, respectively. Genetic distance scale bars are shown for each tree and bootstrap support >70% is shown with asterisks. Pre-ART plasma was not available in participants A01, A08, A10, A13, A14. For participant A09, only the Subtype B sequences are displayed here to allow for assessment of the relatively smaller genetic distances between the pre ART and rebound subtype B sequences. Monoclonal rebound lineages are seen in participants A02 and A12. Polyclonal lineages are seen in participants A01, A06, A08, A09, A10, A13, and A14. From *N Engl J Med.*, Bar et al., *Effect of HIV Antibody VRC01 on Viral Rebound after Treatment Interruption*, 375(21). Copyright © (2016) Massachusetts Medical Society. Reprinted with permission.

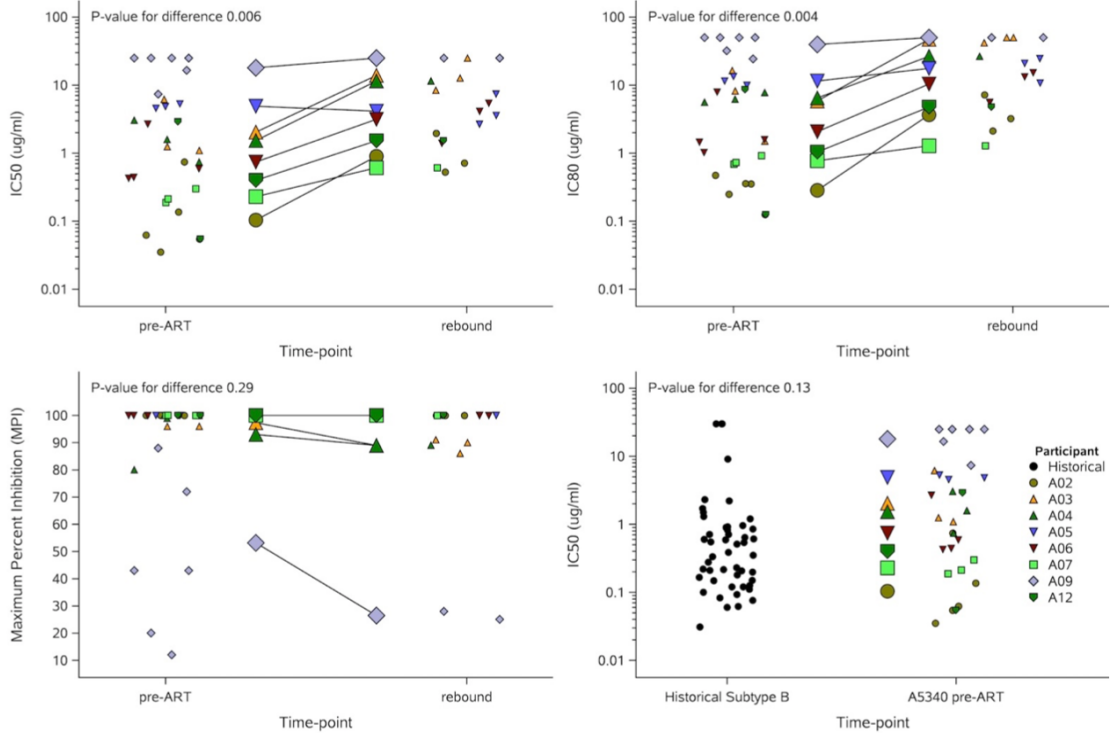


Figure 3.6 VRC01-resistance of pre-cART and rebound viruses.

Pre-ART and rebound Envs from the eight participants with available samples were compared for changes in neutralization sensitivity by IC₅₀ (truncated at 25 $\mu\text{g/mL}$), IC₈₀ (truncated at 50 $\mu\text{g/mL}$) and MPI. Individual Env titers were plotted laterally, while the mean titers per participant were compared between time points centrally. A. By IC₅₀, there was a 3.44 fold increase (two-sided random-effects model p value=0.006). B. By IC₈₀, there was a 3.79 fold increase (two-sided random-effects model p value of 0.004). C. No change seen in MPI. D. There was a statistically non-significant trend towards increased resistance comparing the Pre-ART IC₅₀ titers for the eight A5340 participants (represented as mean of each participant's individual Envs) to the 49 subtype B Envs reported in the 2010 report initially characterizing VRC0125, two-sided random-effects model p=0.13. From *N Engl J Med.*, Bar et al., Effect of HIV Antibody VRC01 on Viral Rebound after Treatment Interruption, 375(21). Copyright © (2016) Massachusetts Medical Society. Reprinted with permission.

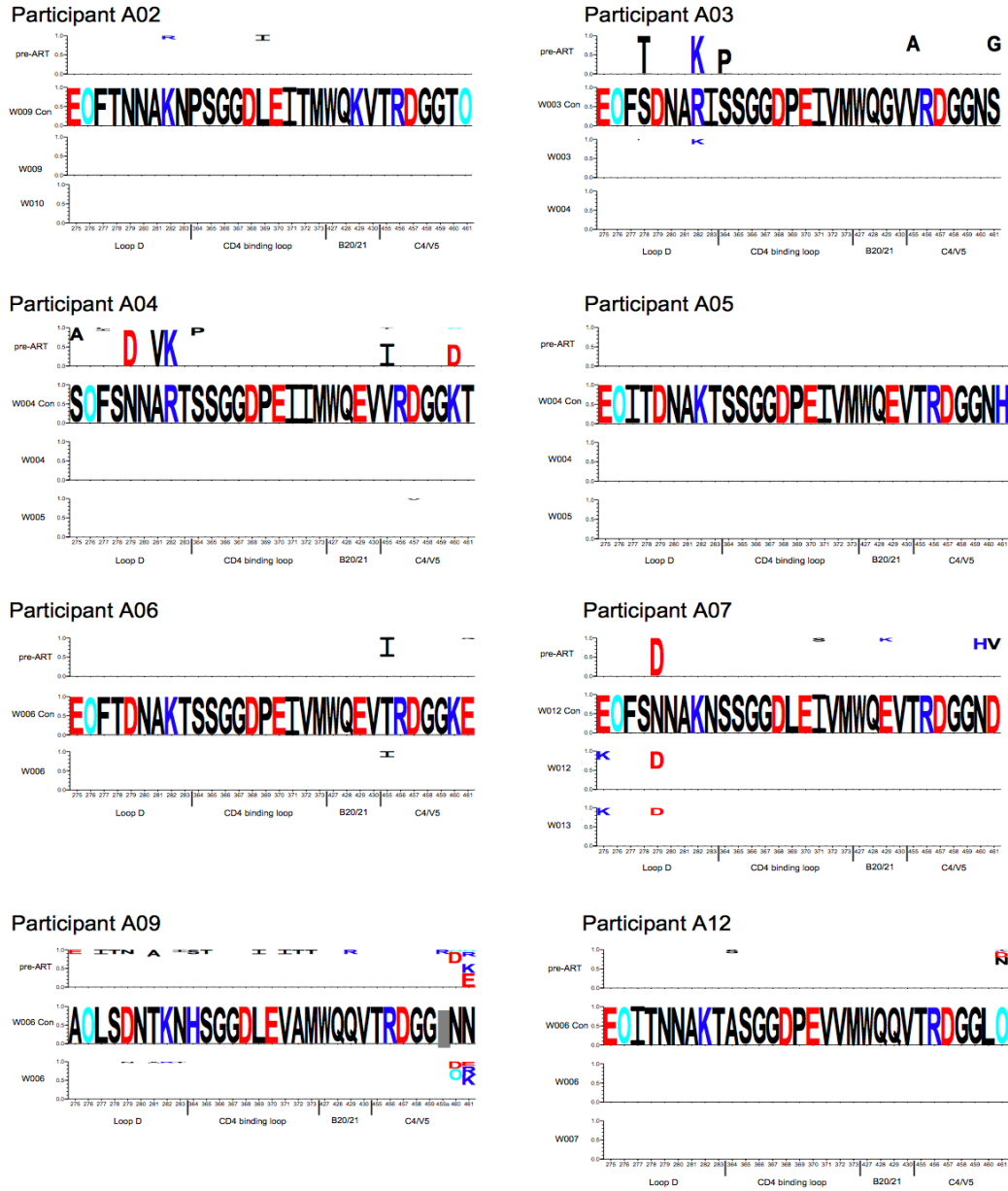


Figure 3.7 VRC01 antibody footprint sequence changes from pre-cART to rebound.

To analyze changes in the predicted VRC01 antibody binding regions between pre-ART and rebound virus populations, modified longitudinal logo plots were generated with the Longitudinal Antigenic Sequences and Sites from Intra-host Evolution (LASSIE) tool¹⁶. The VRC01 binding footprint was represented by Env residues in Loop D, CD4 binding loop, β 20/ β 21 regions, and the base of V5 that are known VRC01 contact residues¹⁷. All sequences were compared to the consensus of the rebound viruses, which is displayed as color-coded, bold letters in the second line. The top line shows amino acid differences in the pre-ART sequences from the rebound consensus. The consensus was generated as a majority-rule consensus using sequences from the earliest time point post-rebound.

Residues were colored as follows: acidic residues (ED) in red, basic residues (HKR) in dark blue, asparagines within N-linked glycosylation sequons (NXS/T, depicted as an "O") in cyan, and all other amino acids in black. Gaps are treated as characters. Several participants, including participants A03 and A04, show substantial changes in the binding footprint between the pre-ART and rebound sequences, suggesting selection for a minor variant to arise in rebound. Other participants show minimal changes in the binding footprint. Between week 1 and 2 of rebound, minimal changes are seen within the VRC01 binding footprint. From *N Engl J Med.*, Bar et al., Effect of HIV Antibody VRC01 on Viral Rebound after Treatment Interruption, 375(21). Copyright © (2016) Massachusetts Medical Society. Reprinted with permission.

Discussion

Passive infusions of CD4bs bNAbs have recently entered the clinical trial pipeline and have shown significant and prolonged viral load reduction in the majority of viremic participants and are now being tested in ATI trials to determine their curative capacity¹. In some individuals, however, bNAb resistant variants prevented successful viral suppression²⁴. These data suggest either that replicating autologous viruses may undergo rapid viral escape during passive infusion, or viruses harbor pre-existing mutations that confer bNAb resistance. In the A5340 clinical trial, I evaluated the effects of VRC01 infusion in the setting of ATI in 13 chronically infected, cART suppressed participants. I hypothesized that chronically infected cART-suppressed participants would harbor a minority population of pre-existing resistant HIV-1 in the viral reservoir, which would decrease the time to first detectable rebound and restrict the clonality of the rebound viral quasispecies. In this study, I used SGS methods and phenotypic analyses of pre-cART and rebound plasma viruses to identify mechanisms that determine viral rebound dynamics during VRC01 infusion.

Multiple VRC01 infusions were found to be safe and well tolerated, with high levels of circulating VRC01 in the plasma. Despite this observation, only a modest delay in the time to viral rebound was observed compared to historical controls, and the majority of participants rebounded during high levels of circulating VRC01 (>50µg/ml). Sequence analyses of pre-cART and rebound viruses from 8 participants show that VRC01 can restrict the clonality of the emerging rebound population. This was specifically observed in participants with a range of VRC01 sensitivities in pre-cART plasma. During VRC01

infusion and ATI, these participants had monoclonal or oligoclonal viral populations that established viral rebound. In contrast, participants with several highly resistant pre-cART viruses, polyclonal rebound populations emerged during rebound. While *de novo* generation of VRC01 resistance cannot be completely eliminated due to sampling limitations, the rapid timing of viral rebound in most participants suggests that pre-existing resistance to VRC01 is the more likely explanation for rapid viral rebound in this clinical trial. Together these data suggest that VRC01 exerts significant pressure on latently infected cells and selects for pre-existing resistant viruses from the reservoir.

It is important to note that sampling of plasma viruses before the initiation of cART only provides a limited assessment of viruses that could possibly reactivate from the viral reservoir. Due to the timing of viral rebound in this study, however, it is more likely that pre-existing resistance drives rapid viral rebound upon ATI and high levels of circulating VRC01. Additionally, our findings of pre-existing VRC01 resistance driving rapid viral rebound were also observed in an independent clinical trial NIH 15-I-0140. In the NIH trial, evidence of selection pressure exerted by VRC01 was identified through sequence analyses, where specific amino acid changes within VRC01 binding epitopes were commonly found among pre-cART and rebound viruses. The NIH trial results were published together with A5340 in Bar et al. *NEJM*, 2016. Additionally, similar findings were observed in a recently conducted bNAb clinical trial testing the safety and efficacy of the more potent CD4 bs bNAb, 3BNC117². Four infusions of 3BNC117 delayed viral rebound for up to 19 weeks in select participants, and further sequence analyses of pre-infusion viral isolates and rebound viruses also show that pre-existing resistance predicts the pattern and timing of viral rebound.

By assessing VRC01 resistance among multiple pre-cART and rebound viruses, I was able to highlight the striking prevalence of VRC01 resistance among the majority of study participants and its relationship to the timing and patterns of viral rebound. Importantly, our finding highlights that minority variants with pre-existing VRC01 resistance can be archived within the viral reservoir and potentially contribute to viral rebound upon VRC01 infusion. This finding presents a significant challenge for future studies testing bNAb efficacy in monotherapy trials, but also highlights the important observation that bNAb monotherapy can exert modest but significant pressure on viruses that emerge from the reservoir.

To determine mechanisms of viral rebound during VRC01 infusion and ATI, I performed sequence analyses of pre-cART and rebound plasma samples and assessed baseline differences in viral diversity. Through these methods, I found that baseline resistance to VRC01 is common. The prevalence of VRC01 resistance in pre-cART plasma was associated with decreased time to viral rebound and the emergence of polyclonal viral lineages upon treatment interruption. These rebounding lineages were also VRC01-resistant. In participants with a diverse pool of VRC01-sensitive and VRC01-resistant viruses, I observed monoclonal or oligoclonal rebound viruses, suggesting VRC01 is also able to restrict the clonality of viruses that can emerge from the latent reservoir. In participants who rebounded beyond week 4, I found monoclonal or oligoclonal populations emerge. One participant, A07, rebounded at 11 weeks as VRC01 plasma levels waned significantly. As expected, this participant harbored VRC01 sensitive pre-cART viruses and maintained sensitivity to VRC01 in its oligoclonal rebound population as well.

Modest delays in viral rebound in combination with the clonal restriction observed in some participants suggest that VRC01 exhibits modest pressure on reactivating viruses from the viral reservoir and is an encouraging finding in the bNAb therapeutic field. While monotherapy of VRC01 may not be potent enough for successful, long-term cART-free remission, other studies analyzing the effect of combination bNAb infusions are promising.

Materials and Methods

Study Design and Oversight

AIDS Clinical Trials Group (ACTG) A5340, was a phase 1, two-step, open-label study of the safety, tolerability, pharmacokinetics (PK) and antiviral activity of the human monoclonal antibody, VRC-HIVMAB060-00-AB (VRC01) in HIV-infected individuals undergoing brief ATI (ClinicalTrials.gov identifier NCT02463227). We enrolled 14 HIV-1 infected men, ages ≥ 18 years, who had a CD4 T-cell count of ≥ 450 cells/ μL , undetectable plasma viral load (< 50 copies/mL) for at least 24 weeks, CD4 nadir > 200 cells/ μL , and no known ART during acute or early infection. We excluded participants receiving non-nucleoside reverse transcriptase inhibitor (NNRTI) based ART due to the prolonged half-life of those drugs and the potential risk for development of resistance^{24,25}. Complete inclusion criteria are presented in the Supplement of this publication.

In Step 1, participants received up to three doses of VRC01 (40mg/kg intravenously) at three-week intervals (see Figure 1). One week after the first dose of VRC01, participants

stopped ART and were followed at weekly intervals until they had confirmed CD4 T-cell count <350 cells/ μ L or return of HIV-1 viremia, defined as HIV-1 RNA \geq 200 copies/ml followed by a confirmation \geq 1000 copies/ml, or three consecutive measurements \geq 200 copies/ml. Upon confirmation of viral rebound or CD4 T-cell decline, participants entered Step 2, when ART was reinitiated and HIV-1 viral load was followed until below 50 copies/ml.

The primary objectives of the study were to assess the safety and tolerability of multiple doses of VRC01 administered in individuals with well controlled viral replication and to estimate the proportion of participants with return of viremia in the presence of high levels of bNAb at 8 weeks of ATI. Secondary objectives were frequency of rebound viremia at 4 weeks and the evaluation of the PK parameters of the product. Key exploratory objectives were the frequency of development of antibodies against VRC01 and the genetic and phenotypic characterization of the rebound HIV-1 viruses.

The study was powered for 13 evaluable participants, which provided 95% power to detect a difference of 40% (*i.e.*, return of viremia by 8 weeks in 50% vs. 90% in historical controls)²¹ using a one-sided test with a significance level of 0.05. The time to viral rebound was compared with historical controls from other treatment interruption trials conducted by the AIDS Clinical Trials Group (ACTG)²¹. Details of the control group, participant monitoring, and laboratory and statistical methods are outlined in the online supplement.

The study was conducted at two ACTG sites: the University of Pennsylvania and the University of Alabama Birmingham. All participants provided written informed consent.

All the authors vouch for the accuracy and completeness of the data and the fidelity of the study to the protocol.

Study inclusion criteria

In addition to HIV-specific criteria, exclusion criteria included known treatment during acute infection, previous receipt of a humanized or human mAb, treatment with systematic glucocorticoids or other immunomodulators, active hepatitis B or C virus infection, ongoing opportunistic infection(s), history of an AIDS-defining illness, history of severe allergic reactions, abnormal laboratory values, inadequate venous access, and weight >115 or <53 kilograms. A plasma or serum specimen before the initiation of ART was required for at least 8 participants.

VRC01 antibody product

The VRC01 antibody product was manufactured by the NIAID/Vaccine Research Center (VRC) using recombinant DNA technology in the mammalian Glutamine Synthetase Gene Expression System in the Chinese hamster ovary (CHO) cell line developed by Lonza Biologics (Slough, UK). The 40 mg/kg dosing strategy was chosen based on the observed 14 day half-life in aviremic HIV-infected individuals in prior trials^{1,2}.

Adverse Events Monitoring

Diagnosis, signs and symptoms, and laboratory results were graded using version 2.0 of the Division of AIDS (DAIDS) adverse events (AEs) grading table, and assessed for relationship to VRC01 by the core study team. Post-entry, sites were required to report all signs and symptoms of grade 2 or higher, as well as all solicited signs and symptoms that were grade <2 from an infusion report card asking participants about injection site

pain, redness, swelling and induration, as well as systematic AEs like feeling unwell, muscle aches, headache and chills during the 7 days after receipt of the antibody. All diagnoses identified by the ACTG criteria for clinical events and other diseases were additionally required to be reported. DAIDS AEs grading table described at: <http://rsc.tech-res.com/safetyandpharmacovigilance/gradingtables.aspx>. ACTG criteria described at <http://reprivetrial.org/wp-content/uploads/2014/11/Appendix100.pdf>.

Historical ACTG data on control ATI group

There have been six previous ACTG clinical trials that have utilized analytical treatment interruptions (ATI). A total of 61 participants were on suppressive non-NNRTI ART started during chronic infection and received no immunologic interventions. At week 4 of the ATI the proportion of participants with virologic suppression <200 copies/mL was 13% (8/61), and at week 8 it was 3% (2/61) (Fig. 3.3C) For the comparison with historical controls we used participants in ACTG trials that were receiving non-NNRTI-based regimens because of the prolonged half-life of NNRTIs artificially delayed the return of viremia.

Power calculations

We planned to enroll 15 participants; all receiving VRC01. We assumed a 15% loss to follow-up or non-protocol required study treatment discontinuation, to have a total of 13 evaluable participants for planned per-protocol analysis, using the binomial distribution and the conservative assumption that in the absence of an intervention 90% will have a return of viremia within 8 weeks of treatment interruption, we had 95% power to detect a difference of 40% (i.e., return of viremia by 8 weeks in 50%) using a one-sided test with

a significance level of 0.05. Regarding the assessment of safety, the sample size of 15 VRC01-treated participants would provide a 90% probability of observing a VRC01-related AE that would occur in 14% or more of treated participants. After enrollment of 13 evaluable participants for the primary efficacy analysis, recruitment was stopped with a total of 14 participants receiving VRC01.

Trial outcome analysis

For analysis of time to first confirmed HIV-1 RNA ≥ 200 copies/ml during the ATI, HIV-1 RNA measurements were binned at the nearest scheduled week. The cumulative probability of remaining virologically suppressed (i.e. no confirmed HIV-1 RNA ≥ 200 copies/ml) was calculated by Kaplan-Meier methods, and at 4 and 8 weeks 90% confidence intervals (CI) were generated using the Clopper-Pearson exact method. Comparison to historical ACTG data was by the one-sided Fisher's exact test, and Spearman's rank correlation coefficients were calculated to assess the relationship between pre-ART and study entry variables with time to first confirmed HIV-1 RNA ≥ 200 copies/ml. For the safety analysis, all participants exposed to VRC01 were included, and the percentage of participants experiencing a grade 3 or higher AE was calculated along with a 95% Clopper-Pearson exact CI.

VRC01 plasma concentration measurements and modeling

Quantification of VRC01 concentrations in participant serum and individual participant noncompartmental PK analysis were performed as previously described². Briefly, VRC01 serum concentration quantification was performed in 96-well plates on a Beckman

Biomek–based automation platform using the anti-idiotypic mAb 5C9. Pharmacokinetic data were fit to a two compartment population model using the computer program NONMEM (version 7.2).

Viral RNA extraction, cDNA synthesis, single genome sequencing (SGS)

SGS enables proportional representation of the complex HIV-1 virus quasispecies with linkage across the sequenced region with minimal in vitro errors⁴. Viral RNA extraction, cDNA synthesis, and SGS were performed to amplify gp41 or gp160 env as previously described^{4,5}. Amplicons were directly sequenced and chromatograms were inspected for evidence of priming from multiple templates or introduction of PCR error in early cycles.

Phylogenetic analyses

Sequences from each participant were aligned using ClustalW⁶ and alignments were adjusted as necessary by visual inspection. Regions in within-participant alignments that could not be unambiguously aligned were removed from subsequent phylogenetic analyses. Maximum Likelihood (ML) phylograms for each participant were inferred using PhyML version 3⁷, which jointly estimates the tree and the parameters of the evolutionary model. Evolutionary model classes for within-participant data sets were selected using jModelTest version 2.1.4^{7,8} using the AICc criterion⁹. Within-participant alignments were aligned sequentially using ClustalW. Hypervariable regions as defined in Los Alamos National Laboratory HIV Sequence Database Variable Region Characteristics webtool (http://www.hiv.lanl.gov/content/sequence/VAR_REG_CHAR/) and other regions that could not be unambiguously aligned were removed from the alignment used for the phylogenetic analysis encompassing all of the sequences. Pairwise diversity estimates were performed by DIVEIN¹⁰. Assessment for phylogenetic

clustering within individual participant's sequences was performed by Slatkin-Maddison and Hudson's nearest neighbor tests¹¹⁻¹³. To determine the clonality of rebound viremia, sequences were analyzed by a previously described model of neutral virus evolution^{4, 14}, which assumes virus undergoes rapid expansion without selection. Under this model, low-diversity sequence lineages display a star-like phylogeny and a Poisson distribution of mutations, coalesce to an unambiguous founder sequence enabling estimates of time from a most recent common ancestor (MRCA)^{4, 14,15}. Pairwise nucleotide Hamming distances were calculated using code from the Los Alamos National Laboratory HIV database Variable Region Characteristics webtool (http://www.hiv.lanl.gov/content/sequence/VAR_REG_CHAR/) and other regions that could not be unambiguously aligned were removed from the alignment used for the phylogenetic analysis encompassing all of the sequences (Fig S3). Pairwise diversity estimates were performed by DIVEIN¹⁰. Assessment for phylogenetic clustering within individual participant's sequences was performed by Slatkin-Maddison and Hudson's nearest neighbor tests¹¹⁻¹³. To determine the clonality of rebound viremia, sequences were analyzed by a previously described model of neutral virus evolution^{4, 14}, which assumes virus undergoes rapid expansion without selection. Under this model, low-diversity sequence lineages display a star-like phylogeny and a Poisson distribution of mutations, coalesce to an unambiguous founder sequence enabling estimates of time from a most recent common ancestor (MRCA)^{4, 14,15}. Pairwise nucleotide Hamming distances were calculated using code from the Los Alamos National Laboratory HIV database Poisson Fitter version 2 tool. In calculating Hamming distances, gaps were excluded. For rebound virus populations that met these criteria ($p > 0.05$ in goodness-of-fit to Poisson distribution), recent clonal expansion from a single virus was interpreted to indicate a single virus rebounded from latency to found systemic virus replication during rebound. If rebound sequences violated the conditions

of this model, it was interpreted that more than one virus rebounded from latency to found rebound viremia. All sequences were deposited in GenBank (accession number: KX587007-KX587459).

Env gene cloning and pseudovirus production.

Select env sequences from throughout the pre-ART phylogeny and those representing the consensus sequence of low-diversity rebound lineages were molecularly cloned for the production of pseudovirus and phenotypic analyses as described previously^{4,5}. Briefly, to reduce the probability of generating molecular env clones with Taq polymerase errors, we reamplified from the first-round PCR product under the same nested PCR conditions but used only 25 cycles. Correctly sized amplicons identified by gel electrophoresis were gel-purified by using the QIAquick gel purification kit according to the recommendations of the manufacturer (Qiagen), ligated into the pcDNA3.1 Directional Topo vector (Invitrogen Life Technologies), and transformed into competent TOP10 E. coli bacteria. Bacteria were plated on LB agar plates supplemented with 100 µg/ml ampicillin and cultured at 25°C for 3 days. Single colonies were selected and grown overnight in liquid LB broth at 30°C with 225 rpm shaking followed by plasmid isolation. Finally, each molecular clone was sequence-confirmed to be identical to the previously determined env sequence of the plasma env amplicon. Pseudovirus was prepared by transfecting overnight cultured 3×10^6 293T cells in 10cm² tissue culture dishes with 4 µg of rev/env expression plasmid and 4 µg of HIV-1 backbone: using Fugene 6 (Roche Applied Science, Indianapolis, IN). Pseudovirus containing culture supernatants were harvested 2 days after transfection, cleared of cellular debris by low-speed centrifugation and stored in aliquots at -80°C. Viruses were titrated on TZM-bl reporter cells (8129; NIH AIDS Research and Reference Reagent Program), which

contain a Tat-inducible luciferase and a β -galactosidase gene expression cassette. Infectious titers were measured on 24-well plates based on β -galactosidase production, representing the number of infection events per μL of virus stock (IU/ μL) as described previously¹⁸.

Neutralization assays

Virus neutralization by VRC01 was assessed on TZM-bl cells as described previously¹⁸. TZM-bl cells were seeded at 1×10^4 per well and cultured in 96-well plates overnight. Virus stocks dilutions were made to final concentrations of DMEM containing 6% FBS and 40 $\mu\text{g}/\text{mL}$ DEAE dextran (Sigma-Aldrich, St. Louis, MO) to achieve 2000 IU/well. Equal volume virus dilutions and two to five-fold serially diluted mAbs were mixed and incubated at 37°C for 1 h. Supernatants were then removed and 80 μL of these mixtures were added. Media-only and virus-only control wells were included as background and 100% infectivity, respectively. Luciferase activity was measured after 48 h incubation in 37°C using Bright-Glo per the manufacturer's instructions (Promega). All assays were done in triplicate in each of at least two independent experiments. To calculate the concentration of antibody that neutralized 50% (IC50), and 80% (IC80), of virus infection the antibody dose-response curves were fit with a four parameter logistic regression equation using Prism 5.0 (GraphPad Software Inc. San Diego, CA). When 50% or 80% neutralization was not achieved at the 50 $\mu\text{g}/\text{ml}$ concentration of VRC01, the IC50 or IC80 was recorded as 50 $\mu\text{g}/\text{ml}$. Maximal percent inhibition was calculated by determining the change in infectivity at 50 $\mu\text{g}/\text{ml}$.

VRC01 neutralization resistance analysis

For comparison of pre-ART and rebound VRC01 resistance by cloned Envs, multilevel random effects models (random intercept and slope) were fitted to account for multiple clones per participant at each time-point, and a one-sided p-value for the estimated difference in pre-ART and rebound resistance was calculated. Analysis was performed on the log₁₀ scale for IC₅₀ and IC₈₀. For comparison of pre-ART IC₅₀ to an historical subtype B panel, we used a one-sided exact Wilcoxon rank-sum test to compare the mean pre-ART log₁₀ IC₅₀ in A5340 to the historical subtype B panel. For analysis, IC₅₀ values were truncated at 25 µg/ml and IC₈₀ values were truncated at 50µg/ml. Analyses were performed in SAS version 9.4. The historical subtype B panel IC₅₀ values were obtained in a methodologically similar assay performed in a different laboratory¹⁹.

Acknowledgement: First and foremost, I thank all study volunteers for their participation in the A5340 clinical trial. I also thank Drs. Pablo Tebas and Katharine Bar for their role in designing the clinical trial. The NIH AIDS Reagent Program for providing HIV-specific mononuclear antibodies, Gerald H. Learn for single genome sequencing and phylogenetic analyses, and all staff of the Center for AIDS Research (CFAR) at the University of Pennsylvania for their technical assistance (P30-AI045008). This work was supported by an award from the National Institute of Allergy and Infectious Diseases (NIAID) (U01AI068636); grants from the Penn Center for AIDS Research (P30 AI045008), the Penn Clinical Trials Unit (AI069534), the University of Alabama at Birmingham (UAB) Center for AIDS Research (P30 AI027767), the UAB Clinical Trials Unit (AI069452), the AIDS Clinical Trials Group Statistical and Data Analysis Center (UM1 AI068634), the NIAID (1-R21-AI118431, for A5340 viral analyses), a Ruth L.

Kirschstein National Research Service Award (F30 AI112426, to Dr. Kreider), and a T32 Training Grant in HIV Pathogenesis (2T32AI007632).

References

1. Marasco WA, Sui J. The growth and potential of human antiviral monoclonal antibody therapeutics. *Nat Biotechnol* 2007; 25: 1421-34.
2. Brekke OH, Sandlie I. Therapeutic antibodies for human diseases at the dawn of the twenty-first century. *Nat Rev Drug Discov* 2003; 2: 52-62.
3. Burton DR, Mascola JR. Antibody responses to envelope glycoproteins in HIV-1 infection. *Nat Immunol* 2015; 16: 571-6.
4. Halper-Stromberg A, Nussenzweig MC. Towards HIV-1 remission: potential roles for broadly neutralizing antibodies. *J Clin Invest* 2016; 126: 415-23.
5. Wu X, Yang ZY, Li Y, et al. Rational design of envelope identifies broadly neutralizing human monoclonal antibodies to HIV-1. *Science* 2010; 329: 856-61.
6. Ko SY, Pegu A, Rudicell RS, et al. Enhanced neonatal Fc receptor function improves protection against primate SHIV infection. *Nature* 2014; 514: 642-5.
7. Pegu A, Yang ZY, Boyington JC, et al. Neutralizing antibodies to HIV-1 envelope protect more effectively in vivo than those to the CD4 receptor. *Sci Transl Med* 2014; 6: 243ra88.
8. Mascola JR, Stiegler G, VanCott TC, et al. Protection of macaques against vaginal transmission of a pathogenic HIV-1/ SIV chimeric virus by passive infusion of neutralizing antibodies. *Nat Med* 2000; 6: 207-10.
9. Gautam R, Nishimura Y, Pegu A, et al. A single injection of anti-HIV-1 antibodies protects against repeated SHIV challenges. *Nature* 2016; 533: 105-9.
10. Chun TW, Moir S, Fauci AS. HIV reservoirs as obstacles and opportunities for an HIV cure. *Nat Immunol* 2015; 16: 584-9.
11. Davey RT Jr, Bhat N, Yoder C, et al. HIV-1 and T cell dynamics after interruption of highly active antiretroviral therapy (HAART) in patients with a history of sustained viral suppression. *Proc Natl Acad Sci U S A* 1999; 96: 15109-14.
12. Chun TW, Davey RT Jr, Engel D, Lane HC, Fauci AS. Re-emergence of HIV after stopping therapy. *Nature* 1999; 401: 874-5.

13. The Strategies for Management of Anti-retroviral Therapy (SMART) Study Group. CD4+ count-guided interruption of antiretroviral treatment. *N Engl J Med* 2006; 355: 2283-96.
14. Li JZ, Etemad B, Ahmed H, et al. The size of the expressed HIV reservoir predicts timing of viral rebound after treatment interruption. *AIDS* 2016; 30: 343-53.
15. Balazs AB, Chen J, Hong CM, Rao DS, Yang L, Baltimore D. Antibody-based protection against HIV infection by vectored immunoprophylaxis. *Nature* 2012; 481: 81-4.
16. Johnson PR, Schnepf BC, Zhang J, et al. Vector-mediated gene transfer engenders long-lived neutralizing activity and protection against SIV infection in monkeys. *Nat Med* 2009; 15: 901-6.
17. Chun TW, Murray D, Justement JS, et al. Broadly neutralizing antibodies suppress HIV in the persistent viral reservoir. *Proc Natl Acad Sci U S A* 2014; 111: 13151-6.
18. Barouch DH, Whitney JB, Moldt B, et al. Therapeutic efficacy of potent neutralizing HIV-1-specific monoclonal antibodies in SHIV-infected rhesus monkeys. *Nature* 2013; 503: 224-8.
19. Schoofs T, Klein F, Braunschweig M, et al. HIV-1 therapy with monoclonal antibody 3BNC117 elicits host immune responses against HIV-1. *Science* 2016; 352: 997-1001.
20. Shingai M, Nishimura Y, Klein F, et al. Antibody-mediated immunotherapy of macaques chronically infected with SHIV suppresses viraemia. *Nature* 2013; 503: 277-80.
21. Klein F, Halper-Stromberg A, Horwitz JA, et al. HIV therapy by a combination of broadly neutralizing antibodies in humanized mice. *Nature* 2012; 492: 118-22.
22. Caskey M, Klein F, Lorenzi JC, et al. Viraemia suppressed in HIV-1-infected humans by broadly neutralizing antibody 3BNC117. *Nature* 2015; 522: 487-91.
23. Ledgerwood JE, Coates EE, Yamshchikov G, et al. Safety, pharmacokinetics and neutralization of the broadly neutralizing HIV-1 human monoclonal antibody VRC01 in healthy adults. *Clin Exp Immunol* 2015; 182: 289-301.
24. Lynch RM, Boritz E, Coates EE, et al. Virologic effects of broadly neutralizing antibody VRC01 administration during chronic HIV-1 infection. *Sci Transl Med* 2015; 7: 319ra206.
25. Keele BF, Giorgi EE, Salazar-Gonzalez JF, et al. Identification and characterization of transmitted and early founder virus envelopes in primary HIV-1 infection. *Proc Natl Acad Sci U S A* 2008; 105: 7552-7.

26. Rothenberger MK, Keele BF, Wietgreffe SW, et al. Large number of rebounding/founder HIV variants emerge from multifocal infection in lymphatic tissues after treatment interruption. *Proc Natl Acad Sci U S A* 2015; 112(10): E1126-34.
27. Kearney MF, Wiegand A, Shao W, et al. Origin of rebound plasma HIV includes cells with identical proviruses that are transcriptionally active before stopping of antiretroviral therapy. *J Virol* 2015; 90: 1369-76.
28. Bednar MM, Hauser BM, Zhou S, et al. Diversity and tropism of HIV-1 rebound virus populations in plasma level after treatment discontinuation. *J Infect Dis* 2016; 214: 403-7.
29. Parrish NF, Gao F, Li H, et al. Phenotypic properties of transmitted founder HIV-1. *Proc Natl Acad Sci U S A* 2013; 110: 6626-33.
30. Zhou T, Georgiev I, Wu X, et al. Structural basis for broad and potent neutralization of HIV-1 by antibody VRC01. *Science* 2010; 329: 811-7.
31. Kong R, Louder MK, Wagh K, et al. Improving neutralization potency and breadth by combining broadly reactive HIV-1 antibodies targeting major neutralization epitopes. *J Virol* 2015; 89: 2659-71.
32. Bouvin-Pley M, Morgand M, Meyer L, et al. Drift of the HIV-1 envelope glycoprotein gp120 toward increased neutralization resistance over the course of the epidemic: a comprehensive study using the most potent and broadly neutralizing monoclonal antibodies. *J Virol* 2014; 88:13910-7.
33. Binley JM, Lybarger EA, Crooks ET, et al. Profiling the specificity of neutralizing antibodies in a large panel of plasmas from patients chronically infected with human immunodeficiency virus type 1 subtypes B and C. *J Virol* 2008; 82: 11651-68.
34. Lynch RM, Tran L, Louder MK, et al. The development of CD4 binding site antibodies during HIV-1 infection. *J Virol* 2012; 86: 7588-95.
35. Gray ES, Madiga MC, Moore PL, et al. Broad neutralization of human immunodeficiency virus type 1 mediated by plasma antibodies against the gp41 membrane proximal external region. *J Virol* 2009; 83: 11265-74.
36. Bar KJ, Tsao CY, Iyer SS, et al. Early low-titer neutralizing antibodies impede HIV-1 replication and select for virus escape. *PLoS Pathog* 2012; 8(5): e1002721.
37. Chun TW, Stuyver L, Mizell SB, et al. Presence of an inducible HIV-1 latent reservoir during highly active antiretroviral therapy. *Proc Natl Acad Sci U S A* 1997; 94: 13193-7.
38. Finzi D, Blankson J, Siliciano JD, et al. Latent infection of CD4+ T cells provides a mechanism for lifelong persistence of HIV-1, even in patients on effective combination therapy. *Nat Med* 1999; 5: 512-7.

39. Wong JK, Hezareh M, Günthard HF, et al. Recovery of replication-competent HIV despite prolonged suppression of plasma viremia. *Science* 1997; 278: 1291-5.
40. Fischl MA, Richman DD, Grieco MH, et al. The efficacy of azidothymidine (AZT) in the treatment of patients with AIDS and AIDS-related complex. *N Engl J Med* 1987; 317: 185-91.
41. Larder BA, Darby G, Richman DD. HIV with reduced sensitivity to zidovudine (AZT) isolated during prolonged therapy. *Science* 1989; 243: 1731-4.
42. Hammer SM, Squires KE, Hughes MD, et al. A controlled trial of two nucleoside analogues plus indinavir in persons with human immunodeficiency virus infection and CD4 cell counts of 200 per cubic millimeter or less. *N Engl J Med* 1997; 337: 725-33.
43. Gulick RM, Mellors JW, Havlir D, et al. Treatment with indinavir, zidovudine, and lamivudine in adults with human immunodeficiency virus infection and prior antiretroviral therapy. *N Engl J Med* 1997; 337: 734-9.
44. Delaney M. The development of combination therapies for HIV infection. *AIDS Res Hum Retroviruses* 2010; 26: 501-9.

CHAPTER 4

HIV-1 Latent Reservoir Size and Diversity are Stable Following Brief Treatment Interruption

This work was published in the following publication:

Salantes DB, Zheng Y, Mampe F, Srivastava T, Beg S, Lai J, Li JZ, Tressler RL, Koup RA, Hoxie J, Abdel-Mohsen M, Sherrill-Mix S, McCormick K, Overton ET, Bushman FD, Learn GH, Siliciano RF, Siliciano JM, Tebas P, Bar KJ. *Journal of Clinical Investigation*. 2018. Pii: 120194. doi: 10.1172/JCI120194.

Abstract

Analytical treatment interruption of cART in HIV-infected individuals is an important component of HIV-1 cure strategy clinical trials. While brief, closely monitored ATIs are generally considered to be clinically safe^{1,2}, the effect of transient rebound viremia on the size and composition of the latent reservoir is unknown. In the previously described ACTG clinical trial A5340 (presented in Chapter 3 of this thesis), the safety and tolerability of passively infused CD4 bs bNAb, VRC01, was tested under ATI conditions in chronically infected participants. Only a modest delay in viral rebound was observed in the majority of participants compared to ATI studies without immunotherapeutic intervention. Phenotypic and genotypic analyses of available pre-cART viruses from these participants identified a high prevalence of pre-existing VRC01 resistance, which was associated with viral rebound kinetics. Nine participants underwent leukapheresis prior to ATI and six months after rapid re-suppression of plasma viremia with cART. In this study, I applied quantitative and qualitative analyses on archived leukapheresis and plasma samples collected prior to, during and after ATI in order to determine the effect of ATI on the size and composition of the latent reservoir. Additionally, through SGS methods, I also identified large, clonally expanded viruses from Quantitative Viral Outgrowth Assays (QVOA) and genetically intact proviruses in resting CD4 T cells, though these expanded clones fail to accurately predict viruses that reactivate in vivo. Taken together, these results demonstrate that brief ATI with transient viremia does not substantially impact the diversity of the peripheral viral reservoir, though the discordance between large, clonally expanded lineages identified by QVOA and proviral DNA sequencing and rebounding viruses highlight the challenges in using current latent reservoir assays to accurately predict viruses that will reactivate in vivo.

Introduction

Successful introduction of combination antiretroviral therapy (cART) in HIV-1 infected individuals can lead to rapid suppression of plasma viremia, resulting in a dramatic decline in HIV-associated morbidity and mortality. Despite effective cART, HIV persists primarily in long-lived resting memory CD4⁺ T cells and latently infected cells remain stable with a half-life of approximately 44 months³⁻⁹. The slow decay of the viral reservoir prevents HIV eradication with cART alone. Additionally, once cART is removed, multiple latently infected cells can contribute to recrudescence of plasma viremia¹⁰⁻¹⁶. These infected cells are the target of curative strategies aiming to achieve cART-free remission and complete eradication of the latent reservoir. However, in the absence of nonviral biomarkers to accurately identify changes in the size or composition of the reservoir, analytical treatment interruptions (ATI) of cART are required to determine efficacy of the novel therapeutic strategy^{17,18}. Brief ATIs have recently been shown to be well-tolerated in infected participants and have been a useful tool in identifying the genotypic and phenotypic characteristics of viruses that “break-through” therapeutic intervention¹³. Additionally, plasma viremia observed during ATIs interruption is rapidly suppressed upon re-initiation of the participant’s original cART regimen. The effect of transient viremia on the latent reservoir during ATI, however, is unknown. In this study, I performed quantitative and qualitative analyses on latently infected cells in nine participants from the previously described AIDS Clinical Trials Group (ACTG) clinical trial, A5340 (described in Chapter 3 of this thesis). The trial found that three infusions of the broadly neutralizing antibody VRC01 was safe and well-tolerated, but only modestly delayed the time to viral rebound compared to historical controls. Phenotypic and

genotypic analyses of pre-cART and rebound viruses determined that VRC01 was able to restrict the clonality of rebound viruses, though pre-existing resistance to VRC01 led to rapid viral rebound in the presence of high concentrations of plasma VRC01 in the majority of participants. Upon collection of two consecutive plasma samples with viral loads greater than 1,000 copies per milliliter, cART was reinitiated and all participants achieved rapid suppression back to undetectable levels. Here, I determine the impact of transient viremia with ATI by assessing the relationship between autologous viruses derived from pre-cART plasma, rebound plasma, and PBMCs archived before and six months after trial completion. I show that ATI does not substantially alter the size or diversity of the peripheral latent reservoir. Additionally, I also observed a high prevalence of clonally-expanded replication-competent and genetically intact latent viruses, which confounded attempts to successfully identify viruses that will reactivate in vivo upon ATI.

Results

Patient population

Nine individuals participated in this component of the ACTG clinical trial A5340, undergoing multiple blood draws and two leukapheresis and rectal biopsies. In this study, I analyzed plasma and/or PBMC samples from four time points (Fig 4.1); Plasma samples were obtained prior to ART initiation (available in 5 participants) and at the first and second week of virus rebound after ATI. Plasma and PBMCs obtained by leukapheresis at trial entry (prior to VRC01 administration or ATI) and six months after plasma virus suppression <200 copies/ml with ART re-initiation were also studied.

Further patient demographics information can be found in Table 4.1. Prior to the post-ATI leukapheresis, participants' plasma virus was suppressed <200 copies/ml on cART for a median of 34 weeks (range 23-44 weeks) and 35 weeks (range 23-43 weeks) prior to the post-ATI rectal biopsy.

Quantitative measures of reservoir change

We performed several assays to quantitatively estimate within-person changes in the size of the peripheral latent reservoir. Using PBMCs obtained during cART suppression of viremia prior to ATI and six months after virus suppression on cART (Figure 4.1), we selected CD4⁺ T cells and measured copies of total HIV-1 DNA and cell-associated RNA by quantitative PCR (Figure 4.2). Total DNA levels ranged from 21.4 to 1791.2 copies/million CD4⁺ T cells pre-ATI and 25.4 to 1564.5 copies/million CD4⁺ T cells post-ATI. No significant change between the within-person pre- and post-ATI values was observed, with a median (Q1, Q3) change of 0.08 (-0.13, 0.18) log₁₀ copies/million cells, $P=0.313$. Similarly, we did not observe any significant changes in cell-associated RNA levels between pre- and post-ATI samples. RNA measures ranged from 6.1 to 10,834.7 copies/million cells with a median (Q1, Q3) change of -0.05 (-0.15, 0.2) log₁₀ copies/million cells, $P=0.734$.

To determine the composition of replication-competent viruses from the latent reservoir, we used the same PBMC samples pre- and post-ATI, and quantified the total number of resting CD4⁺ T cells using a quantitative virus outgrowth assay (QVOA). We found that the values for infectious units per million cells (IUPM) ranged from 0.033 to 16.248 IUPM pre-trial and 0.023 to 8.35 IUPM post-trial. There was no evidence suggesting significant within-person change, with a median (Q1, Q3) change of 0.3 (-0.16, 0.63) log₁₀

copies/million cells, $P=0.652$. We also performed single copy assay (SCA) to detect low-level viremia in plasma collected during suppressive ART before and after the trial (Fig. 4.2). With a limit of detection of <0.5 copies/ml, 3 participants remained undetectable before and after ATI, 3 participants were above detectable at both timepoints, 1 participant went from just above detection (0.53 copies/ml) to undetectable, while the remaining 2 went from undetectable to 2.14 and 2.19 copies/ml, respectively.

Several reports between latency measures have demonstrated a lack of correlation between IUPM, HIV DNA, and SCA measures^{7,9,19}. Here, we tested the association between the three quantitative assessments at baseline, post-trial, and in the change between timepoints. We identified a modest correlation between total DNA in CD4 T cells and replication-competent virus (IUPM) by QVOA, with Spearman correlation coefficients of 0.68 and ($P=0.06$) at baseline, 0.83 ($P=0.01$) at Step 3, and 0.79 ($P=0.02$) for the change between baseline and post-ATI (Figure 4.3). No correlation between ca-RNA and other measures was detected. An association between undetectable plasma virus by SCA and lower DNA and IUPM by QVOA was also seen. We also did not observe any detectable virus in pre- or post-ATI samples in rectal tissues in the majority of participants, however, we believe this was due to a technical issue that occurred during tissue processing.

Phylogenetic analysis of reservoir change

To further evaluate whether brief ATI and transient viremia altered the genetic composition of the viral reservoir, I used phylogenetic analyses to assess the viral quasispecies in pre-ATI, rebound, and post-ATI archived samples. Due to limited sequence yield, Participant A14 was not included in this analyses. For the remaining

eight participants, I sequenced full length HIV-1 Env using gp160 nested primers on viruses replicating in p24+ culture wells of the pre- and post-trial QVOA assays. QVOA wells were cultured with limiting dilutions of resting CD4+ T cells, therefore, in order to eliminate cultures with multiple HIV-1 templates single genome sequencing methods were used to identify culture wells with single templates and present the consensus sequence of individual *envs* represented in individual culture wells (see methods). I then compared QVOA-derived *env* sequences with SGS-derived gp160 *env* from plasma samples sampled prior to cART initiation (pre-cART viruses), and plasma viruses collected during the first and second rebound time points during ATI. These samples were then analyzed collectively in a maximum likelihood (ML) phylogenetic tree, where all participant sequences clustered independently (Fig. 4.4).

Clonal populations are prevalent within replication competent peripheral latent reservoir

ML phylogenetic trees of each individual participant's gp160 *env* sequences from the three observed time points in this study show a range of diversity in pre-cART viruses and low-diversity lineages during rebound with a maximum within-patient diversity (range, 0.87%-6.1%) and tree structures indicative of chronic infection. Viral rebound was polyclonal for 7 participants, showing multiple genetically distinct, low-diversity rebound lineages supporting the hypothesis that rebound lineages arise from multiple latently infected cells and replicates systemically within weeks of ATI^{7,14,15}. When assessing QVOA-derived sequences, I observed an interesting phenomenon in QVOA sequence analyses, where multiple groups of identical *env* sequences are represented in dependent culture wells. While whole genome analyses was not used in this study, the sequences were generated through *env* specific primers with a clonal prediction

score of 95, indicating a high likelihood that these identical *env* sequences also reflected identical whole genomes²⁰. While definitive proof of clonal expansion of latently infected cells requires integration site analysis of identical viruses from different cells, modeling and empiric studies support the hypothesis that multiple identical gp160 *env* sequences are indicative of in vivo clonal expansion²⁰⁻²³.

Given that QVOA assays require 14 to 21 days of ex vivo stimulation and that the in vitro error rate of HIV RT can cause an accumulation of errors during this period^{21,24-26}, in my analyses of clonal variants, I included viral sequences with up to two nucleotide polymorphisms as a clonal lineage. All participants with more than two QVOA sequences available per time point (A01, A02, A06, A08, A09 and A13), were found to have clonal lineages through these methods. In four participants with more than 20 QVOA sequences available, clonal lineages comprised 68% of the total QVOA-derived viruses assessed. A01 is a striking example of substantial clonal expansion, where the replication-competent viruses from this participant comprised of 41 of 43 identical viruses (95%) that were derived from pre-trial as well as post-trial QVOA samples. Furthermore, we identify 6 of 11 (55%) identical QVOA viruses from participant A02 representing two clonal lineages, and multiple expanded lineages in participant A08, representing 6 distinct lineages of 2 or more sequences, representing 48% (14 of 29) of QVOA-derived viruses (Fig. 4.5).

Minimal enrichment of rebound sequences in the post-trial latent reservoir.

I next assessed whether enrichment of rebound sequences could be observed in the post-trial latent reservoir by comparing the genetic relatedness of rebound lineages to pre-trial and post-trial QVOA lineages. I hypothesized that brief ATI would not lead to a substantial accumulation of rebound viruses in the viral reservoir, indicated by the limited number of identical post-trial QVOA and rebound sequences compared to pre-trial QVOA sequences. In participants A01, A02, A05, A09 and A13 (Fig. 4.4, Fig. 4.5). I did not find any evidence of post-trial QVOA sequences clustering with or near rebound viruses. In contrast, I did identify two identical rebound and post-trial QVOA sequences, as well as a minor lineage with both pre- and post-trial QVOAs. These data suggest possible enrichment of the viral reservoir during viral rebound in this participant. In addition, I identified 2 participants with small or low-diversity viral reservoirs before ATI, which made phylogenetic interpretation of rebound and QVOA sequences more challenging. Participant A07, for example, had a very small replication-competent reservoir, with only one pre-trial QVOA well available for assessment, and no available wells post-trial, which prevented an accurate qualitative assessment of the reservoir at pre- and post-trial time points. In addition, participant A06 contained a very narrow within-patient diversity (maximum difference of 3 nucleotides or 0.12%), containing rebound, pre- and post-trial QVOA sequences, which prevented us from accurately distinguishing between discrete lineages. Together, I found that the frequencies of pre-trial QVOA sequences (77%) and post-trial QVOA sequences (33%) aligned with this rebound virus as suggesting the preexistence of this lineage before ATI, rather than enrichment of this lineage from rebound viremia. Overall, in 5 of 6 evaluable participants, limited relatedness of rebound and QVOA viruses suggests that transient viral rebound does not substantially alters the composition of the latent reservoir.

Limited relatedness of pre-ATI QVOA to rebound sequences.

I next asked whether pre-ATI QVOA sequences represent replication-competent viruses that could reactivate upon treatment interruption. This analyses would be a useful tool in predicting rebound viruses, which is of considerable interest to the HIV cure field. Sequence analyses of pre-trial QVOA show a lack of correlation to rebounding virus populations, and was especially notable in participants with large expanded clones of pre-trial QVOA viruses, as indicated in participant A01. Interestingly, while participant A01 contained 93% (13 of 14 sequences) identical pre-trial QVOA viruses, none of these viruses from this replication competent expanded clone were sampled during ATI. Instead, four genetically distinct, clonal lineages reactivated during ATI. This was also observed in two other participants with clonal pre-trial QVOA lineages. In participant A02, where 55% (5 of 9 sequences) from pre-trial QVOA made up two expanded clonal lineages, though neither of these expanded clones reactivated in vivo. In participant A09, 30% (3 of 10 sequences) of pre-trial QVOA viruses made up a single clone, though the 7 distinct lineages that arose in vivo during rebound do not represent this in vitro expanded clone. These results suggest that in most chronically-infected cART suppressed participants, sampling of pre-trial QVOA viruses often leads to the identification of large, clonally expanded populations, though these populations are not able to predict the viral population that reactivates upon ATI. Exceptions to this finding were found in participants A07 and A02, where narrow diversity and limited reservoir size prevented accurate distinction between rebound and QVOA lineages, and in participant A08, where two pre-trial QVOA sequences were related to a minor rebound virus population (with 4-7 nucleotide differences).

Neutralization sensitivity to VRC01 and autologous plasma.

Given that the majority of participants in this study contained clonally expanded, replication-competent viruses that did not expand in vivo, I next asked whether one potential mechanism preventing their expansion was related to the in vivo conditions during rebound. High concentrations of VRC01 were circulating in the plasma at the time of rebound in all participants with the exception of participant 07, who rebounded at 11 weeks with waning plasma concentrations. Previous analyses of rebound virus sensitivity to VRC01 determined that the prevalence of VRC01 resistance is high, and contributes to the timing and clonality of the rebound virus population. Additionally, in Chapter 2 of this thesis I describe a role for autologous antibodies during rebound in restricting the replication of select neutralization-sensitive viral populations at longitudinal rebound timepoints. Therefore, I hypothesized that large, clonally expanded viruses derived by QVOA were not represented in the rebounding virus population upon ATI and VRC01 infusion due to increased VRC01 sensitivity and circulating autologous antibody responses generated at the time of viral rebound.

To test this, I generated HIV-1 Env pseudotype viruses from the cloned consensus sequence of distinct QVOA, rebound, and pre-cART lineages from participants A01, A02, A06, and A09 (as shown in Figures 4.4 and 4.5). These pseudotypes were assessed for neutralization sensitivity (by IC80) to VRC01. Interestingly, I found no differences in VRC01 neutralization curves across QVOA, rebound, and pre-ART *envs* in either participant. To determine whether autologous antibodies had a differential role in restricting viral replication during ATI, the same Env pseudoviruses were tested for sensitivity to autologous plasma collected at first detectable viral rebound. This timepoint contained both the exogenously administered VRC01 as well as circulating polyclonal autologous neutralizing Abs (Figure 4.6). Although the limited number of

available Env pseudotypes for each participant prevented robust statistical comparisons, across all participants, I observed a trend toward greater sensitivity to autologous plasma in QVOA viruses compared to rebound viruses for all participants, suggesting autologous antibodies generated at the time of viral rebound may inhibit replication-competent, clonally expanded viruses from rebounding during ATI and VRC01 infusion.

Phylogenetic analysis of intact gp160 env from resting CD4+ T cell proviral DNA.

While sequencing of QVOA viruses allows for an assessment of replication-competent viruses within the viral reservoir, sampling depth is extremely limited and provides only a minimal estimate of viruses that could potentially reactivate under ATI conditions. To address this, I performed SGS on proviral DNA from resting CD4+ T cells collected before and up to six months after ATI. While the majority of proviruses in the reservoir have been shown to be defective variants^{23,27-29}, I restricted my analyses to sequences without hypermutations, multiple templates, or incomplete gp160 open reading frames. Through these methods, I generated 546 intact sequences (median 70 per participant). By including these sequences into the ML phylogenetic trees containing pre-cART, rebound, and pre- and post-trial QVOA sequences, I identified additional evidence of clonal expansion within the viral reservoir (Fig. 4.7 and Fig. 4.8). Similar to QVOA sequence analyses, I found that all 8 participants harbored multiple populations of identical proviral DNA sequences, with clonal populations comprising a range of 5% to 78% of the total sequenced proviral DNA population. Interestingly, I also found a low degree of overlap between proviral DNA and QVOA sequences. Participants A02 and A13, for example, contained expanded clones that comprised 61% and 78% of the proviral DNA population, respectively (Fig. 4.7, Fig. 4.8). , though these expanded populations did not match the clonal populations observed in pre- or post-trial QVOA

analyses. This low level of overlap between proviral and QVOA sequences was observed across all participants. Participant A01 was another striking example, where the 95% clonal population observed by QVOA represented only 2% of the proviral DNA sequences samples (Fig. 4.7). In contrast, participant A09 did contain matched proviral DNA and QVOA sequences (Fig. 4.8).

While proviral DNA sequencing expanded the pool of latent viruses in each participant, similar to QVOA analyses, the vast majority of participants (A01, A02, A05, A06, A08 and A09) did not contain overlapping proviral DNA and rebound sequences. In addition, expanded clonal populations identified in pre-trial proviral DNA (A02 and A13) also did not predict rebounding viruses. The only exception to this finding was participant A07, and supports the hypothesis that this participant contains a limited reservoir compared to all participants, with a small pool of replication-competent identical to near identical latent viruses. Together, these data support the findings of my QVOA analyses that transient viremia during brief ATI does not substantially change the composition of the latent reservoir.

Statistical comparisons of virus populations.

We also sought to determine the relatedness of these distinct viral compartments through genealogical sorting indices (GSI) (Table 4.2)³⁰. The GSI tests the phylogenetic similarities of two sequence groups, with the null hypothesis that the virus populations were the same; GSI values range from 0 (complete interspersed) to 1 (complete monophyly), with statistical significance indicating greater than random segregation between groups. Through these analyses, we found that the majority of participants had

highly interspersed latent pre- and post-ATI virus populations. Participant A08 was the only participant in this study with a statistically and significantly high GSI value, suggesting that the composition of the replication-competent viruses changes over time. For the remainder of the participants, these highly interspersed pre- and post-ATI sequence sets support the concept that ATI does not substantially alter the sampled reservoir.

To determine statistical relatedness of pre- and post-ATI sequences of QVOA and proviral DNA sequences, pre- and post-ATI sequences were grouped together and QVOA and proviral DNA viruses were compared. Interestingly, through these analyses we found that in 5 of 6 evaluable participants (those with >2 QVOA sequences per time point), there were significant ($P < 0.05$) differences between QVOA and proviral DNA viruses sampled from the same leukapheresis-derived resting CD4+ T cells. When comparing QVOA and proviral DNA viruses with rebound viruses, we found that latent viral sequences differed significantly ($P < 0.001$) from rebound.

We also used a non-tree-based method to examine sequence differences among the same virus populations. Here, we tested the null hypothesis that the distributions of Levenshtein edit distance were the same when comparing virus populations with themselves and with other virus populations (Fig. 4.8). Similar to the GSI results, we found highly similar LDs among pre- and post-ATI QVOA and proviral DNA sequences. Then, we grouped the pre- and post-ATI sequences together and compared proviral DNA with QVOA sequences (Fig. 4.8, right box for each participant). When we grouped pre- and post-ATI sequences together and compared proviral DNA with QVOA sequences, we found statistical significance in the same participants as with the GSI

method, with the exception of participant A09, in whom an extremely high intrapopulation genetic diversity pre-vented distinction between QVOA and proviral DNA sequences. Finally, comparisons of rebound sequences with QVOA and proviral DNA showed highly significant differences in all participants except those with limited or narrow QVOA sequence populations (A06 and A07). Thus, both statistical methods supported phylogenetic analysis results suggesting that ATI did not substantially change the composition of the reservoir and that the QVOA, proviral DNA, and rebound virus populations all differed substantially from each other.

Tables

Characteristic

Male sex, <i>n</i> (%)	9 (100%)
Age (yr) at entry, median <i>n</i> (Q1, Q2)	43 (36, 47)
Race, <i>n</i> (%)	
Black or African American	4 (44%)
White	5 (56%)
Ethnicity, <i>n</i> (%)	
White non-Hispanic	4 (44%)
Black non-Hispanic	3 (33%)
Hispanic	2 (22%)
Baseline CD4 ⁺ T cell count (cells/ml), median <i>n</i> (Q1, Q3)	874 (599, 1,026)
Nadir CD4 ⁺ T cell count (cells/ml), <i>n</i> (%)	
201–500	8 (89%)
>500	1 (11%)
Years on ART at entry, median <i>n</i> (min, max)	4.8 (3.6, 14.5)
ART regimen at study entry, <i>n</i> (%)	
INSTI based	6 (67%)
PI based	3 (33%)
Total no. of wk off ART during ATI, median <i>n</i> (min, max)	6 (3, 13)
Total no. of wk with detectable viremia (>200 copies/ml) during ATI, median <i>n</i> (min, max)	5 (4, 6)
Total no. of wk from viral suppression (<200 copies/ml) on ART to post-ATI leukapheresis, median <i>n</i> (min, max)	34 (23, 43)

INSTI, integrase strand transfer inhibitor; max, maximum; min, minimum; PI, protease inhibitor.

Table 4.1 Baseline, clinical, and study characteristics from A5340 Step 3. This work was reprinted with permission from the Journal of Clinical Investigation.

Participant	QVOA pre- and post-ATI		Proviral DNA pre- and post-ATI		QVOA vs. proviral DNA		QVOA vs. rebound		Proviral DNA vs. rebound	
	Before ATI	After ATI	Before ATI	After ATI	QVOA	Proviral DNA	QVOA	Rebound	Proviral DNA	Rebound
A01	0	0.061	0.029	0.13	0.42 ^A	0	0.89 ^A	0.84 ^A	0.87 ^A	0.56 ^A
A02	0	0.012	0.19 ^B	0.2 ^A	0.2 ^A	0.43 ^A	0.86 ^A	1.0 ^A	0.94	1.0 ^A
A05	0.33	0	0.13	0.10	0.10	0	0.15 ^B	0.46 ^B	0.67 ^A	0.30 ^A
A06	0.166	0.05	0.048	0.10 ^B	0.10 ^B	0.12 ^B	0.54 ^A	0.53 ^A	0.49 ^A	0.50 ^A
A07	NA	NA	0.06	NA	NA	NA	NA	NA	0.12 ^B	0.55 ^A
A08	0.19	0.34 ^B	0.063	0.16	0.16	0.29 ^A	0.032	0.38 ^A	0.62 ^A	0.16 ^B
A09	0.05	0	0.06	0.11	0.11	0.079	0.53 ^A	0.50 ^A	0.61 ^A	0.4 ^A
A13	0.13	0	0.088 ^B	0.39 ^A	0.39 ^A	0.11 ^B	0.64 ^A	0.16 ^B	0.21 ^A	0.48 ^A

^A*P* < 0.001; ^B*P* ≥ 0.001 to *P* ≤ 0.05.

Table 4.2 Genealogical Sorting Indices. This work was reprinted with permission from the Journal of Clinical Investigation.

Figures

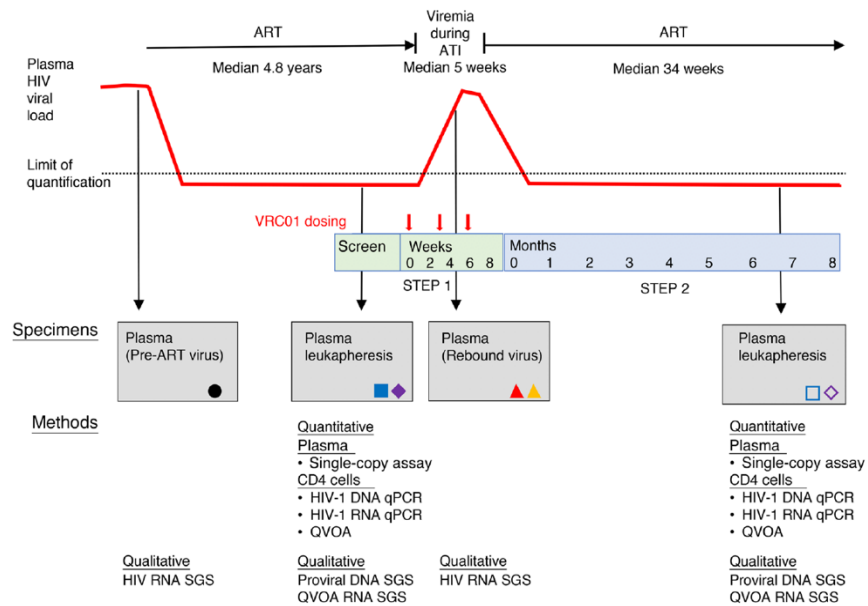


Figure 4.1 A5340 Step 3 Study Schema. The A5340 clinical trial schema is shown at the top, with the type and timing of clinical specimens obtained for the present study shown in the center, and the assays performed shown at the bottom. This work was reprinted with permission from the Journal of Clinical Investigation.

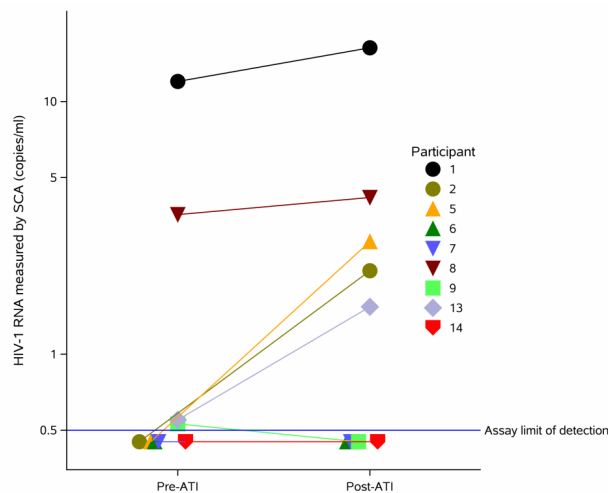


Figure 4.2 Single copy assay. Single copy assay was performed to detect low-level viremia in plasma collected during suppressive ART before and after the trial. With a

limit of detection of <0.5 copies/ml, 3 participants remained undetectable before and after ATI, 3 participants were above detectable at both timepoints, 1 participant went from just above detection (0.53 c/ml) to undetectable, while the remaining 2 went from undetectable to 2.14 and 2.19 copies/ml, respectively. This work was reprinted with permission from the Journal of Clinical Investigation.

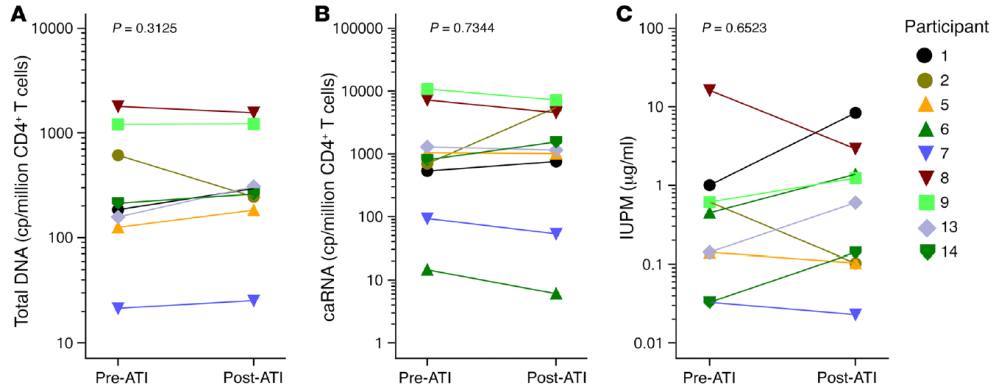


Figure 4.3 Quantitative measures of reservoir change. Pre-ATI and post-ATI values (Obtained at study entry and more than 6 months after viral suppression following cART reinitiation, respectively) of total HIV-1 DNA in CD4+ T cells. A. Cell-associated HIV-1 RNA (caRNA) in CD4+ T cells, B. and the frequency of resting CD4+ T cells bearing replication-competent virus (IUPM) C. are shown for each participant. Total DNA is not shown for participant A06 because the values were below detectable levels at both timepoints. P values shown in A-C indicate the significance of the within-participant changes and were determined by Wilcoxon signed-rank test. This work was reprinted with permission from the Journal of Clinical Investigation.

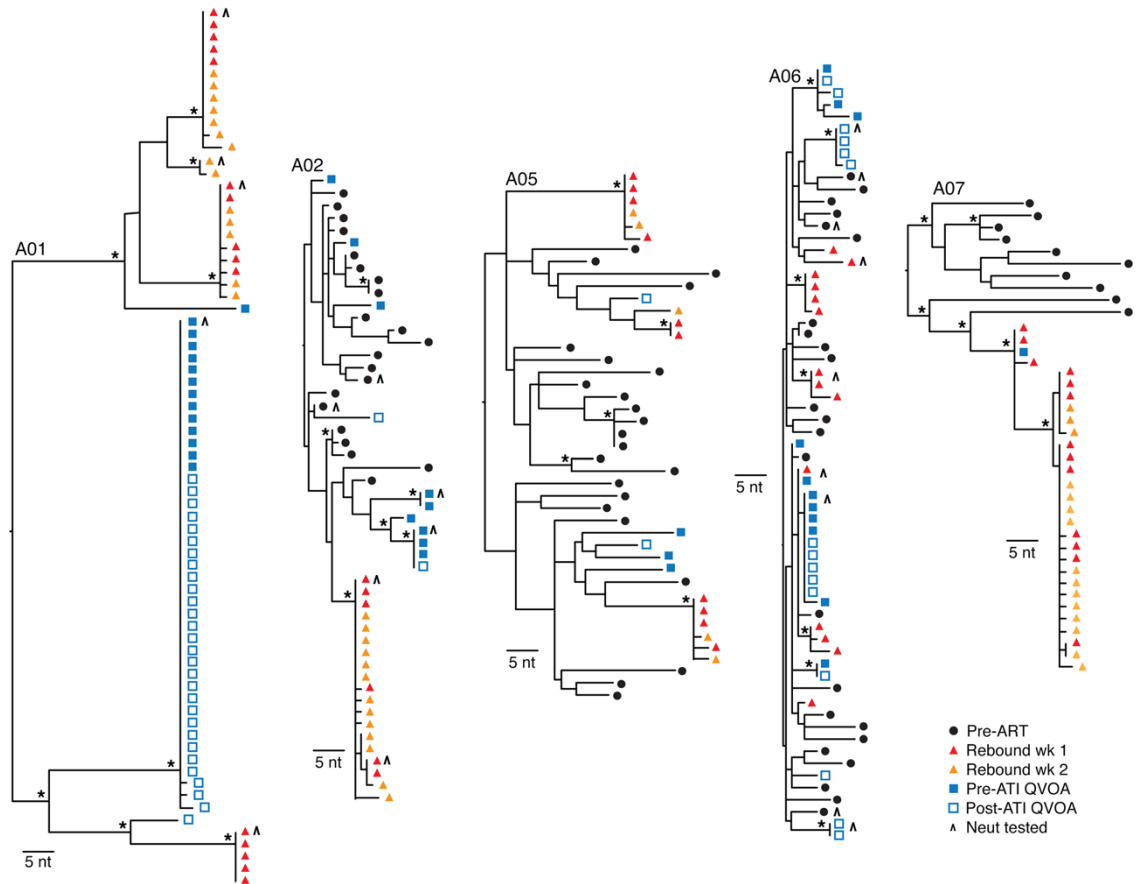


Figure 4.4 ML phylogenetic trees of SGS-derived gp160 env sequences from pre-ART plasma, rebound plasma, and replication-competent latent viruses (Participants A01, A02, A05, A06, A07). Env sequences from pre-ART plasma are shown as black circles, sequences from rebound plasma from the first and second weeks of detectable viremia after ATI are shown as red and orange triangles, respectively, and sequences from virus supernatant from individual pre- and post-ATI p24+ QVOA culture supernatants are shown as solid blue or open blue squares. Genetic distance is shown by the scale bar, indicating 5 nucleotides (or ~0.2% difference). Bootstrap values above 70 are indicated by asterisks. Envs tested for neutralization sensitivity in participants A01, A02, and A06 are indicated with an inverted v (^). Populations of identical QVOA sequences are seen in participants A01, A02, and A06, including a single dominant clone in participant A01 representing 95% of all QVOA sequences. Rebound sequences are generally distinct from QVOA sequences, except in participant A06, in which limited genetic diversity challenged distinction and in A07, in which the single QVOA sequence aligned with a rebound lineage. This work was reprinted with permission from the Journal of Clinical Investigation.

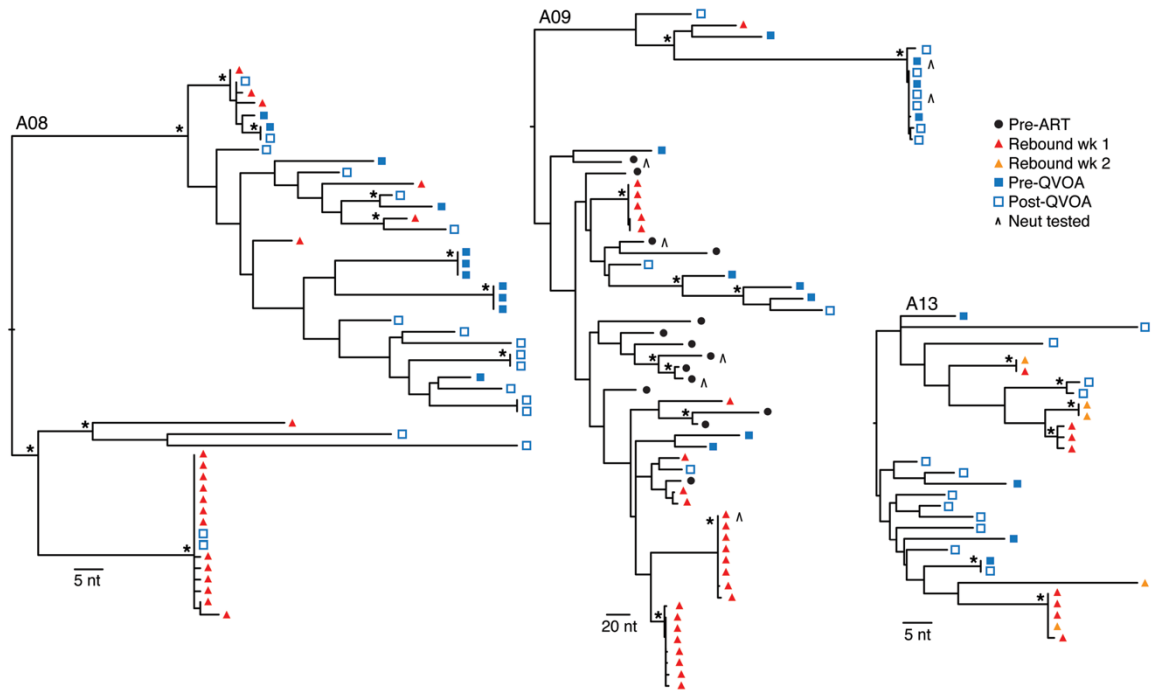


Figure 4.5 ML phylogenetic trees of SGS-derived gp160 env sequences from pre-ART plasma, rebound plasma, and replication-competent latent viruses (A08, A09, A13). Participants A08, A09, and A13 shown above. Genetic distance is shown by the scale bar, indicating 5 nucleotides (or ~0.2% difference) for participants A08 and A13, and 20 nucleotides (~0.8% difference) for participant A09. Envs tested for neutralization sensitivity in participants A09 are indicated with an inverted λ . Populations of identical QVOA sequences are seen in participants A08, A09, and A13. Viral rebound sequences are distinct from QVOA sequences in participants A09 and A13; in participant A08, some pre- and post-ATI QVOA sequences are identical or nearly identical to rebound lineages. This work was reprinted with permission from the Journal of Clinical Investigation.

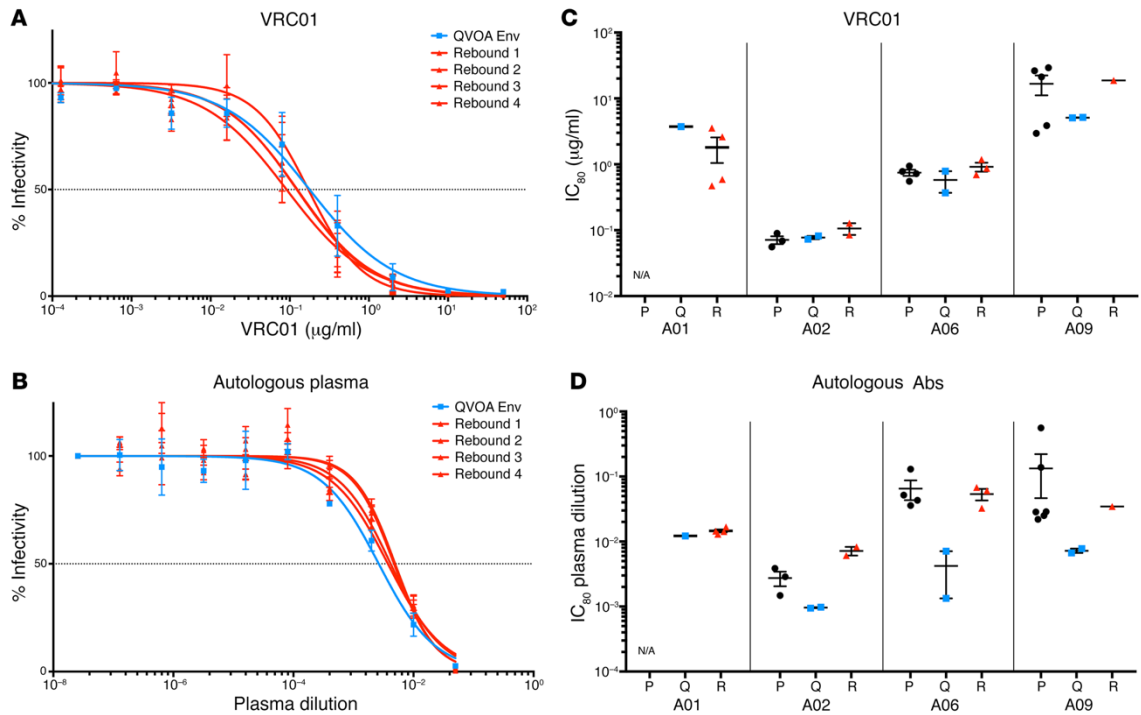


Figure 4.6 Neutralization sensitivity to VRC01 and autologous plasma at the time of viral rebound. Representative Envs from 4 participants were cloned and tested as pseudoviruses in infectivity assays for sensitivity to VRC01 and autologous plasma. Representative infectivity curves for the rebound and QVOA Envs for participant A01 are shown against VRC01 (A) and autologous plasma (B). All assays were performed in triplicate, and the mean infectivity \pm SEM for each dilution is shown. The mean IC₈₀ for virus inhibition against VRC01 (C) and autologous plasma (D) is shown for 4 participants. Pre-ATI viruses are shown in black, QVOA viruses in blue, and rebound viruses in red. This work was reprinted with permission from the Journal of Clinical Investigation.

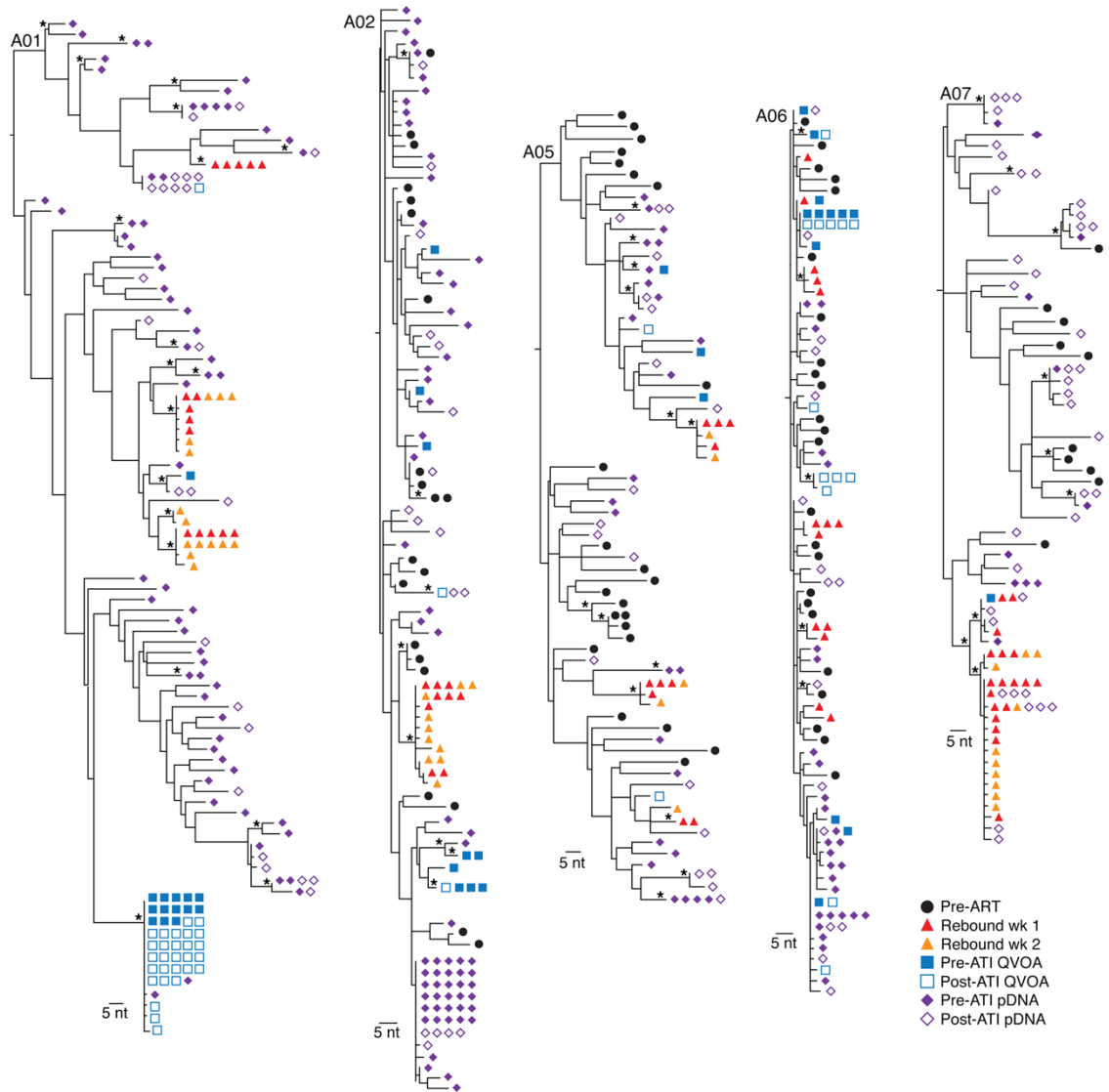


Figure 4.7 ML phylogenetic trees of SGS-derived gp160 env sequences from pre-ART plasma, rebound plasma, replication-competent latent viruses, and genetically intact proviral DNA (Participants A01, A02, and A05–A07). Env sequences from pre-ART plasma are shown as black circles, sequences from rebound plasma from the first and second weeks of detectable viremia after ATI are shown as red and orange triangles, respectively, sequences from virus supernatant from pre- and post-ATI individual p24+ QVOA culture well supernatants are shown as solid blue or open blue squares, and sequences from pre- and post-ATI proviral DNA (pDNA) are shown as solid purple or open purple diamonds. For clearer visualization, identical sequences are aligned horizontally in rows of 5. Genetic distance is shown by the scale bar, indicating 5 nucleotides (or ~0.2% difference) in all trees. Bootstrap values above 70 are indicated by asterisks. Populations of identical proviral DNA sequences are seen in all participants, including a large clonal population in participant A02 comprising 61%

of total proviral DNA sequences. In general, the larger clonal populations of proviral DNA sequences show limited or no overlap with the larger QVOA clones. This work was reprinted with permission from the Journal of Clinical Investigation.

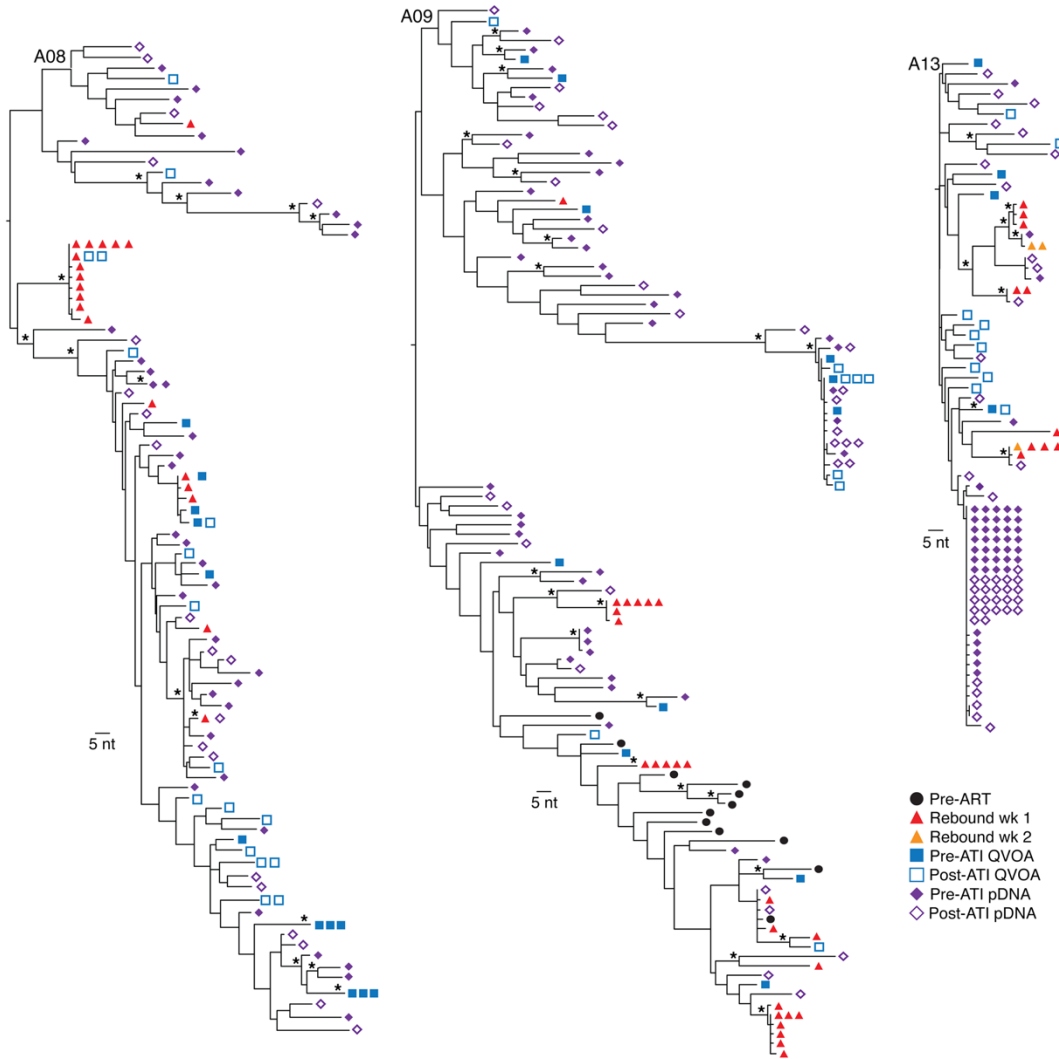


Figure 4.8 ML phylogenetic trees of SGS-derived gp160 env sequences from pre-ART plasma, rebound plasma, replication-competent latent viruses, and genetically intact proviral DNA (Participants A08, A09 and A13). Populations of identical proviral DNA sequences were found all participants, including a single clone comprising 78% of the proviral DNA sequences for participant A13, which was not sampled in the QVOA sequences. This work was reprinted with permission from the Journal of Clinical Investigation.

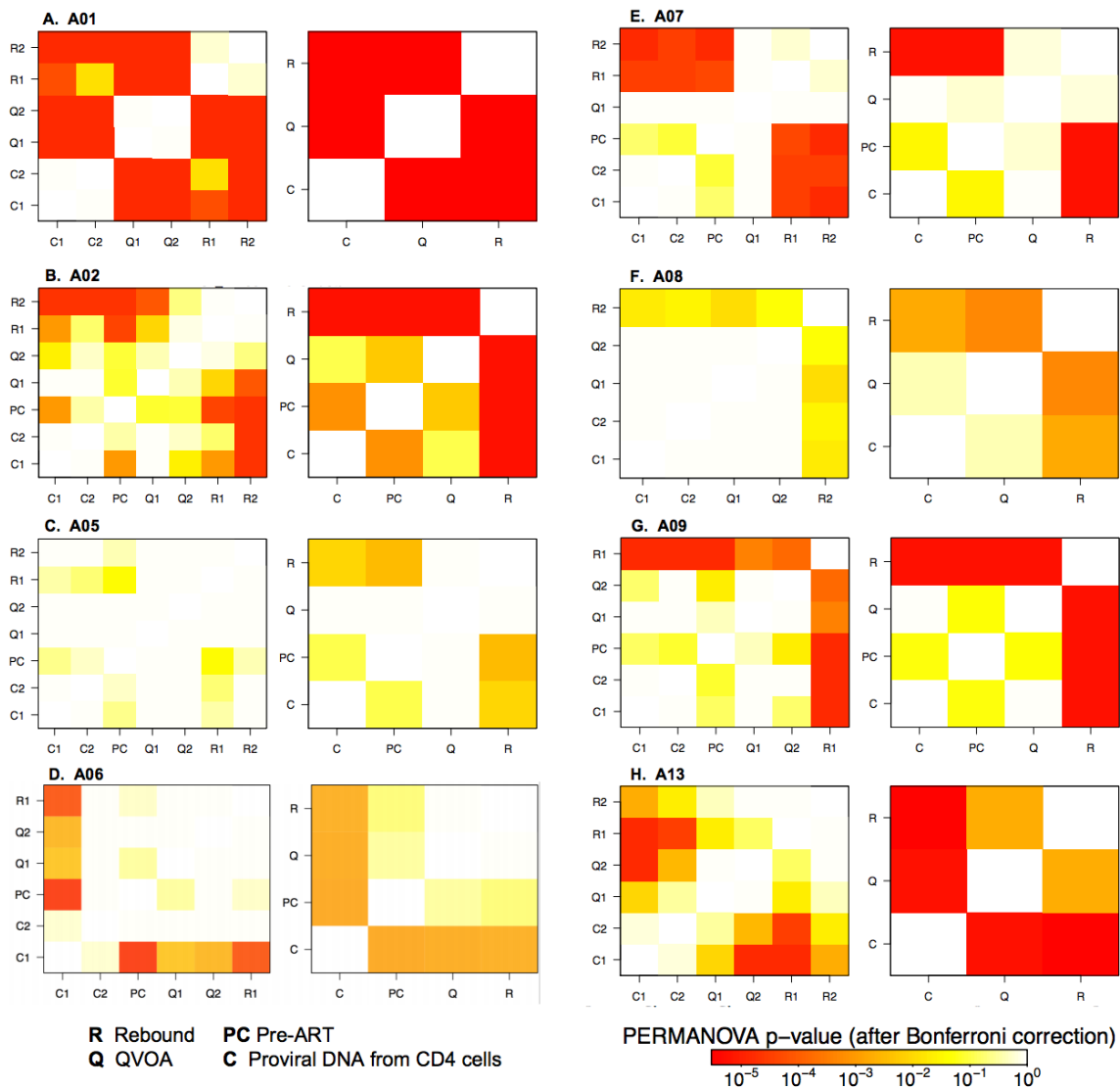


Figure 4.9 Comparisons of pairwise Levenshtein Distances between virus populations. For each participant, pairwise Levenshtein edit distance between nucleotide sequences sets are shown. Rebound sequences are labeled R, QVOA sequences are labeled Q, Proviral DNA sequences are labeled C, and pre-ART sequences are labeled PC. In the box on the left, comparisons between viruses from each timepoint are shown (i.e., Q1 is pre-ATI QVOA sequences and Q2 is post-ATI QVOA sequences). In the box on the right, sequences from the pre- and post-ATI samples are combined. Statistical significance by PERMANOVA after Bonferroni correction for multiple comparisons is indicated by the heat map. This work was reprinted with permission from the Journal of Clinical Investigation.

Discussion

ATIs are a valuable tool commonly used in HIV curative trials to assess the efficacy of novel curative therapies in the absence of cART^{1,17,31,32}. While closely monitored ATIs prevent long periods of viral replication without intervention, there are several safety concerns with altering the size and composition of the viral reservoir during rebound. Using a unique collection of pre-trial and post-trial samples available from clinical trial A5340 (Fig. 4.1), we were able to assess the effect of brief ATI with transient rebound viremia in HIV-infected individuals. Participants in this study reinitiated their original cART regimen and remained virally-suppressed for at least 6 months before post-trial samples were collected in order to ensure sampling of latently infected cells. In this study, we found no statistical increase in the size of the latent reservoir through measurements of viral transcripts by total HIV-1 DNA, cell-associated RNA, or IUPM. Collectively, these data suggest that the latent reservoir does not expand during ATI. While HIV DNA and RNA measures have not previously been shown to correlate with the number of replication-competent viruses assessed in QVOA assays due to the high number of defective viruses present in the viral reservoir, our measurements of HIV-1 DNA and RNA correlate with IUPM, suggesting our sampling methods are measuring a biologically relevant population of viruses.

To determine whether ATI can change the composition of the viral reservoir, we next performed QVOA assays on resting CD4⁺ T cells collected from pre-trial and post-trial time points and assessed the diversity of latent replication-competent viruses that expanded *in vitro*. Through SGS and phylogenetic analyses, I found that QVOA viruses

from pre- and post-trial time points had minimal nucleotide changes and were distinct from the rebounding virus population in the majority of participants. I also observed two exceptions to this finding in participant A07 and A02, where the reservoir size was small (A07) or narrow (A02), thus preventing distinction between rebound viruses and QVOA viruses.

While QVOA assays are a useful measure of replication-competent viruses from the latent reservoir, these methods can be highly resource intensive^{18,33}, and provide only a limited snapshot of the viral reservoir. Therefore, we sought to increase the number of HIV sequences in our analysis by sequencing proviral DNA from resting CD4+ T cells from pre- and post-trial leukapheresis time points. Proviral DNA sequencing substantially increase the number of HIV *env* sequences from latently infected cells. Similar to QVOA sequence analyses, I found that genetically intact proviral DNA from pre- or post-trial time points did not align with rebounding viruses in most participants. Like QVOA viruses, I also found that while large, clonally expanded lineages were prevalent in proviral DNA (Fig 4.6-4.7), these sequences are still not predictive of viral rebound. An additional finding in our sequence analyses was that pre- and post-trial proviral DNA sequences remained stable over time. This is in contrast to a recently published study that have suggests latently infected, clonally expanded cells wax and wane over time³³. This was supported by non-tree based statistical testing, where no statistical differences can be observed between pre- or post-trial samples, even in participants with small or narrow viral reservoirs. Collectively, these data suggest that brief ATIs followed by rapid viral suppression with cART do not substantially increase the size or diversity of the latent reservoir. This finding is significant, in that future curative trials will need to

determine drug efficacy in individuals who initiated cART early in infection, where the reservoir is potentially smaller and less diverse^{34–36}.

The observation of large identical lineages in QVOA and proviral DNA sequences from pre- and post-trial time points is also notable, as it supports the hypothesis that clonal expansion of latently infected cells is prevalent and may also contribute to the size and diversity of the viral reservoir over time^{23,24,27–29,37}. While we did not perform integration site analysis in this study, the primers used in our analyses are 95% likely to predict identical whole-genome sequencing, while mathematical modeling supports the finding that identical sequences are highly likely to predict clonally expanded cell populations^{20,22,23,38}.

In the A5340 clinical trial, increased VRC01 sensitivity was associated with delayed rebound kinetics and clonal restriction of viruses that arose from the latent reservoir. In this study, *in vitro* neutralization assays with VRC01 did not identify increased sensitivity to VRC01 in QVOA viruses compared to autologous pre-cART and rebound viruses, suggesting VRC01 is not implementing a “sieve effect” on the latent viral pool. Previous studies have suggested autologous plasma may exert selective pressure on rebounding variants during ATI, and are described in greater detail in Chapter 2 of this thesis. Using the same Env pseudotypes and heat-inactivated autologous plasma from first detectable rebound, I tested the hypothesis that autologous antibodies also exert selection pressure on rebounding viruses during ATI and VRC01 infusion. While the number of Env pseudotypes tested was limited, I found that QVOA viruses had increased sensitivity to autologous antibodies, suggesting that autologous antibodies may drive the selection of rebound.

In summary, these results provide reassurance that brief, closely monitored ATIs with rapid resuppression of cART do not substantially alter the size or composition of the latent reservoir. These findings are especially important for future HIV cure trials that will need to assess the efficacy of each therapeutic strategy under the context of ATI in chronically infected individuals³⁹.

Materials and Methods

Study participants

The ACTG clinical trial A5340 (ClinicalTrials.gov NCT02463227) tested the safety and ability of the bNAbs VRC01 to maintain viral suppression during ATI. The study design, approvals, and results were published previously (17). All A5340 trial participants who opted to undergo leukapheresis were included in this study (n = 9). Participant A14 was excluded from the qualitative analysis because of an insufficient number of rebound plasma *env* sequences and a limited number of p24+ QVOA wells.

Quantification of total HIV-1 DNA and cell-associated RNA

CD4+ T cells were isolated from PBMCs using an EasySep Human CD4+ T cell Enrichment Kit (STEMCELL Technologies). Cellular RNA and DNA from isolated CD4+ T cells were purified using the AllPrep DNA/RNA Kit (QIAGEN) as specified by the manufacturer, quantified using a NanoDrop ND-1000 spectrophotometer (Thermo Fisher Scientific), and normalized to cell equivalents by qPCR using human genomic TERT for DNA and RPLP0 expression for RNA (Life Technologies, Thermo Fisher Scientific).

Total cellular HIV-1 DNA and RNA were quantified with a qPCR TaqMan assay using the LTR-specific primers F522-43 (5'-GCCTCA-ATAAAGCTTGCCTTGA-3'; HXB2522-543) and R626-43 (5' GGGCGCCACTGCTAGAGA-3'; 626-643), coupled with a FAM-BQ probe (5'-CCAGAGTCACACAACAGACGGGCACA-3') using the QuantStudio 6 Flex Real-Time PCR System (Applied Biosystems). The cell-associated HIV-1 DNA copy number was determined using a reaction volume of 20 μ l with 10 μ l of 2X TaqMan Universal Master Mix II with UNG (Life Technologies, Thermo Fisher Scientific), 4 pmol of each primer, 4 pmol probe, and 5 μ l DNA. Cycling conditions were 50°C for 2 minutes, 95°C for 10 minutes, and then 60 cycles of 95°C for 15 seconds and 59°C for 1 minute. The cell-associated HIV-1 RNA copy number was determined in a reaction volume of 20 μ l with 10 μ l of a 2 \times TaqMan RNA-to-Ct 1-Step Kit (Life Technologies, Thermo Fisher Scientific), 4 pmol of each primer, 4 pmol probe, 0.5 μ l reverse transcriptase, and 5 μ l RNA. Cycling conditions were 48°C for 20 minutes, 95°C for 10 minutes, and then 60 cycles of 95°C for 15 seconds and 59°C for 1 minute. For HIV-1 DNA measurements, external quantitation standards were prepared from the ACH-2 cell line in a background of HIV-1-negative human cellular DNA and calibrated to the Virology Quality Assurance (VQA) (NIH DAIDS) cellular DNA quantitation standards. For HIV RNA measurements, external quantitation standards were prepared from full-length NL4-3 RNA, followed by copy number determination using the Abbott RealTime assay (Abbott Diagnostics) and calibrated to VQA HIV-1 RNA standards. Patient specimens were assayed with up to 800 ng total cellular RNA or DNA in replicate reaction wells and the copy number determined by extrapolation against a 7-point standard curve (1-10,000 cps) performed in triplicate. DNA values for 1 participant measured under the limit of detection with fewer than 21.4 copies/million CD4+ T cells were censored at 21.4 copies/million CD4+

T cells throughout the analyses. DNA values for A06 are not shown because of assay failure secondary to a primer mismatch.

Single-copy assay

Residual plasma HIV viremia was measured using the validated ultrasensitive integrase single-copy assay (iSCA)⁴⁰. Plasma from the participants was spiked with an internal RCAS virion²⁶ standard, and qPCR reactions were performed with a Roche LightCycler 480 system using primers and probes specific to a conserved area of the HIV integrase gene.

QVOA

Resting CD4+ T cells (30.5 million) from leukapheresis derived PBMCs from individual HIV-1–infected participants and purified by 2-step magnetic bead depletion (CD4+ T cell Isolation Kit and CD69 Microbead Kit II, both from Miltenyi Biotec). Resting CD4+ T cells were then serially diluted 5-fold, briefly cocultured with a 10-fold excess of γ -irradiated allogeneic PBMCs from uninfected donors, and stimulated with RPMI containing phytohemagglutinin (PHA) (Remel), 10% FBS 100 U/ml IL-2 (Novartis), and 1% T cell growth factor (produced by the Siliciano laboratory as previously described, ref. 44). Media were removed 1 day after mitogen stimulation, and target MOLT-4/CCR5 cells were added to fresh media to propagate replication-competent HIV-1. The ratios of target cells were 1×10^7 to 1×10^6 patient resting CD4+ T cells to 2.5×10^6 target cells. Five days after stimulation, culture media were replaced, and cells in each well were split. Supernatants from each well were then assessed for p24 protein by qPCR and ELISA to determine the presence of replication competent virus on days 14 and 21 (Alliance HIV-1 p24 antigen ELISA Kit, PerkinElmer). The frequency of latently infected cells among the

input resting CD4⁺ T cells was calculated by a ML method, as described previously, and expressed as IUPM, and 95% CIs for individual IUPM determinations were ± 0.7 log IUPM, or 5-fold⁴¹. Using the ML method, samples without replication-competent virus were assessed in analyses as the limit of detection of the assay, based on cell input. Supernatant from wells containing replication-competent virus was then collected and processed by SGS methods.

SGS of replication-competent virus from QVOA wells

Viral RNA from p24⁺ wells collected in MOLT-4/CCR5 QVOA assays was extracted using the QIAmp viral RNA Mini Kit (QIAGEN) according to the manufacturer's instructions. HIV cDNA was generated by incubating 30 μ l template RNA with 3 μ l 10 mM dNTPs and 0.75 μ l of 20 μ M antisense primer R3B3R (5'-ACTACTTGAAGCACTCAAGGCAAGCTTTATTG-3') for 5 minutes at 65°C to denature the RNA, followed by reverse transcription using SuperScript III Reverse Transcriptase (Life Technologies, Thermo Fisher Scientific) according to the manufacturer's instructions. Amplification of gp160 env genes was performed by nested PCR using Platinum Taq High Fidelity Polymerase (Life Technologies, Thermo Fisher Scientific) as previously described³¹. In order to ensure that a majority of sequences would be generated from a single template, cDNA was diluted to yield less than 30% PCR-positive products on a precast 1% agarose gel (Thermo Fischer Scientific). Three to eight amplicons per QVOA sample were sequenced on an Illumina MiSeq platform; only wells with identical consensus sequences (85% identity at each nucleotide position) were used for analysis. Divergent sequences derived from the same QVOA well indicate evidence of multiple viruses, and were excluded from analysis. Sequences that contained stop codons, large deletions, or mixed bases were also excluded from further

analysis. Sequences were codon aligned using MUSCLE in the Geneious suite (version 8.1.7), manually refined, and gap-stripped. Phylogenetic trees were inferred using ML/rapid bootstrapping in RAxML, version 8, run on the Cyberinfrastructure for Phylogenetic Research (CIPRES) Science Gateway (<http://www.phylo.org/>). Evolutionary models were chosen for each participant data set using jModelTest (version 2.1.4), and model parameters were estimated concurrently with the phylogram topology. Trees were mid-point rooted and visualized using MEGA, version 621, and bootstraps greater than 70 are shown in the figures. All sequences were deposited in GenBank (accession numbers MH263749 and MH264427).

SGS of proviral DNA from pre- and post-trial resting CD4+ T cells

Viral DNA was extracted from multiples of 4 million resting CD4+ T cells from pre- and post-trial time points according to the manufacturer's instructions (QIAamp DNA Mini and Blood Mini Kit, QIAGEN). Amplification of gp160 env genes was performed as described above. Amplicons were run on precast 1% agarose gels (Thermo Fisher Scientific), and bands of appropriate size were directly sequenced on the Illumina MiSeq platform. Sequences were inspected for evidence of priming from multiple templates, stop codons, large deletions, or introduction of PCR error in early cycles; a threshold of 85% identity at each nucleotide position was used. Only sequences with full gp160 env ORFs and no evidence of multiple templates were used in analysis. Sequences were codon aligned using MUSCLE in the Geneious suite (version 8.1.7), manually refined, and gap-stripped.

Env cloning, pseudovirus titering, and neutralization assays

Select env sequences from pre-ART, rebound, and pre-trial QVOA samples were molecularly cloned for the production of pseudovirus and phenotypic analyses as described previously¹. Amplicons identified by gel electrophoresis were gel purified using the QIAquick Gel Purification Kit (QIAGEN), ligated into the pcDNA 3.1 Zeo(+) Expression Vector (Invitrogen, Thermo Fisher Scientific), and transformed into NEB 5-alpha Competent E. coli (New England BioLabs). Transformed bacteria (100 µl) were plated onto Luria broth (LB) agar plates supplemented with 50 µg/ml ampicillin and cultured at 37°C for 24 hours. Single colonies were selected and grown overnight in liquid LB broth at 37°C with shaking at 250 rpm, followed by plasmid isolation. Finally, each molecular clone was sequence confirmed against the reference env amplicon using the Illumina MiSeq platform. Pseudovirus was prepared as described previously¹. Culture supernatants were harvested 48 hours after transfection, and pseudoviruses were titrated on TZM-bl reporter cells. Virus neutralization by VRC01 or heat-inactivated autologous plasma collected at the first detectable rebound was assessed on TZM-bl cells as described previously¹. All assays were performed in triplicate in each of at least 2 independent experiments. To calculate the concentration of VRC01 or dilution of autologous plasma that neutralized 50% (IC50) and 80% (IC80) of the viral infection, the Ab dose-response curves were fitted with a 4-parameter logistic regression equation using GraphPad Prism 5.0 (GraphPad Software). The bNAb VRC01 was obtained from the NIH AIDS Reagent program.

Statistics

Given the small sample size (n = 9), nonparametric tests were used for all comparisons. The test for within-person changes from pre-ATI to post-ATI in measures of the latent reservoir was performed using a Wilcoxon signed-rank test. Spearman's correlation

testing was used to test the association between measures. Analyses were conducted in SAS, version 9.4 (SAS Institute). A P value of less than 0.05 was considered statistically significant.

GSI

To assess similarities between sampled virus populations, within-person ML phylogenies of combinations of QVOA sequences, proviral DNA sequences, and viral rebound sequences were inferred using PhyML version 3.0, and GSI values were calculated using the genealogical Sorting R package (<http://molecularevolution.org/software/phylogenetics/gsi/download>)³⁰. Statistical significance was assessed by randomly permuting character states across the tips of the tree 10,000 times. Nonsignificant values indicate the absence of compartmentalization (P values were corrected for multiple tests).

Pairwise PERMANOVA of LDs

For each participant, we calculated the pairwise PERMANOVA of the LD between nucleotide sequence sets that were aligned and gap-stripped. We then performed pairwise comparisons between all sample populations using PERMANOVA to test the null hypothesis that the centroids and spreads of the 2 populations were the same. P values were adjusted by Bonferroni's correction for the number of tests [$n \times (n - 1)/2$].

Study approval

The ACTG clinical trial A5340 was conducted under approval of the IRBs of the University of Pennsylvania and the University of Alabama at Birmingham. Written

informed consent was obtained from all participants. The study protocols and results were published previously¹.

Acknowledgement: I am grateful for the technical assistance from the NGS Sequencing Core (Catharine Bahari, Andrew Smith, and Alex Shazad), Gerald H. Learn for sequence and phylogenetic analyses, Scott Sherrill-Mix for GSI and Levenshtein distance analyses, and the study volunteers of the ACTG A5340 clinical trial, who participated in the present study. The A5340 clinical trial was supported by the NIAID (U01AI068636); the Penn Center for AIDS Research (P30 AI045008); the Penn Clinical Trials Unit (AI069534); the UAB Center for AIDS Research (P30 AI027767), the UAB Clinical Trials Unit (AI069452); and the ACTG Statistical and Data Analysis Center (UM1 AI068634). A5340 viral analyses were supported by the NIAID (1-R21-AI118431); the Penn Center for AIDS Research Viral and Molecular Core (P30 AI045008); the BEAT-HIV: Delaney Collaboratory to Cure HIV-1 Infection by Combination Immunotherapy (UM1AI26620); and CARE: Delaney Collaboratory for AIDS Eradication (UM1AI126619).

References

1. Bar, K. J. *et al.* Effect of HIV Antibody VRC01 on Viral Rebound after Treatment Interruption. *N. Engl. J. Med.* **375**, 2037–2050 (2016).
2. Caskey, M. *et al.* 3BNC117 a Broadly Neutralizing Antibody Suppresses Viremia in HIV-1-Infected Humans. *Nature* **522**, 487–491 (2015).
3. Hill, A. L., Rosenbloom, D. I. S., Fu, F., Nowak, M. A. & Siliciano, R. F. Predicting the outcomes of treatment to eradicate the latent reservoir for HIV-1. *Proc. Natl. Acad. Sci. U.S.A.* **111**, 13475–13480 (2014).
4. Pinkevych, M. *et al.* HIV Reactivation from Latency after Treatment Interruption Occurs on Average Every 5-8 Days--Implications for HIV Remission. *PLoS Pathog.* **11**, e1005000 (2015).

5. Finzi, D. *et al.* Latent infection of CD4+ T cells provides a mechanism for lifelong persistence of HIV-1, even in patients on effective combination therapy. *Nat. Med.* **5**, 512–517 (1999).
6. Siliciano, J. D. *et al.* Long-term follow-up studies confirm the stability of the latent reservoir for HIV-1 in resting CD4+ T cells. *Nat. Med.* **9**, 727–728 (2003).
7. Crooks, E. T. *et al.* Vaccine-Elicited Tier 2 HIV-1 Neutralizing Antibodies Bind to Quaternary Epitopes Involving Glycan-Deficient Patches Proximal to the CD4 Binding Site. *PLOS Pathogens* **11**, e1004932 (2015).
8. Blankson, J. N. *et al.* Biphasic decay of latently infected CD4+ T cells in acute human immunodeficiency virus type 1 infection. *J. Infect. Dis.* **182**, 1636–1642 (2000).
9. Poon, A. F. Y. *et al.* Quantitation of the latent HIV-1 reservoir from the sequence diversity in viral outgrowth assays. *Retrovirology* **15**, (2018).
10. Davey, R. T. *et al.* HIV-1 and T cell dynamics after interruption of highly active antiretroviral therapy (HAART) in patients with a history of sustained viral suppression. *PNAS* **96**, 15109–15114 (1999).
11. Chun, T. W., Davey, R. T., Engel, D., Lane, H. C. & Fauci, A. S. Re-emergence of HIV after stopping therapy. *Nature* **401**, 874–875 (1999).
12. Li, J. Z. *et al.* The Size of the Expressed HIV Reservoir Predicts Timing of Viral Rebound after Treatment Interruption. *AIDS* **30**, 343–353 (2016).
13. Rothenberger, M. K. *et al.* Large number of rebounding/founder HIV variants emerge from multifocal infection in lymphatic tissues after treatment interruption. *PNAS* **112**, E1126–E1134 (2015).
14. Alexander, T. H. *et al.* Changes in CD4+ T-Cell Differentiation Phenotype During Structured Treatment Interruption in Patients With Chronic HIV-1 Infection. *JAIDS Journal of Acquired Immune Deficiency Syndromes* **34**, 475 (2003).
15. Moltó, J. *et al.* Influence of Prior Structured Treatment Interruptions on the Length of Time without Antiretroviral Treatment in Chronically HIV-Infected Subjects. *AIDS Research and Human Retroviruses* **20**, 1283–1288 (2004).
16. Papasavvas, E. *et al.* Randomized, Controlled Trial of Therapy Interruption in Chronic HIV-1 Infection. *PLoS Med* **1**, (2004).
17. Kutzler, M. A. & Jacobson, J. M. Treatment interruption as a tool to measure changes in immunologic response to HIV-1. *Current Opinion in HIV and AIDS* **3**, 131 (2008).
18. Siliciano, J. D. & Siliciano, R. F. Assays to Measure Latency, Reservoirs, and Reactivation. *Curr. Top. Microbiol. Immunol.* (2017). doi:10.1007/82_2017_75

19. Sharaf, R. R. & Li, J. Z. The Alphabet Soup of HIV Reservoir Markers. *Curr HIV/AIDS Rep* **14**, 72–81 (2017).
20. Laskey, S. B., Pohlmeyer, C. W., Bruner, K. M. & Siliciano, R. F. Evaluating Clonal Expansion of HIV-Infected Cells: Optimization of PCR Strategies to Predict Clonality. *PLOS Pathogens* **12**, e1005689 (2016).
21. Hosmane, N. N. *et al.* Proliferation of latently infected CD4⁺ T cells carrying replication-competent HIV-1: Potential role in latent reservoir dynamics. *J. Exp. Med.* **214**, 959–972 (2017).
22. Bui, J. K. *et al.* Proviruses with identical sequences comprise a large fraction of the replication-competent HIV reservoir. *PLOS Pathogens* **13**, e1006283 (2017).
23. Lee, G. Q. *et al.* Clonal expansion of genome-intact HIV-1 in functionally polarized Th1 CD4⁺ T cells. *J Clin Invest* **127**, 2689–2696 (2017).
24. Mansky, L. M. & Temin, H. M. Lower in vivo mutation rate of human immunodeficiency virus type 1 than that predicted from the fidelity of purified reverse transcriptase. *J. Virol.* **69**, 5087–5094 (1995).
25. Das, K. & Arnold, E. HIV-1 reverse transcriptase and antiviral drug resistance. Part 1. *Curr Opin Virol* **3**, 111–118 (2013).
26. Palmer, S. *et al.* New real-time reverse transcriptase-initiated PCR assay with single-copy sensitivity for human immunodeficiency virus type 1 RNA in plasma. *J. Clin. Microbiol.* **41**, 4531–4536 (2003).
27. Ho, Y.-C. *et al.* Replication-Competent Noninduced Proviruses in the Latent Reservoir Increase Barrier to HIV-1 Cure. *Cell* **155**, 540–551 (2013).
28. Cohn, L. B. *et al.* HIV-1 integration landscape during latent and active infection. *Cell* **160**, 420–432 (2015).
29. Bruner, K. M. *et al.* Defective proviruses rapidly accumulate during acute HIV-1 infection. *Nat. Med.* **22**, 1043–1049 (2016).
30. Cummings, J.-S., Cairo, C., Armstrong, C., Davis, C. E. & Pauza, C. D. Impacts of HIV infection on Vgamma2Vdelta2 T cell phenotype and function: a mechanism for reduced tumor immunity in AIDS. *J. Leukoc. Biol.* **84**, 371–379 (2008).
31. Scheid, J. F. *et al.* HIV-1 antibody 3BNC117 suppresses viral rebound in humans during treatment interruption. *Nature* **535**, 556–560 (2016).
32. Rosás-Umbert, M. *et al.* Virological and immunological outcome of treatment interruption in HIV-1-infected subjects vaccinated with MVA-B. *PLoS ONE* **12**, e0184929 (2017).

33. Wang, Z. *et al.* Expanded cellular clones carrying replication-competent HIV-1 persist, wax, and wane. *Proc. Natl. Acad. Sci. U.S.A.* **115**, E2575–E2584 (2018).
34. Jaafoura, S. *et al.* Progressive contraction of the latent HIV reservoir around a core of less-differentiated CD4⁺ memory T Cells. *Nat Commun* **5**, 5407 (2014).
35. Ananworanich, J. *et al.* HIV DNA Set Point is Rapidly Established in Acute HIV Infection and Dramatically Reduced by Early ART. *EBioMedicine* **11**, 68–72 (2016).
36. Ananworanich, J. *et al.* Markers of HIV reservoir size and immune activation after treatment in acute HIV infection with and without raltegravir and maraviroc intensification. *J Virus Erad* **1**, 116–122
37. Clarridge, K. E. *et al.* Effect of analytical treatment interruption and reinitiation of antiretroviral therapy on HIV reservoirs and immunologic parameters in infected individuals. *PLOS Pathogens* **14**, e1006792 (2018).
38. Satou, Y. *et al.* Dynamics and mechanisms of clonal expansion of HIV-1-infected cells in a humanized mouse model. *Scientific Reports* **7**, 6913 (2017).
39. Sneller, M. C. *et al.* A randomized controlled safety/efficacy trial of therapeutic vaccination in HIV-infected individuals who initiated antiretroviral therapy early in infection. *Sci Transl Med* **9**, (2017).
40. Cillo, A. R. *et al.* Improved single-copy assays for quantification of persistent HIV-1 viremia in patients on suppressive antiretroviral therapy. *J. Clin. Microbiol.* **52**, 3944–3951 (2014).
41. Laird, G. M. *et al.* Rapid Quantification of the Latent Reservoir for HIV-1 Using a Viral Outgrowth Assay. *PLOS Pathogens* **9**, e1003398 (2013).

CHAPTER 5

Discussion

Overview

In HIV-infected individuals, daily cART can effectively and durably suppress plasma viral loads to undetectable levels; however, cART is unsuccessful as a curative strategy for HIV due to the persistence of the latent reservoir despite cART. In most individuals, when cART is discontinued, latently infected cells residing in the viral reservoir can reactivate and establish systemic rebound viremia within 4 weeks¹⁻⁶. These long-lived, persistently infected cells are the target of novel curative strategies for HIV. Without known nonviral biomarkers to accurately assess how these strategies affect the latent reservoir, ATIs are currently the preferred method to test efficacy of interventions by assessing the duration of viral suppression in the absence of cART. Clinical trials utilizing ATIs with novel curative strategies against HIV present a unique opportunity to assess the virologic and immunologic consequences of rebound viremia and determine mechanisms of treatment failure. Early studies utilizing ATIs for this purpose have primarily focused on the viral kinetics and initial diversity of the rebound viral quasispecies. The effects of ATI on both the evolution of HIV and host immune responses, however, are poorly understood. In this thesis, I use longitudinal SGS, molecular cloning, and neutralization assays on archived plasma and PBMC samples from two previously conducted clinical trials to better understand the virologic and immunologic events occurring during brief and extended periods of ATI. These data address the initial clonality of rebounding HIV-1 variants (Chapter 2), the effect of host-derived and passively infused neutralizing antibodies on viral evolution (Chapters 2, 3 and 4), as well as changes in the size and composition of the latent reservoir during brief periods of transient viremia (Chapter 4). These results provide important quantitative and qualitative information regarding the effect of rebound on viral and host immune

dynamics and will inform our understanding of mechanisms of both treatment failure and success for curative strategies for HIV.

Clonality of the viral rebound quasispecies

One previously published ATI study has shown that the expansive initial diversity of recrudescence viremia is consistent with viral replication arising from multiple latently infected cells⁴. The in vivo processes governing viral evolution of the rebound quasispecies, however, are unknown. In this thesis, I use single genome amplification and direct amplicon sequencing (SGS) of HIV-1 env to determine the precise genotypic diversity of individual plasma-derived and proviral HIV-1 variants over multiple time points during extended ATI. These methods provide a snapshot of the peripheral diversity and clonality of the rebounding viral quasispecies in chronically-infected participants over time and inform our understanding of viral evolution under ATI conditions. I hypothesized that the plasma virus population would rapidly accumulate diversity through the continuous stochastic activation of genetically distinct latent viruses coupled with the ongoing evolution of early rebound viruses. Consistent with my hypothesis, as described in Chapter 2 of this thesis, I observed that at baseline, the viral quasispecies had a substantial increase in inpatient diversity at first detectable rebound (maximum diversity 6.07%) compared to early time points during acute viremia in the same patients (maximum diversity 0.47%)^{3-5,7}.

With access to archived plasma samples from subsequent ATI time points, I was also able to investigate patterns of viral evolution during rebound. Rather than the continuous and random evolution of early rebound variants, which would be consistent with a

Poisson-Fitter model of viral evolution in the absence of selective pressures, I instead observed that select viral lineages were no longer sampled at later time points, indicating that a population bottleneck had occurred in the participants studied. In participant S25, for example, I observed complete replacement of the viral quasispecies at the time of first detectable rebound after only four additional weeks of treatment interruption. This rapid replacement of early viral lineages suggests that anti-HIV host immune responses are rapidly emerging during ATI and preventing select variants from replicating.

Importantly, further visual inspection of gp160 env sequences within participants showed that clonal expansion of replication-competent viruses was common. In Chapters 2 and 3, I found that multiple clonal lineages arose from latency to establish rebound viremia. This finding was also observed in Chapter 4 of this thesis, where large, expanded clonal lineages of full length gp160 env were identified in proviral DNA from resting CD4+ T cells. This is in contrast to previously published data suggesting that defective viruses, characterized by large internal deletions or APOBEC3-mediated mutations, are often found in expanded T cell clones, while replication-competent viruses exist in quiescent, non-expanding cells^{7,8}. Using nested PCR and SGS, I was able to selectively amplify and sequence viruses containing full length gp160, and identified multiple clonal replication-competent viruses within both the plasma virus population and the PBMC-derived latent reservoir. My data, in agreement with previously published reports, supports the hypothesis that clonally expanded cells contribute to the persistence of the replication-competent reservoir^{1,7}. These findings complicate efforts to eradicate HIV, as current therapies targeting the reservoir function under the assumption that clonal expansion does not substantially contribute to the replication-competent viral quasispecies⁹.

The clinical trials used for describing the diversity and clonality of the rebound viral quasispecies have several important limitations. First, the study sizes were limited to 11 (Chapter 2), 13 (Chapter 3), and 9 (Chapter 4) male participants. Future work should use larger, more diverse cohorts with extensive sampling to ensure that these studies have the statistical power to be more informative. Second, the rebound period described in Chapters 3 and 4 was brief (only 2 weeks), preventing extensive analyses of latently infected cells that could have emerged at later ATI time points. Third, all participants studied initiated cART during chronic infection. Viral diversity during chronic infection is significantly greater than what is observed during acute infection¹⁰⁻¹². Therefore, our findings regarding rebound clonality cannot be extrapolated to patients who initiated cART during acute infection. Fourth, all viruses analyzed in this thesis were from the peripheral blood; as multiple reports have described that the majority of HIV target cells reside in lymphoid tissues that may be sanctuary sites for HIV replication, this may be considered a limitation of our studies^{4,13}. Additionally, recent work in a mouse model for HIV-1 has shown that clonally expanded HIV-1 infected cells are distributed in multiple organs, and frequently integrate into genes associated with lymphocyte activation, proliferation, and chromatin regulation¹⁴. Future work should consider sampling diverse anatomical sites, such as lymphoid tissues, and should also focus on identifying the molecular drivers of clonal expansion to inform future interventions that will need to target cell-intrinsic mechanisms to prevent reservoir persistence.

Rebound kinetics to evaluate effect of treatment

Viral kinetic modeling has been used to better understand the within-host dynamics of HIV-1 viral replication and the effects of antiretroviral therapy¹⁵⁻¹⁷. Modeling of viral

kinetics during rebound for these same purposes has not been previously described. The A5340 clinical trial provided the first opportunity to understand rebound viral kinetics in the context of high circulating plasma concentrations of VRC01. In Chapter 3 of this thesis, I hypothesized that VRC01 infusions would result in a significant delay in the time to viral rebound compared to historical controls by exerting selective pressure on VRC01-sensitive latent reservoir viruses. Consistent with my hypothesis, 38% of VRC01 trial participants remained suppressed at week 4 of ATI compared to 13% of patients in historical controls^{3,4}. In Participants A02 and A07, detectable viremia emerged at 8 and 11 weeks respectively, and corresponded with IC50 neutralization titers <1 µg/ml. This was in contrast to the remaining 11 participants who experienced rapid viral rebound and had an identifiable proportion of viruses from the plasma virus population that had moderate resistance to VRC01 (range, 1.9 to >50.0 µg/ml). These findings suggest that viral rebound kinetics can be used to evaluate the efficacy of bNAb infusions in participants who have pre-existing bNAb resistant and sensitive viruses.

SGS and neutralization assays elucidate mechanisms of failure.

In addition to viral kinetics, the phenotype of circulating plasma viruses can also be used to elucidate mechanisms of treatment failure. In Chapter 3 of this thesis, I explored whether SGS could elucidate mechanisms of VRC01 failure by identifying genetic patterns in the rebound viral quasispecies. It is important to note that regardless of the time to viral rebound, resistance to VRC01 increased almost universally in rebound plasma viruses (mean increase by a factor of 3.44, $P=0.006$ by a two-sided random-effects model) compared to pre-cART plasma viruses. Interestingly, sequence analyses on participants with early rebound revealed two patterns: 1) polyclonal VRC01-resistant

viruses, and 2) monoclonal VRC01-resistant viruses. Further analyses on pre-cART viruses showed that prevalent pre-existing VRC01 resistance was associated with polyclonal rebound while varying pre-existing VRC01 resistance was associated with monoclonal/oligoclonal rebound. This pattern of polyclonal rebound is similar to what is observed in baseline ATI trials without additional intervention^{4,18,19}, suggesting VRC01 exerted no selective pressure on viruses re-emerging from latency. In contrast, select participants with variable pre-cART virus susceptibility to VRC01 had monoclonal/oligoclonal viral rebound, consistent with the recrudescence of a single, clonally expanded virus. Phenotypic analyses of these monoclonal lineages revealed increased resistance to VRC01 compared to pre-cART variants, suggesting VRC01 is able to restrict the outgrowth of diverse HIV-1 variants emerging from the reservoir. Finally, as expected, SGS on late rebounding Participants A02 (8 weeks) and A07 (11 weeks) revealed VRC01-sensitive pre-cART viruses along with sensitive monoclonal/oligoclonal rebound lineages. Together, these data suggest that SGS can identify the effects of the in vivo selective pressure exerted by VRC01 through the emergence of polyclonal or monoclonal/oligoclonal rebound lineages, while neutralization assays on these lineages can be used to further validate VRC01 sensitivities in vitro.

The finding that pre-existing resistance to VRC01 was common in the majority of participants (9 of 11 participants) was surprising, since they had not been previously exposed to VRC01. While autologous antibodies against the CD4 binding site (CD4bs) of HIV-1 Env are common, potent broadly neutralizing CD4bs antibodies take years to develop and the precise immunologic and virologic mechanisms guiding the evolution of these antibodies in vivo is unclear²⁰. Specific amino acid changes within the VRC01

antibody-binding site, however, did reveal changes near or within the VRC01 epitope (V5 and CD4-binding loop), suggesting VRC01 was applying specific selective pressure on rebounding variants.

Env evolution and host immune responses during ATI

While other ATI studies have shown that first detectable rebound arises from multiple, latently infected cells and establishes substantial diversity compared to HIV-1 transmission^{10,21}, no data on the evolution of *env* under ATI conditions currently exists. With access to longitudinal plasma samples from up to 47 weeks of viral rebound, we had the unique opportunity to assess *env* evolution during ATI. These data provided an important baseline assessment of viral rebound dynamics over multiple ATI time points. Using SGS analyses, we find that maximum diversity rapidly increases over time (range of 1.1% to 11.6% within 4 weeks of ATI), as multiple diverse viral lineages emerge and early rebounding lineages evolve throughout the course of ATI. Phylogenetic analyses of rebound diversity over time revealed two important findings: 1) select early lineages were no longer sampled and therefore were probably cleared by later time points, and 2) identical rebound viruses experience stochastic activation or evolve (persist). An important caveat to these analyses is the limited sampling depth and potential recombination events that may account for substantial population shifts. However, with recent clinical data describing neutralization sieve-effects mediated by VRC01³, I asked whether host immune responses may also contribute to the evolution of the viral quasispecies during the first weeks of rebound.

Assessments of adaptive immunity during ATI in previously conducted clinical trials were primarily focused on measures of T cell activation² and viral rebound kinetics. Given that the autologous antibody response takes six months or longer to develop strain-specific neutralizing breadth against earlier viruses²²⁻²⁷, few studies have focused on the kinetics of strain-specific neutralizing antibody responses arising during viral rebound. I hypothesized that autologous antibody responses generated during rebound will exert selective pressure on neutralization-sensitive rebound variants, thus preventing replication during subsequent ATI time points. To test this hypothesis, I developed Env pseudotypes from persisting and cleared viral lineages and assessed neutralization potency of autologous plasma from contemporaneous and longitudinal time points through TZM-bl neutralization assays. I found that Env pseudotypes from cleared viral lineages had a significant increase in sensitivity to autologous plasma compared to persisting lineages by the second ATI time point ($p=0.0286$), suggesting a host-mediated sieving effect on rebounding variants at early ATI time points. Furthermore, persisting lineages were also found to have increased sensitivities to autologous plasma at later ATI time points, suggesting that the neutralizing autologous antibody response against early rebounding variants is dynamic and is able to evolve over time. The selective pressure exerted by autologous neutralizing antibodies generated during rebound was further supported in Chapter 4 of this thesis. Large, clonally expanded QVOA-derived viruses that failed to expand during ATI were found to be more sensitive to autologous antibodies generated during viral rebound than rebounding viruses. Interestingly, I also found that QVOA-derived viruses maintained similar levels of resistance to VRC01. My findings highlight the complex virus-host immune dynamics during ATI, and I conclude that passively infused and host-derived neutralizing antibodies can provide strong

selective pressure on viruses emerging from rebound, thereby influencing the evolution of HIV in its host.

Safety of ATI

An important clinical finding in ACTG A5340 was that brief, closely monitored ATI with VRC01 infusion was safe and well tolerated, and all participants were able to achieve rapid viral suppression upon re-initiation of their original cART regimen. The effects of ATI on the size and composition of the peripheral reservoir with transient viremia, however, are unknown. In Chapter 4 of this thesis, I asked whether substantial changes in the viral reservoir could be observed through quantitative and qualitative assessment of latent reservoir viruses collected from pre-ATI and post-ATI (at least 6 months of cART resuppression) time points. Levels of HIV-1 DNA, RNA, and infectious units per million (IUPM) as determined by QVOA showed no significant within-person changes between pre- and post-ATI resting CD4+ T cell samples, suggesting transient viremia during rebound does not quantitatively affect the size of the viral reservoir. Next, I performed SGS on ex vivo-derived QVOA viruses from pre- and post-ATI time points. These sequences were analyzed against rebound and pre-cART viruses from the same participant in order to determine the phylogenetic relationship between PBMC and plasma-derived viruses. Upon examination, I found that participants do not experience substantial changes in the diversity of viruses found in the PBMC-derived latent reservoir, nor were pre-ATI latent reservoir viruses able to accurately predict which viruses would reactivate in vivo. These data suggest that in most participants, the phylogenetic composition of virus populations induced from or directly sequenced from resting CD4+ T cells are remarkably stable over a 9-12 month period between samplings, despite transient viremia during brief ATI. Interestingly, I observed two

exceptions to this pattern: in participants with low measures of the viral reservoir as assessed by IUPM and HIV-DNA, as well as participants with narrow virus diversity throughout pre-cART, rebound, and QVOA. Importantly, as curative strategies begin to test therapeutic efficacy under prolonged periods of ATI and viral rebound, these analyses will need to be reconsidered in the future.

Discordance between ex-vivo derived latent reservoir viruses and rebound

In addition to confirming that ATI did not substantially change the size or composition of the reservoir in Chapter 4, in all participants with at least two latent viruses to assess, large, clonally expanded viral lineages were found in the PBMC-derived latent reservoir and were genetically distinct from pre-cART and rebound plasma viruses. This observation coincides with recently published clinical trials that have identified clonal expansion within the peripheral viral reservoir²⁸⁻³⁰. In my analyses, I found that across all participants, 68% of QVOA and 52% of proviral DNA viruses were clonal. Within participants, I also found that the total percentage of identical sequences varied (between 2% to 96%). However, even when the majority of pre-ATI latent reservoir viruses display a single expanded clone, no members of this clonal population reactivated in the two weeks of ATI. These findings reveal that the rebound viral quasispecies is a minor variant within the viral reservoir that is not able to be sampled through QVOA methods, thus preventing QVOA from accurately predicting viruses that would reactivate during ATI in our studies.

We also observed noticeably different distributions of expanded clones in the QVOA and intact genes of individual participant, further confirmed by GSI values and pairwise LD analyses, suggesting our methods sampled distinct viral populations. When I compared

sequences from rebound and latent viruses I observed striking discordance between the two groups. This finding highlights that SGS analyses of HIV-1 *env* from QVOA and proviral HIV-1 DNA is an inefficient method to predict the genotype of viruses that will rebound, and that rebounding variants comprise only a small fraction of a potentially large and diverse latent reservoir with the capacity to reactivate over time. Similarly, ex vivo-stimulation of resting CD4 + T cells in QVOA assays represent a small fraction of replication-competent reservoir viruses, and limiting latent cell collection to leukapheresis-derived peripheral cells further reduces sampling depth. While these results show discordance between reservoir and rebound viruses, they also highlight the complexity of the viral reservoir and the underlying factors that govern virus reactivation and evolution during ATI. Future studies utilizing ATI methods should explore increasing sampling depth to include latently infected cells in lymphoid tissue, single-cell integration analyses to identify cellular regulators of expansion in vivo, and SGS analyses of rebounding viruses from prolonged ATI periods to determine if clonally expanded cells eventually reactivate over time. Additionally, current assays used to assess the diversity of the latent reservoir ex vivo should consider that large, clonally expanded cells may potentially confound viral diversity assessments with an extremely limited snapshot of replication-competent viruses within the reservoir.

In conclusion

The virologic and immunologic dynamics of HIV-1 rebound can be elucidated through SGS, molecular cloning of Env, and neutralization assays on plasma viruses, ex-vivo activated QVOA viruses, and proviral DNA. Understanding which viruses emerge from rebound, persist during subsequent rebound time points, and escape humoral immune pressures can further inform mechanistic correlates of curative therapy efficacy. These

studies also provide important information on the neutralization potency of the autologous antibody response generated during ATI. While humoral immune responses at rebound have not been shown to affect viral kinetics^{31,32}, through these analyses I found that neutralizing antibody responses at this point in time are strain-specific, emerge shortly after viral rebound, and are able to exert significant pressure on select viral lineages, preventing ongoing replication at subsequent ATI time points. Future studies should consider building on these findings to determine whether neutralizing antibodies can provide additive or synergistic selective pressure in combination with curative therapies to suppress viral escape from genetically diverse viral variants emerging from the viral reservoir during ATI.

References

1. Clarridge, K. E. *et al.* Effect of analytical treatment interruption and reinitiation of antiretroviral therapy on HIV reservoirs and immunologic parameters in infected individuals. *PLOS Pathogens* **14**, e1006792 (2018).
2. Papasavvas, E. *et al.* Analytical antiretroviral therapy interruption does not irreversibly change pre-interruption levels of cellular HIV: *AIDS* **32**, 1763–1772 (2018).
3. Bar, K. J. *et al.* Effect of HIV Antibody VRC01 on Viral Rebound after Treatment Interruption. *N. Engl. J. Med.* **375**, 2037–2050 (2016).
4. Rothenberger, M. K. *et al.* Large number of rebounding/founder HIV variants emerge from multifocal infection in lymphatic tissues after treatment interruption. *PNAS* **112**, E1126–E1134 (2015).
5. Caskey, M. *et al.* 3BNC117 a Broadly Neutralizing Antibody Suppresses Viremia in HIV-1-Infected Humans. *Nature* **522**, 487–491 (2015).
6. Li, H. *et al.* Envelope residue 375 substitutions in simian–human immunodeficiency viruses enhance CD4 binding and replication in rhesus macaques. *Proc Natl Acad Sci U S A* **113**, E3413–E3422 (2016).
7. Ho, Y.-C. *et al.* Replication-Competent Noninduced Proviruses in the Latent Reservoir Increase Barrier to HIV-1 Cure. *Cell* **155**, 540–551 (2013).
8. Cohn, L. B. *et al.* HIV-1 integration landscape during latent and active infection. *Cell* **160**, 420–432 (2015).
9. Murray, A. J., Kwon, K. J., Farber, D. L. & Siliciano, R. F. The Latent Reservoir for HIV-1: How Immunologic Memory and Clonal Expansion Contribute to HIV-1 Persistence. *The Journal of Immunology* **197**, 407–417 (2016).
10. Keele, B. F. *et al.* Identification and characterization of transmitted and early founder virus envelopes in primary HIV-1 infection. *PNAS* **105**, 7552–7557 (2008).
11. Worobey, M. *et al.* Direct evidence of extensive diversity of HIV-1 in Kinshasa by 1960. *Nature* **455**, 661–664 (2008).
12. Beerenwinkel, N., Günthard, H. F., Roth, V. & Metzner, K. J. Challenges and opportunities in estimating viral genetic diversity from next-generation sequencing data. *Front. Microbiol.* **3**, (2012).
13. Deleage, C. *et al.* Impact of early cART in the gut during acute HIV infection. *JCI Insight* **1**, (2016).
14. Satou, Y. *et al.* Dynamics and mechanisms of clonal expansion of HIV-1-infected cells in a humanized mouse model. *Scientific Reports* **7**, 6913 (2017).

15. Ho, D. D. *et al.* Rapid turnover of plasma virions and CD4 lymphocytes in HIV-1 infection. *Nature* **373**, 123–126 (1995).
16. Wei, X. *et al.* Viral dynamics in human immunodeficiency virus type 1 infection. *Nature* **373**, 117–122 (1995).
17. Canini, L. & Perelson, A. S. Viral Kinetic Modeling: State of the Art. *J Pharmacokinet Pharmacodyn* **41**, 431–443 (2014).
18. Bednar, M. M. *et al.* Diversity and Tropism of HIV-1 Rebound Virus Populations in Plasma Level After Treatment Discontinuation. *J Infect Dis* **214**, 403–407 (2016).
19. Kearney, M. F. *et al.* Origin of Rebound Plasma HIV Includes Cells with Identical Proviruses That Are Transcriptionally Active before Stopping of Antiretroviral Therapy. *J Virol.* **90**, 1369–1376 (2016).
20. Lynch, R. M. *et al.* The Development of CD4 Binding Site Antibodies during HIV-1 Infection. *Journal of Virology* **86**, 7588–7595 (2012).
21. Maldarelli, F. *et al.* HIV Populations Are Large and Accumulate High Genetic Diversity in a Nonlinear Fashion. *Journal of Virology* **87**, 10313–10323 (2013).
22. Moody, M. A. *et al.* Strain-Specific V3 and CD4 Binding Site Autologous HIV-1 Neutralizing Antibodies Select Neutralization-Resistant Viruses. *Cell Host & Microbe* **18**, 354–362 (2015).
23. Richman, D. D., Wrin, T., Little, S. J. & Petropoulos, C. J. Rapid evolution of the neutralizing antibody response to HIV type 1 infection. *Proc Natl Acad Sci U S A* **100**, 4144–4149 (2003).
24. Wei, X. *et al.* Antibody neutralization and escape by HIV-1. *Nature* **422**, 307–312 (2003).
25. Kelly, H. R. *et al.* Neutralizing antibody patterns and viral escape in HIV-1 non-B subtype chronically infected treatment-naive individuals. *Human Antibodies* **14**, 89–99 (2005).
26. Derdeyn, C. A., Moore, P. L. & Morris, L. Development of broadly neutralizing antibodies from autologous neutralizing antibody responses in HIV infection: *Current Opinion in HIV and AIDS* **9**, 210–216 (2014).
27. Moog, C., Fleury, H. J., Pellegrin, I., Kirn, A. & Aubertin, A. M. Autologous and heterologous neutralizing antibody responses following initial seroconversion in human immunodeficiency virus type 1-infected individuals. *Journal of Virology* **71**, 3734–3741 (1997).
28. Lee, G. Q. *et al.* Clonal expansion of genome-intact HIV-1 in functionally polarized Th1 CD4⁺ T cells. *J Clin Invest* **127**, 2689–2696 (2017).

29. Lorenzi, J. C. C. *et al.* Paired quantitative and qualitative assessment of the replication-competent HIV-1 reservoir and comparison with integrated proviral DNA. *PNAS* **113**, E7908–E7916 (2016).
30. Hosmane, N. N. *et al.* Proliferation of latently infected CD4+ T cells carrying replication-competent HIV-1: Potential role in latent reservoir dynamics. *J. Exp. Med.* **214**, 959–972 (2017).
31. Pappasavvas, E. *et al.* Randomized, Controlled Trial of Therapy Interruption in Chronic HIV-1 Infection. *PLoS Med* **1**, (2004).
32. McLinden, R. J. *et al.* Association of HIV neutralizing antibody with lower viral load after treatment interruption in a prospective trial (A5170). *AIDS* **26**, 1452 (2012).